THOR'S HAMMER: DESIGN AND MANUFACTURING PROCESS OPTIMIZATION OF CAST COMPONENTS

2021 SFSA Cast in Steel Competition: Technical Report

Penn State Behrend Student Team Members:

Kristen Collins, Senior Mechanical Engineer
Jackson Craig, Senior Mechanical Engineer
Matt Gielarowski, Senior Mechanical Engineer
Austin Hankey, Senior Mechanical Engineer

Penn State Behrend Faculty Advisor:

Dr. Paul Carl Lynch, Ph. D Assistant Professor of Industrial Engineering

Penn State Behrend Industry Sponsors:

PRL Regal Cast, Lebanon, PA

Urick Ductile Solutions, Erie, PA

Background and Problem Statement

Background:

Traditionally, steel components for commercial and military applications have relied upon forging from wrought product to produce the unique balance of strength, hardness, ductility, and toughness required of these products. However, research within the metal casting industry has suggested that through the utilization of such techniques as fluid flow simulation, solidification modeling, and clean melting, casting can be used to create components with properties identical to forged components. Additionally, advancements in the printing of molds, cores, and patterns are continuously increasing the capability of casting to produce complex designs. Each year, the Steel Founder's Society of America (SFSA) hosts a competition which focuses on the use of modern casting tools such as these to design and manufacture components that are typically produced with forging operations. This project involves participation in this year's Cast in Steel competition to create a cast model of Thor's Hammer. The creation of this cast hammer will try to validate the research that a properly processed casting can match the properties of forged components. The focus of the competition is in the creative implementation of the casting process to the fullest extent to produce a final design that is easily identifiable as the Marvel movie representation of Thor's Hammer. Additionally, the functionality of the hammer will be evaluated based on a series of performance tests and expert revision. The specific tasks associated with each test are not disclosed to the design teams prior to the competition. However, it can be expected that the design will be tested in functions equivalent to that of a sledgehammer during demolition.

In accordance with the competition limitations, the hammer in its completion, with both the head and the handle included, must be within the weight and length limitations of 6 lbs and 20 inches. The hammer must consist at least partially of components that have been cast with steel, though a specific percentage is not required. In compliance with the stipulation of being "easily recognizable as Thor's Hammer" in terms of aesthetics, the head design will be a scale, either full or decreased, of the original 5 in by 5 in by 8 in dimensions. Within the competition testing, the design must be fully functional in the completion of tasks associated with a regular hammer, and primarily, in the high impact applications associated specifically with Thor's Hammer. Little to no facial or structural deformation should occur under the loads induced throughout the performance tests. A combination of various manufacturing processes, including heat treatments, hipping, welding, and machining, may be used in addition to casting so as to meet the criteria for both the design and the capability. A variety of tactics, including but not limited to, CAD optimization, material selection, FEA, and fluid flow simulations, will be utilized to create a model of the highest functionality possible.

Problem Statement:

Design and manufacture a predominantly cast steel representation of Thor's Hammer given SFSA's competition specifications.

Critical Technical Challenges

- Design the hammer to undergo a series of unknown tests with unknown parameters
    - As part of the competition, the performance tests are not revealed to contestants
- Design the hammer to take impact without deformation
    - Must withstand at least the average loads associated the functions of a hammer
- Choose the manner of resembling the original model
    - Will be either full scale or scaled down from the original
    - Based on our interpretation of what classifies as "easily recognizable"
- Choose the degree of solidity of the hammer head while also meeting the weight limitation
    - A solid cast would require a reduction in the volume of the head to nearly $1/10^{th}$ of the original based on the density of steel
    - Increased proximity to full scale requires decreased solidity of the head
- Determine the capabilities of the design in withstanding loads based on dimensional and solidity choices
- Access the proper fluid flow software for realistically and accurately simulating casting processes
- Conduct flow simulations to model the design-specific casting procedure and ensure the design provides the conditions necessary to produce a successful cast
- Choose the method of casting capable of accurately producing the choice of scale and solidity
- Choose the construction method for the handle that will provide the necessary strength and durability without significantly hindering the weight
- Design method for creating a rigid handle that connects to the hammer's internal structure
- Determine the additional manufacturing processes needed to finish the hammer

Overview of Project Objectives

The over-arching objective associated with this project is to gain an understanding of the multitude of factors that affect a cast component and gain experience in completing the steps necessary for producing the final product. The project begins at the initial design step to design a castable Thor's hammer and follows the component all the way through to the final manufacturing, finishing, and material testing. Doing so will involve self-completion of many of the procedures that typically relied on outsourcing to complete in previous years of competition participation. In the initial design stage, concept generation will be conducted where various designs will be produced and then narrowed down based on specified criteria. In this case, the components of each concept must not only be achievable by way of casting, but they must also uphold the competition-given limitations. After the designs are narrowed down to the best contenders, prototypes will be made to analyze the design functionality and determine any possible performance flaws. This phase will utilize 3D printing and design optimization within CAD to fine-tune the remaining designs. Analytical analysis will then be conducted within ANSYS to test the strength capability of each proposed hammer. This will clarify which design can maintain the most strength and resistance to deformation while also adhering to the 6 lb weight restriction. Upon selecting the most optimal model, mold design and fluid simulations will be conducted to ensure that the hammer dimensions are able to be cast based on the limitations given by the industry sponsor. Once the mold designs are created, they will be sent to the industry sponsor where they will print the molds and pour the molten steel into them to produce Thor's hammer. This year's industry sponsors will only be providing services for the mold manufacturing and the metal pouring. Finally, the casted hammers will be sent back from the industry partner, where the group will then implement various post processing techniques to prepare the hammer for competition testing along with conducting various material testing to analyze the hammer's material properties.

Description of Competition Limitations

In the competition outline given by SFSA, there are primarily only three non-negotiable rules that all participants' hammer designs must follow: the weight must be within 6 pounds, the length must be within 20 inches, and at least a portion of the hammer's components must be cast with an alloy of steel. Thor's Hammer is a one-handed hammer, and the size constraints are near the upper limit of one-handed hammers. Though not explicitly stated in the description, it can be inferred that the head is the component of the hammer for which casting is intended to be utilized. The head is both the primary functioning element of the tool and the major element that will be tested, therefore, casting the head aligns with the competition's overall intent to highlight the capabilities of casting. Other factors to consider for success in the judgement process include overall quality, uniqueness of features, and functionality in the performance testing. However, only vague statements are made regarding these areas without provided metrics, therefore, the only strict rules governing submissions remain as those previously stated.

With limitations being set in only these three designated areas, many of the key design choices are left up to the discretion of the designers. A wide variety of designs can be generated

based on the strategy used to meet the requirements, as well as each team's interpretation of Thor's Hammer itself. The biggest influence on the chosen strategy, however, which is universal to all teams regardless of the design inspiration, is the difficulty in combining a 6 lb weight limit with the use of a steel alloy. Using a solid casting for the head would require that the dimensions be significantly scaled down from the original Marvel or Viking renditions. Therefore, any attempt to create a head of sizeable dimensions requires a very innovative casting design on behalf of each team. The contestants must determine how to structure the casted portion of the head such that it is within the designated weight but also maintains the structural integrity needed to perform as a hammer. This includes the scale of the outer dimensions, the internal geometries, specific alloy used, and so on. Furthermore, because additional non-cast elements are permitted, as well as various post processing operations such as machining; grinding; and welding, there are seemingly endless methods as to how the teams can transition from the appearance of the casting to the overall design appearance.

Hammer Design Rationale: Marvel vs. Viking Mythology

At the very base of this design process is determining what defines Thor's Hammer and differentiates it from the average hammer. While the answer is ultimately up to the discretion and interpretation of each team, there are two main depictions of Thor's Hammer: Marvel's rendition of Mjolnir seen in the comics and movies and the traditional version of Mjolnir from Viking Mythology. Though both have a similar mystical history and serve very similar functions, they are quite different in their structure and design. The historic Old Norse version has an almost triangular head that comes to a point at the center, similar to a cross peen, but tapers to two flat faces. Typically, the hammer is a single piece made of entirely of metal, with a short handle and extremely intricate detailing throughout. Marvel's Thor's Hammer is characterized by a large, rectangular head with two square striking faces, resembling a blacksmith sledgehammer or mallet. This version has a longer leather-wrapped handle that is separate piece from the head.

Figure #: Viking Mythology Representation

Figure #: Marvel Representation

Given these two existing constructions of Thor's hammer, our team chose the version depicted in the Marvel series as the inspiration behind our design. In terms of complying with the ease of recognition aspect of the competition, we felt that the Marvel version of the hammer was much more well-known and would generate a lot more enthusiasm at being brought to life. In terms of the casting portion of the competition, our team believed first and foremost that the Marvel version would be more practical given the weight limitation. While the original Viking rendition of the hammer consists of a continuous piece of solid metal for both handle and head, the Marvel version consists of separate components where metal appears to only be used for the head. Though it would be possible to generate a casting to resemble the Viking hammer and appear as if it were one solid casting in its entirety, we felt this would come at a cost in terms of structural integrity and size. Because the Marvel version already accounts for a handle that does not visually resemble metal, we felt that this would give us more leeway to compensate for weight by using lighter materials for elements other than the head structure.

Functional Model

Though determining the aesthetic and structural inspiration for the design is a key initial step, visual recognition as Thor's Hammer is only one criterion for judgement. The hammer must also be able to successfully perform the tasks associated with a hammer that will be executed during competition. Therefore, the next step before making any major design choices was to consider how the hammer works as a complete system. The diagram below gives the functional model for the hammer, including the inputs required (left) and the outputs generated (right) by its use. Treating the hammer as the system itself, the user initiates the operation by picking up the hammer and applying work to raise it. Due to gravity, the hammer obtains potential energy associated with the height it is raised to. With gravity aiding downward motion, the user then re-applies work into swinging the hammer, converting the gravitational potential energy into kinetic energy. At the base of the swing, the hammer interacts with the third input, the surface of impact, creating the impact itself. Finally, this contact between the hammer and the surface produces three outputs in the form of sound, heat, and deformation. By creating this systematic breakdown of the hammer into its abstract functions, we were able to get a better understanding of what constitutes a working system.

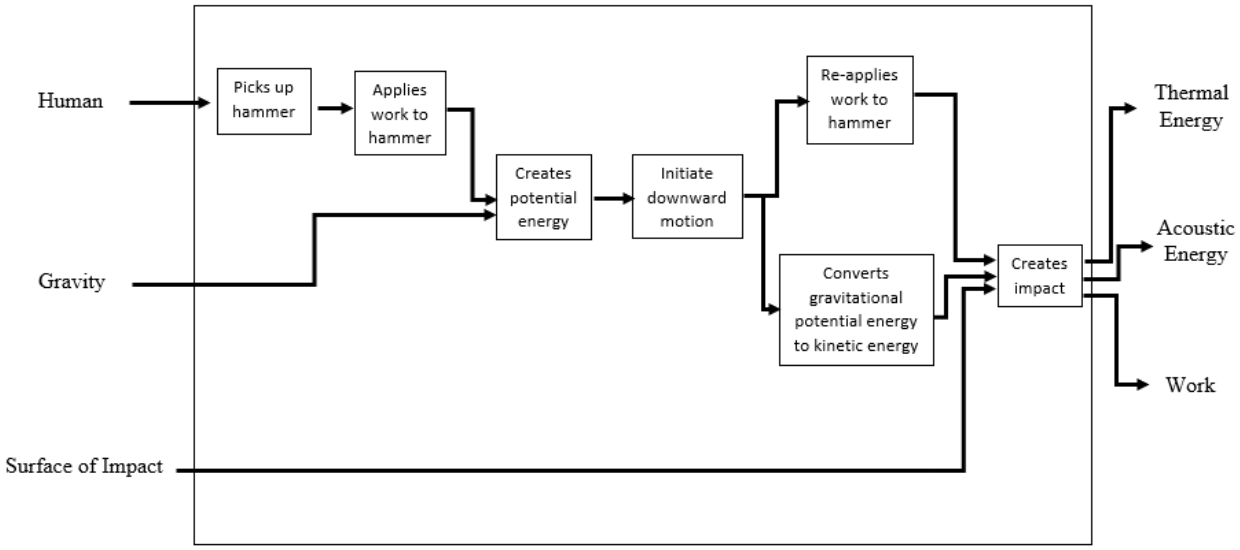

Material Selection

In order to prove the casting capabilities of the material and highlight the intent of SFSA in hosting the competition, the design must include elements cast from an alloy of steel. Based on the factors of judgement within the competition and the standard function of the tool being produced, the specific alloy selected was AF96-28. While designated as the desired material by the Penn State faculty member who is sponsoring this project, prior research with the alloy conducted by the members of this team also factored into the overall selection.

This alloy is designed to exhibit high-performance properties similar to a high strength steel at a decreased cost of production. While comparable to 4130 steel in terms of its low to medium carbon content and low alloying, AF96-28 has significant adjustments to its composition that contribute to its cost reduction and improvement of characteristics relevant to use in this competition. This is from both a base material property and manufacturability standpoint, including yield strength; hardness; and impact toughness as well as castability, heat treatability, and weldability.

First and foremost, the level of carbon content in this alloy ranges from about 0.24% to a maximum of .32% by weight, which is slightly lower than the standard 4130 steel. This offers high strength, hardness, and potential for hardenability, but remains low enough such that it does not significantly reduce the toughness of the alloy. This is important in terms of the competition because the hammer must withstand testing with little to no plastic deformation.

Notably, this alloy includes higher levels of both chromium and silicon as compared to a steel such as 4130, between 2.00-3.00% and around 1.5% respectively. The increased Chromium contributes to the good hardenability, high strength, and temper resistance provided by the alloy. One of the qualities of AF96 that is most applicable to this competition stems from the larger amount of silicon. Silicon reduces the coarsening of epsilon carbide to cementite which preserves

smaller, semi-coherent carbides. Because of this, silicon offers enhanced fluidity when in the molten phase for casting, and also enhanced toughness after solidification.

Several of the advantages of this alloy also stem from the constituents not included in its composition that a typical high strength steel does include. AF96 uses relatively low levels of nickel and is void of any intentionally added tungsten or cobalt. Tungsten specifically, due to its high cost and limited supply, is the alloying element that makes many traditional steels expensive. Furthermore, its high melting point and very high density also contributes to difficulty in processing traditional steels. The exclusion of this constituent makes AF96 a more cost effective and workable option.

Additional information regarding the properties of AF96, as well as the specifics of its invention, can be found within the patent referenced in Appendix A.

Design Specifications

Upon completing the previous preliminary steps, the next portion of the project was dedicated to establishing what the hammer needed to provide based on the requirements of the competition. The purpose this step was to translate the general needs from the competition description into precise and concrete descriptions of what the hammer must do. It was important to come up with requirements that were actually measurable, with a metric that could be used for gaging whether or not the final product truly met the spec. Given that the competition description was rather limited in explicit "needs" for the hammer, especially due to the fact that the testing circumstances are unknown, this task required a significant amount of deliberation. Apart from the rules clearly outlined for the hammer's weight, length, and material composition, the other specifications were based largely on how the group anticipated that the hammer be tested and on existing engineering standards for comparable types of hammers. Interviews were also conducted with our university faculty sponsor, as well as with Kim Schumacher and Diana David of the SFSA team, in order to receive guidance and get a better understanding of the hammer's application.

Using all of the information gathered, the group established the conditions we felt were necessary to produce a successful version of Thor's hammer. While most are uncompromisable constraints, several are high-priority goals, the achievement of which would benefit the overall quality. Listed in the table below is this list of design specifications. Included is the marketing spec based on either the explicit requirements of the hammer by SFSA or those that our group deduced, and the engineering spec giving the specific metric that governs the marketing. Following these are the rationales for each value selected, the method that will be used to measure if the metric is met, and lastly, the classification of each specification as either a constraint or a goal. For those classified as constraints, the chart also lists the area of society, or realistic constraint, applicable to that specification.

One important thing to note pertains to the metric corresponding to recognizability of the hammer outlined in Specification 4. This specification states that the dimensions of the hammer

must be kept within 85% of the original dimensions of Thor's hammer. The rationale behind this stems from how the size of the user of our hammer compares to the size of the actor using the original prop in the movies. The original hammer is 5" by 5" by 8" and is used by an actor who is 6'2" and roughly 200 lbs. Assuming our user as the average male with height 5'8" and weight 160-180 lbs, the overall size of our user is about 85% of the size of the user of the original. As a result, we determined that an 85% scaled-down model of the original would look the same in our user's hand as the original does in the hand of the actor. In other words, the reduction of the hammer size is proportional to the reduction of the user.

A second important notice is in relevant to the metric first cited in Specification 6 and used successively in the specifications to follow. This 6500 lb value is used throughout the specs as the maximum force that the hammer is likely to see during competition. The loads a hammer can see during use vary significantly based on the user, the object being hit, the weight of the hammer, and so on, making it difficult to find a typical value as a basis. Additionally, because information was not disclosed regarding what type of impacts the hammer would experience, the group had to determine a reasonable estimate for the loading conditions it must be capable of withstanding. To do so, a case study was conducted by our team. The study involved a sample group of our assumed users, males of average height and weight, swinging hammers similar in size and weight to the competition restrictions. The force value was then found by measuring the amount of deformation each user inflicted on a lead slug given the velocity of their swing. An in-depth description of this case study can be found in Appendix B.

Lastly, pertaining to the castability of the design described in Specification 3, the exact values listed for the minimum wall thickness and filet radii were added after the completion of the concept selection for the casting method (detailed in the succeeding sections). These values are unique to each casting method such that proper fluidity can be achieved within the mold during pouring. As the exact method of casting the group would use was not determined at the time of compiling the design specifications, these values were left as unknowns until after concept selection.

Marketing Spec	Engineering Spec	Rationale for Value	Metric Evaluation	Constraint vs. Goal
1.) The design must be within the designated weight and length constraint.	A.) The hammer must not exceed an overall weight of 6 lbs.	In accordance with the competition design specifications outlined by SFSA.	Inventor estimations based on densities of steel alloys and potential dimensions. A scale will be used for final weight validation of the prototype.	Constraint (Manufacturability)
	B.) The hammer must not exceed overall length of 20 inches.			
2.) The hammer must consist	A.) The cast material will be AF-9628.	As created by the SFSA, the competition	Pass or Fail	Constraint (Manufacturability)

partially of cast component.		centers on the casting capabilities of steel. Sponsor designated AF-9628 as the specific steel alloy.		
	B.) The hammer will consist of at least 2/3 cast elements by weight.	SFSA's competition description calls for "utilizing casting to the fullest extent".	Weight of all cast parts as compared to the 6 lb limit. Weight calculations using alloy densities and Inventor design dimensions.	Goal-Priority 1
3.) The design dimensions must be castable.	A.) The design must not have any wall or web thicknesses less than 1/4 inches.	Limitations of fluid flow within the mold during the specific casting method. Values given by sponsor and industry recommendation.	Inventor/CAD designing and fluid flow simulations	Constraint (Manufacturability)
	B.) The design must contain fillets of at least 1/8 inches to eliminate sharp edges or corners to allow geometries to be cast.			
4.) The hammer should be easily recognizable as Marvel's "Thor's Hammer".	A.) The final outside dimensions of the head should be kept within 85% of the original 5 in by 5 in by 8 in (face to face dimensions) to resemble the iconic heft of the movie version.	Based on the original dimensions and aesthetic appearance of the licensed replica of the movie prop found in Marvel's Thor. The average male at height 5'8" and 160-180 lbs is roughly 85% of the size of the actor who plays Thor (6'2" and 200 lbs).	Design development with Inventor/CAD to adjust internal dimensions to meet weight requirements with these outer dimensions. Comparison of prototype dimensions and appearance to the online-sourced information on the licensed replica to check for aesthetic accuracy.	Goal-Priority 1
	B.) The hammer should have a surface roughness between 3.2 to 0.4 micrometers (Ra) after post-processing to produce visual sheen akin to the original. *	Sponsor recommendation for the hammer to have a finish between machined and ground.	Comparison of finish to surface roughness charts after post-processing	
5.) The hammer faces should be hard enough to withstand impacts associated with common hammer functions.	All striking faces shall be hardened to 45-60 HRC or equivalent.	According to the specifications outlined for Category 54 hammer heads (Sledge) outlined in ASME B107.400.	Rockwell Hardness tests conducted in accordance with ASTM E18	Constraint (Durability)

6.) The hammer will be designed based on the user capabilities of the average male.	The hammer must withstand a minimum impact load of 6500 lbs without plastically deforming, based on the swing velocity and force generating capacity of an average male (160-180 lbs).	Values estimated using experimental impact testing and dynamic analysis on swing generated by a sample of average males with tools of similar size and weight. **	Impact testing with charpy bars of cast material and ANSYS/FEA load simulations.	Constraint (Durability)
7.) Hammer must withstand repeated impacts during performance testing.	The hammer must undergo 20 successive full swinging blows by an average male without plastically deforming.	Based on ASME B107.400 standard for striking tools over 64 oz in weight as well as the successive use of the hammer in competition testing.	ANSYS dynamic analysis and personal simulation of conditions using tools/users of similar metrics	Constraint (Durability)
8.) The handle material must be strong enough to withstand hammer use.	The handle must not fail under shear stress when the head is subjected to a 6500 lbs load.	The handle must not fail when the head is subjected to the service load.	Hand Calculations and ANSYS/ FEA analysis to simulate loading conditions. Impact testing on prototype to simulate competition conditions	Constraint (Durability)
9.) The handle must be securely fastened to the head.	Handle shall not loosen or separate when subjected to a static tensile force of 1000 lbf.	Specifications outlined in ASME B107.400 for striking tools consisting of separate head and handle.	Hand calculations and ANSYS/FEA analysis used on designs to simulate the loading conditions. Static tensile testing on prototype to induce specified tensile load.	Constraint (Durability/ Manufacturability)
10.) The hammer should maintain a sound and rigid structure upon impact.	A.) The head shall not permanently deform, crack, or break under the impact load of 6500 lbs.	Quality and performance standards given by ASME B107.400 for striking tools used for the expected functions of our hammer.	ANSYS/FEA simulation of estimated amounts of permanent deformation under expected loading conditions.	Constraint (Durability)
	B.) The striking face shall not compress, mushroom, chip, crack, or spall under the impact load of 6500 lbs.			
11.) The design must be safe for the user throughout use.	A.) The handle shall remain free of cracks and splinters when extended in the horizontal plane and subjected to static load of 250 lbf at a point 10 inches from the top of the head.	250 lbf is the value given by ASME B107.400 for striking tools with a head weight greater than 4 lbs.	ANSYS load analysis using handle dimensions and material and prototype testing under given static load	Constraint (Safety/ Durability)
	B.) Head and handle should be free of	Based on OSHA standard 1926.301 (d)	Inventor 3D modeling	

	nonfunctional sharp edges less than 90° All Sharp corners broken.	for hand tool safety and ASME B107.54 standard for hammer manufacturing.		
12.) The hammer should have an ergonomic handle.	The diameter of the handle without any nonfunctional aesthetic additions should be between 1.125 in and 1.25 in.	Textbook on the Ergonomic Design of Hammer Handles defines this as the optimal size for comfortable use.	Inventor dimensioning to ensure the design is kept to this range. Actual dimension validated with calipers. ANSYS analysis to test if this size range can support the durability requirements.	Goal-Priority 2 (Ergonomics)
13.) Project completion must meet the designated time constraint	All manufacturing, reporting, and video documentation for the competition must be complete and postmarked by March 12th.	SFSA's deadline for submission of the three competition deliverables (hammer, technical report, and summary video) is March 12th.	Pass or Fail	Constraint (Manufacturability)
14.) The project costs will be optimized.	The costs of manufacturing and post-processing should be minimized.	The cost must be within the amount of granted funding as designated by the sponsor.	Sponsor approval of cost analysis and feasibility reports	Goal-Priority 1

*4B.) Post- Processing is allowed as a means to achieve desired surface finish

** 6.) Data sourced from the self-conducted Lead Slug Case Study for Load Estimation. See Appendix for detailed case study description.

Summary of Realistic Constraints

As stated above, in addition to the technical considerations associated with the hammer, the design specifications also outline the broader considerations in the form of realistic constraints that correspond to each engineering requirement. These constraints, such as Sustainability, Environmental, and Ethical, relate mainly to the well-being of society and the quality of life. Linking the aspect of the product to the general area of society that its production may affect ensures that we as designers take the time to truly understand the design problem and anticipate potential hazards. The goal is to make decisions with the best judgement in order to address these concerns. The realistic constraints associated with the design of the hammer include:

- Manufacturability
    - Specification 1: The design must be within the weight and length constraints of 6 lbs and 20 inches
    - Specification 2: The hammer must consist partially of components cast from an alloy of steel

- Specification 3: The design must have wall thicknesses greater than 1/4 in and fillets of at least 1/8 inches to ensure castability
- Specification 9: The handle must have a connection to the head that remains rigid under a tensile load of 1000 lbf
- Specification 13: All manufacturing, reporting, and video documentation must be complete and submitted to SFSA by March 12th.

- Durability
  - Specification 5: The hammer faces should be hardened to between 45 and 60 HRC in order to withstand impacts associated with common hammer functions
  - Specification 6: The hammer must withstand a minimum load of 6500 lbs upon impact when swung by an average male
  - Specification 7: The hammer must withstand 20 successive full swinging blows of 6500 lbs
  - Specification 8: The handle must be strong enough to avoid shear failure during an impact load of 6500 lbs
  - Specification 10: The hammer should maintain a sound and rigid structure with little to no permanent deformation under the impact load of 6500 lbs

- Safety
  - Specification 11A: The handle shall remain free of cracks and splinters when extended in the horizontal plane and subjected to static load of 250 lbf
  - Specification 11B: Head and handle should be free of nonfunctional sharp edges less than 90°

Applicable Engineering Standards

In order to determine specific metrics and methods of evaluation for each design specification, several published engineering standards were referenced. Given the tool being designed, these standards are based on the safety and functionality of hammers. Those specifications regarding the performance characteristics of the hammer, such as durability and hardness, utilize the ASME Standard for Striking Tools. Those specifications concerned with maintaining the safety of the user utilize the OSHA standard for Hand Tools.

ASME B107.400-2018: Standards for the Quality and Performance of Striking Tools

These standards outline the performance requirements and limitations of use, as well as the test methods to evaluate performance and safety. Category 54 (B107.54) applies specifically to heavy

striking tools including stone sledges and blacksmith sledges, as these hammers function most closely with the expected competition test for the design.

- Specification 5: The striking faces should have hardness values of 45-60 HRC or equivalent after Rockwell hardness testing according to ASTM E18.
- Specification 7: The hammer must withstand 20 successive full swinging blows by an average male of 160-180 lbs
- Specification 9: The handle shall be securely connected so as not to loosen or separate when subjected to a static tensile force of 1000 lbf.
- Specification 10: The head and striking faces shall not crack, mushroom, or deform under the service load of 6500 lbs
- Specification 11A: The handle must withstand the 250 lbf point load without splintering to ensure it will remain safe for the user during service.

OSHA 1926.301: Safety Standards for Hand Tools

This defines the safety and health regulations associated with the use of various hand tools. These apply specifically to the construction industry, as it is anticipated that the design be tested in functions most closely related to those of the construction industry. Component 301(d) of this standard is specifically tailored to hammer safety.

- Specification 11B: The hammer shall be free of sharp edges less than 90° to prevent user injury.

Concept Generation Process

This section defines the process the group used to come up with ideas for every aspect of the producing the hammer, from casting method all the way to the hammer head design. The focus was to formulate potential solutions to each of these aspects such that the necessary functions can be achieved. In order to generate the most diverse design options, the overall concept for the hammer was broken down into four separate categories: the casting method, the hammer head structure, the handle material, and the connection method between head and handle. Each of these categories constitute the major elements of the design, and variations in each of these categories can have a significant effect on the function and quality of the hammer. For the first phase of concept generation, the ideas for the four categories were generated independent of the others. This allowed for the highest level of ingenuity and ensured that initial possibilities in one concept category were not restricted by association with another category. During this process, the focus was to brainstorm as many options as possible, and no ideas were discounted. The feasibility of each idea, as well as the compatibility of ideas between the four categories would be considered in the next phases of concept screening and concept selection.

The generation process was started by having each group member sit down independent of each other and generate as many designs or methods as possible, creating lists and drawing diagrams. Each group member was required to come up with at least 10 designs for each concept category, and they were encouraged to be creative with it. Evidence-based design heuristics for idea generation were used so that each group member could be creative and not get caught with design fixation. Once each of the team members had their 10 design for each component, the group convened to discuss each design individually. Throughout the discussion, pros and cons were made about each design, and as the group discussed together more designs were created. There even various design features taken from multiple initial concepts that were used to create a completely new design. Once all the designs were created and discussed, the concept screening process was able to be carried out. The sections below will explain the generation process for each component and show some of the concepts that were generated. For images of all the concepts that were generated please refer to the appendix.

I. Casting Method

As at least a portion of the hammer must consist of cast components per competition guidelines, the first category to undergo concept generation was the casting method. A very wide variety of casting methods exist that could potentially produce the components needed, each offering their own benefits and characteristics to the parts they make. Some of the major ways the methods tend to differ from each other are in the mold material used, method of inserting metal into the mold, and material compatibility. Because our knowledge of these methods was limited to primarily the traditional and more common options, it was decided that this area would benefit from using a digital source that contains all casting methods. This would give us insight into methods we may not have been aware of that could be considered as possible options. The specific source used for this purpose was the Granta Edupack material and processes database. Within this database, there are three levels, each with a more advanced coverage of data and each containing various subcategories of information, including material and manufacturing processes. Level 3 was used for our purposes to correspond to the level of analysis being done and to provide the widest range of options. Specifically, only the process universe was used within level 3 for this portion. Because the Process Universe further breaks down to include all processes categorized as joining, shaping, and surface treatment, the search was narrowed to only the casting processes since most of the hammer needed to be cast. Given that it was known that the casting must be made of steel, the search was then limited to only those casting processes compatible for steel alloys. While generation intends to include as many ideas as possible, it was not practical to include the casting methods that were unable to comply with the competition's material requirement. No other upfront rules for the competition would immediately discount certain methods as the material did, so the search was not narrowed any further in an effort to leave the casting concepts as open as possible. After the limits were set, a list was generated for all the applicable processes which have been documented below.

Table 1: List of generated casting methods

Centrifugal casting	Evaporative pattern casting, automated	High pressure die casting	Replicast casting
Centrifugally aided casting	Evaporative pattern casting, manual	Investment casting, automated	Rheocasting
Ceramic mold casting	Semi-centrifugal casting	Investment casting, manual	Ferro die casting
CLA/CLV casting	Gravity die casting	Low pressure die casting	Shell casting
CO2/silicate casting	Green sand casting, automated	Plaster mold casting	Squeeze casting
Cosworth casting	Green sand casting, manual	Rammed graphite casting	Thixocasting
Vacuum investment casting	3D Printed sand casting		

II. Head Structure

The next category focused on for this brainstorming portion was the hammer head structure. The head structure presents arguably the most vital component for which to determine a solution. The overall functionality of a hammer and likely its performance in the competition testing is most dependent on the design of the head. Based on this, it was decided prior that most if not all of the head would be produced through casting in order to truly highlight the capabilities of casting. One of the factors then contributing in part to the ideas we came up with was castability. A second factor kept in mind while brainstorming was recognition. Concepts for the head structure were generated with the idea that the hammer must look similar to Marvel's Thor's hammer. As a result, most of the external features of the hammer looked very similar in design on all of the concepts. Where the designs got creative was for the internal structure of the hammer. Adjusting the internal geometries across the concepts was a way to alter both the weight and the strength of the design, which were the last two major factors influencing our ideas. A solid steel Thor's hammer cast to movie dimensions would weigh about 60 lbs. However, the competition guidelines require that the overall hammer be under six pounds and the outer dimensions must remain within 85% of the movie dimensions according to the group's own design specifications. Therefore, a totally solid head was not possible, and a very creative design needed to be generated to stay close to the size of Marvel's Thor's hammer while still being under the 6 lb constraint. However, the group was aware that any adjustments to the internal design would adjust the integrity of the head and its capability to withstand use as a hammer. As a result, many of the designs attempted to include internal structures that reduced the weight as compared to a solid head while also providing strength to perform. These parameters required unorthodox designs to be generated to help narrow the hammer down to the final design. Listed in appendix D1 are pictures of the generated head structure designs.

In addition to the individual head structure concepts that were generated, the group established a potential approach that could apply across multiple head designs for achieving the "solid" external look. Rather than including the four side walls as part of the head designs or attempting to cast them, a "shell" made of sheet metal could be used to connect the striking faces. While the intent of some concepts included casting the side walls as part of the overall design, many focused on the variation in internal structure. For these in particular, the sheet metal shell presented a way to achieve both the recognition factor and the weight limitation. Much of the area in between the faces could remain hollow but appear as if it were solid,

subsequently allowing the outer dimensions to remain closer to 100% scale. These sheet metal walls could be much thinner than any casted wall could due to the minimum thickness requirements for most casting processes, posing further benefits to the weight reduction aspect. Additionally, based on the assumption that the hammer will truly be "used as a hammer" during competition, these sides walls will not be used for impact like the striking faces will, so strength is not as much of a concern. All things considered, it was determined that this approach would be used to give the outer walls, provided that the final selected head concept was one that did not intend to have the side walls cast as part of the design.

III. Handle Materials

Following the head structure concept generation was the generation process for the handle. Unlike the head of the hammer, which must be made at least partially of steel, the handle is not required to be made from any specific material, nor does it have to be cast. With the previous decision to dedicate the casting process primarily to the head structure, it was determined at the beginning of this process that the handle would be a non-cast element separate from the head. The group felt this would give more freedom to implement a wide variety of materials for the handle, as well as simplify its production if it does not have to be uniquely manufactured through casting. This decision also ties back to the original rationale for choosing the Marvel rendition as the design inspiration.

Without the limitation of being made from a castable material, the options for the handle were very broad. To generate a more manageable list of ideas for the handle materials, and one that would be more applicable than a list of any material we could think of, the group utilized several strategies. First, the group generated our own list of materials based on knowledge of typical hammers, experience using sledgehammers, and research into materials commonly used by hammer manufacturers. Using this information, some of the most important considerations for a handle material are that it is strong enough to withstand loading while also being light enough to not throw of the balance of the swing during use. The weight factor is especially relevant in this case, so those considerations influenced our lists. To validate these lists and ensure that mainly materials with appropriate strength to weight ratios were being considered, Granta EduPack was used. For this purpose, the Material Universe within level 1 of the software was used, as this includes more general categories of materials than the extremely specific materials that level 3 includes. Once the universe was selected, a graph was created comparing the material's yield strength vs. the material's density. Only the top 25% of materials that had the highest strength while weighing the least were considered. These results were the compared to the lists we generated, and the materials common to both our lists and the software results were kept. There were, however, some exceptions from our lists that were kept even though the software results did not include them, based on research the group did on commonly used materials for hammer handles. The main examples of this were hickory and fiberglass. The entire list of the hammer materials generated and considered can be seen below in the graph. Additional insight into our written process of generation can also be seen in Appendix D2.

Table 2: List of generated hammer handle materials

Ash	Hickory	Oak	Titanium	Polyethylene	PC/ABS
Steel	Aluminum	Brass	Beryllium	Polypropylene	Bone
ABS	PVC	PLA	Magnesium	PVT	Bamboo
Fiberglass	Carbon fiber	Pine	Kevlar	PET	

IV. Connection Method

Based on the choice for the handle to be a separate element from the head structure, the last category requiring concept generation was for connection methods. These would provide the means for fixing the handle to the head such that it is a complete and usable tool. The generation process for the hammer connection methods began by researching how various materials are attached together. Some connection methods are specific for metal-to-metal, wood-to-wood, and so on, therefore one consideration that needed to be made was the possibility that the hammer and handle be made of two non-similar materials. There had to be a variety of connection methods included that could work between various materials in the case that the hammer, made from steel, must be joined with a handle made of wood or some other non-metal product. Some of the methods were determined from analyzing the specific case of how handles on common hand tools are fastened, while others were generated based on common manufacturing practices. Strength of the connection is also something that the group kept in mind while formulating ideas. All the generated connection methods are listed in the table below and schematics of the generation process are listed in Appendix D3.

Table 3: List of generated handle-to-head affixion methods

Threaded, and glue	Glue	Weld	Hot Rivet
Press fit, and glue	Shrink fit	Lash	Threaded
Taper sleeve, wedge, and glue	Lock pin	Press fit	Epoxy
Solid connection to head	Key	Magnetic	

Concept Screening

After ideas were generated for each of the four categories, the next task was to pass all of the ideas through a concept screening. The goal of concept generation had essentially been to document any possible solutions the group could think of, so the group was left with a multitude of abstract ideas and unorthodox approaches to the design problem. However, the purpose of concept screening was to analyze this collection of initial generated concepts and narrow them down to a smaller more manageable group. It does so by measuring the potential of each concept to pinpoint those that are worth pursuing and eliminate those that are not. This is done using more simplistic criteria such as if the idea is feasible, if it is desirable, or if the group has the resources available to produce it. These criteria were developed for each category in order to produce a list of concepts that are most capable of meeting the design criteria. The following sections describe the screening methods for each particular category, as well as indicate the resulting concepts after screening.

I. Casting Method

For the casting method to be screened down, a few factors had to be taken into consideration. The two factors that were analyzed for each of the casting processes were the relative cost per casting and the part type intended to be made with each casting method. The relative cost index per unit was determined by logging onto the Granta EduPack software and investigating all the viable casting processes and their relative costs. The highest price limit was set around the 50th percentile range which produced a relative cost index of under $500. The reason this limit was chosen was to eliminate a lot of the high dollar processes since the group did not have an unlimited budget for the project. The other limit chosen was the type of parts each casting method was best suited for. For example, centrifugal casting is designed to be used when casting thin-walled cylinders. As a result, since the hammer was going to be of a low batch size and high complexity it was crucial to eliminate casting methods that would not work with the potential designs generated. Table # shows the process used for screening the casting method and table # lists the casting methods that passed concept screening.

Table 4: Concept Screening for the potential casting methods

	Relative cost index (per unit)(USD)- Less than $500	Part type	Rationale for failure	Spec relation
Centrifugal casting	400	Thin walled cylinder	Our cast component is too complex for this method	Spec 4A
Centrifugally-aided casting	150	Small intricate parts	Our cast component is too large for this method	Spec 4A
Ceramic mold casting	200	High complexity	We could not find a ceramic mold casting sponsor	Spec 2A
CLA/CLV casting	1000		The cost is above our desired cost	Spec 14
CO2/silicate casting	1000		The cost is above our desired cost	Spec 14
Cosworth casting	300	Non-ferrous products	Our casting must be of a steel alloy	Spec 2A
Evaporative pattern casting, automated	400	High complexity, automated	We do not have time to use an automated system	Spec 13
Evaporative pattern casting, manual	200	High complexity	Pass	
Ferro die casting	5000		The cost is above our desired cost	Spec 14
Gravity die casting	1000		The cost is above our desired cost	Spec 14
Green sand casting, automated	300	High complexity, automated	We do not have time to use an automated system	Soec 13
Green sand casting, manual	150	High complexity	Pass	
High pressure die casting	4000		The cost is above our desired cost	Spec 14
Investment casting, automated	800		The cost is above our desired cost	Spec 14
Investment casting, manual	300	High complexity	Pass	
Low pressure die casting	2000		The cost is above our desired cost	Spec 14
Plaster mold casting	250	Low melting temps	Our casting must be of a steel alloy	Spec 2A
Rammed graphite casting	200	greater than 176 lbs	Our part can only be 6 lbs	Spec 1 A
Replicast casting	800		The cost is above our desired cost	Spec 14
Rheocasting	800		The cost is above our desired cost	Spec 14
Semi-centrifugal casting	200	Simple axisymmetric shapes	Our part will be too complex for this method	Spec 4A
Shell casting	500		The cost is above our desired cost	Spec 14
Squeeze casting	2000		The cost is above our desired cost	Spec 14
Thixocasting	800		The cost is above our desired cost	Spec 14
Vacuum investment casting	1000		The cost is above our desired cost	Spec 14
3D Printed sand casting	400	High complexity	Pass	

Table 5: List of remaining casting methods after completed screening.

Design	Rationale for Failure
Evaporative pattern casting, manual	Pass
Green sand casting, manual	Pass
Investment casting, manual	Pass
3D Printed sand casting	Pass

II. Head Structure

After designs were generated for the head structure, there needed to be a method used in order to sort through and find the best hammer head designs. The head structure was screened using three criteria: weight requirements met at 85% of the scale, manufacturability, and single

cast component “utilize casting to fullest extent”. The weight requirement criteria was selected because it aligned with the constraint of the project and with SFSA’s competition rules. The group’s goal was to produce a hammer as close to the size of the hammer from the Marvel movies so as a result there had to be screening for designs with a large head size while still weighing under 6 lbs. The next category used to screen the head designs was the manufacturability of the head design. Since a lot of the final machining needed to be done by the group with limited resources, it was crucial to designate whether the design would be simple or complex to manufacture. The final criteria used was whether the casting process was used to the fullest extent”. The guidelines outline by SFSA stated that the casting process needed to be used in a creative manner to get a casting under the 6 lbs. As a result, each design was considered and discussed, because it was crucial that the casting process was displayed instead of taking a solid hammer head and machining it out. As long as the head design met the weight requirements at 85% scale of the movie prop, was simple to machine, and utilized the casting method to the fullest extent, the design was passed on. Below in table # shows how the head structures were screened down and table # shows the final screened head structures.

Table 6: Concept Screening table for potential head structure designs

	Weight Requirement met at 85% size scale	Manufacturability	Single cast component "utilize casting to fullest extent"	Rationale for failure	Spec relation
1	Yes	Simple	No	Is not near net final shape (Requires extensive post processing procedures)	Spec 13
2	Yes	Simple	Yes	Pass	
3	Yes	Complex	Yes	Not able to be manufactured within the project time frame/Rapid Geometry Changes (fluidity issues)	Spec 13
4	Yes	Simple	Yes	Pass	
5	Yes	Simple	No	Is not near net final shape (Requires extensive post processing procedures)	Spec 13
6	Yes	Complex	Yes	Not able to be manufactured within the project time frame/Rapid Geometry Changes (fluidity issues)	Spec 13
7	Yes	Complex	No	Is not near net final shape (Requires extensive post processing procedures)	Spec 13
8	Yes	Complex	Yes	Not able to be manufactured within the project time frame/Rapid Geometry Changes (fluidity issues)	Spec 13
9	Yes	Simple	Yes	Pass	
10	No	Simple	Yes	Due to minimal size, it will not meet the 85% of size requirement	Spec 1A/4A
11	No	Simple	Yes	Due to minimal size, it will not meet the 85% of size requirement	Spec 1A/4A
12	Yes	Complex	Yes	Not able to be manufactured within the project time frame/Rapid Geometry Changes (fluidity issues)	Spec 13
13	Yes	Complex	Yes	Not able to be manufactured within the project time frame/Rapid Geometry Changes (fluidity issues)	Spec 13
14	Yes	Complex	Yes	Not able to be manufactured within the project time frame/Rapid Geometry Changes (fluidity issues)	Spec 13
15	Yes	Complex	No	Is not near net final shape (Requires extensive post processing procedures)	Spec 13
16	Yes	Simple	Yes	Pass	
17	Yes	Complex	No	Is not near net final shape (Requires extensive post processing procedures)	Spec 13
18	Yes	Complex	No	Is not near net final shape (Requires extensive post processing procedures)	Spec 13
19	yes	Complex	Yes	Not able to be manufactured within the project time frame/Rapid Geometry Changes (fluidity issues)	Spec 13

Table 7: List of remaining head structures after completed screening

	Design	Rationale for Failure
2	The Fabricator	Pass
4	Hedgehog	Pass
9	Big bar	Pass
16	Bartholomew	Pass

III. Handle Materials

For the handle materials, the main screening criteria pertained to the strength the material offered as well ats its density. These were selected because they directly correlated to the needs outlined in our design specifications and to one of the main limitations outlined by the competition. It was important to progress only those materials that offered enough strength to withstand use but also a reasonable weight such to not exceed the 6 lb limit. In order to screen the material concepts in terms of strength, the specific criteria used stated that the handle material must have a yield strength of 6.5 ksi or higher. The method for determining this criterion was based on several design specifications. Using the ergonomic range of handle

diameters (1.125 in to 1.25 in) outlined in Specification 12A, the range of cross-sectional areas for the handle was calculated. These areas were then used to estimate the approximate range of stresses the handle must withstand based on expected competition load value of 6500 lbs, as stress is a force applied over an area. This resulted in the value of 6.5 ksi, limited based on the smallest area in the range. Because the handle could not fail under the load of the competition testing, the yield strength of the chosen material must meet or exceed this value. The second criteria for screening the concepts was having a density below .058 lb/in^3. Several tactics went into determining this criterion as well. First, a rough amount of weight was allotted to each of the major components of the hammer: 4 lbs for the head, 0.75 lbs for the handle, 0.25 lbs for connection, and 1 lb for aesthetics. Then, utilizing the average range of handle diameters again, as well as the length of the handle based on an 85% scale of the original, an approximate range of volumes were calculated for the handle. Finally, using the rough weight allotment of 0.75 lbs for the handle, density values were calculated. It was determined that in order to meet the amount of weight designated for use by the handle at the volume estimated, the material density must be below .058 lb/in^3. The table below indicates the material that passed or failed these criteria and is followed by the complete list of screened concepts.

Table 8: Concept Screening table for potential handle materials

	Yield strength of 6.5 ksi or greater	Densities below .058 (lb/in^3)	Rationale for failure	Spec relation
Ash	7.5	0.024	Weaker than hickory with same approximate density	N/A
Steel	42	0.283	Density is too high	Spec 1A/12A
ABS	4	0.038	Yield strength is too low	Spec 8
Fiberglass	100	0.072	Density is too high	Spec 1A/12A
Hickory	8.5	0.025	Pass	
Aluminum	19	0.098	Density is too high	Spec 1A/12A
PVC	6.5	0.049	Pass	
Carbon fiber	560	0.066	Density is too high	Spec 1A/12A
Oak	7	0.034	Weaker than hickory with higher density	N/A
Brass	40	0.299	Density is too high	Spec 1A/12A
PLA	5	0.045	Yield strength is too low	Spec 8
Pine	5	0.019	Yield strength is too low	Spec 8
Titanium	45	0.163	Density is too high	Spec 1A/12A
Beryllium	37	0.067	Density is too high	Spec 1A/12A
Magnesium	21	0.066	Density is too high	Spec 1A/12A
Kevlar	350	0.052	Kevlar is too flexible	N/A
Polyethylene	3.2	0.035	Yield strength is too low	Spec 8
Polypropylene	4.1	0.038	Yield strength is too low	Spec 8
PBT	15	0.059	Density is too high	Spec 1A/12A
PET	7.5	0.050	Pass	
PC/ABS	8.2	0.043	Pass	
Bone	9	0.024	Bone is unfeasible to use	N/A
Bamboo	5.5	0.026	Yield strength is too low	Spec 8

Table 9: List of remaining handle materials after completed screening

Design	Rationale for Failure
Hickory	Pass
PVC	Pass
PET	Pass
PC/ABS	Pass
Fiberglass	Pass

IV. Connection Method

The connection method was screened based on the criteria of common hammer affixion method and useable for multiple types of materials. In essence the criteria was chosen because there was no sense trying to reinvent the wheel. For example, hammer affixion methods have been around for over 100 years and have worked reliably. As a result, the group wanted a connection method that was commonly used on hammers for strength and reliability and also usable on multiple types of materials since a final head structure had not been determined yet.

Table 10: Concept Screening table for potential connection methods

	Common hammer affixion method	Usable for multiple types of materials	Rationale for failure	Spec relation
Hot Rivet	No	No	can only be conducted on metals (weight)	Spec 7
Threaded	Yes	Yes	Inferior to threaded and glue	Spec 7
Taper sleeve, wedge, and glue	Yes	Yes	Pass	
Weld	Yes	No	Must be used w/ steel alloy (weight)	Spec 1A
Glue	No	Yes	Relies solely on glue shear strength	Spec 7
Shrink fit	No	No	Relies on Friction as main mode of connection	Spec 7
Lock pin	No	Yes	Stress concentrator	Spec 7
Key	No	Yes	Stress concentrator	Spec 7
Solid connection to head	Yes	No	Must be used w/ steel alloy (weight)	Spec 1A
Lash	No	Yes	Unreasonable	Spec 7
Press fit	No	Yes	Relies on Friction as main mode of connection	Spec 7
Magnetic	No	No	Unreasonable/requires very limited handle material	Spec 1A/7
Threaded, and glue	Yes	Yes	Pass	
Press fit, and glue	No	Yes	Reliance on friction and glue shear strength	Spec 7
Epoxy	Yes	Yes	Pass	

Table 11: List of remaining connection methods after completed screening

Design	Rationale for Failure
Taper sleeve, wedge, and glue	Pass
Threaded, and glue	Pass
Epoxy	Pass

Initial Inventor Models of Screened Head Structures

In order to make the prototypes CAD models had to first be drafted using Autodesk inventor. In order to eliminate variability between the models each one was created in the same way with one variable (the internal structure) changed between each model. The models began by creating one square face of ¼ inch thickness to serve as the hammer face. A sweep command was then conducted to place the angled flanges along the perimeter of the square face section. That file was then input into an assembly where it was mirrored and set opposite another face at the distance associated with the agreed upon scale. That assembly was then derived to form solid files where the aforementioned internal structures could be extruded from inside face to inside face, spanning the gap and making the solid hammer file. With that the models were adjusted iteratively to fall within the same relative weight to be used as a direct strength to weight comparison later. The models would then be sent off to have finite element analysis conducted on them, along with being 3D printed.

3D Printed Prototypes

With the head structure design concepts narrowed down to the final four that passed through concept screening, the group felt it would be valuable to generate a prototype for each concept as part of the selection process. Prototyping allowed the group to better visualize the designs still in consideration by giving them tangibility and to gain insight into the potential flaws or advantages of each. In terms of the method used to generate the prototypes, the group selected FDM 3D printing. There were several reasons for this selection, the first being that each of the four members of this team had their own printer and filament at their disposal. With such immediate access to these resources and technology, this was the most practical because it would not require the group to obtain any additional materials. This also made it possible for each member to individually produce one of the four designs. The second reason this method was chosen is that 3D printing was the most accurate way to reproduce the digital models that were already created in Inventor. The software integrated with 3D printers is designed to be compatible with CAD and inventor models. It works by slicing the 3D models into layers and translating them into instructions that the printer can follow, which then deposits filament layer by layer until the model is complete. This allowed us to produce 100% scale models that replicated each of the four digital head structure designs down to the exact dimension, including all of the relevant design details. Lastly, it was our idea that how the printer would produce each design, by building layers of the melted filament, would loosely simulate how the molten metal would fill up a mold in casting. Any particular difficulty encountered with printing certain elements of each design could translate to issues that may be encountered when attempting to cast the design. If aspects of the geometries could not be printed successfully, they would likely prove difficult to cast as well. This proves especially relevant considering that the molds eventually used for casting, which would be nearly direct negatives of the Inventor model of the selected design, would also be 3D sand printed.

For production, the prototypes were printed based on the initial inventor models previously described, including all of the key internal and external design details such as the angled flanges extending from the square faces and filets to eliminate the sharp corners. The only adjustments involved splitting the models into separate components, such that the faces and internal structures were individual parts, and adding in connection methods. This was done based on geometry limitations for 3D printing, as the overhangs and bridges each model had as a single component made them impossible to print. Prototypes were printed to 100% scale of the dimensions provided by each of these models. While each of the four prototypes had a varying internal structure, several dimensions were kept consistent across all prototypes as they were across all of the inventor models, including a face thickness of 0.25 inches, a facial area of 10.19 square inches, and a face-to-face length of 6.8 inches. As discussed, it was determined that for three out of the four head structures, the casted portion would consist of the faces connected by the varying cross-beam and the overall appearance would be achieved with a shell of sheet metal. Because the purpose of the prototypes was to examine the differences between the designs, which existed only in each of their internal structures, the external shells were not printed for three of the four designs. The exclusion was the “Fabricator”, as the whole concept of this design included casting the head as a hollow block with the side walls as well as the striking faces. As each team member was responsible for printing a select head structure, the printing conditions varied across the prototypes in terms of the specific printer, the printing software, the filament,

and the printing parameters. Shown below is a table summarizing the various settings used for each prototype. The sample screen shot below shows the print preview one of the models, Big Bar, as an STL file loaded into the Cura software. Following this screenshot are the pictures of the completed prototypes for each head structure.

Table 12: Summary of Printing Conditions for the four head structure prototypes

Summary of Settings for 3D Printed Prototypes				
	The Fabricator	**The Hedgehog**	**The Bartholemew**	**Big Bar**
Printer Model	Bibo	ANET A6	Creality Ender 3V2	Creality Ender 3
Software	Prusa	Cura	Cura	Cura
Filament	PLA	PLA	PLA	PLA
Nozzle Temperature °F	220	210	210	205
Bed Temperature °F	60	70	70	70
Infill Pattern	Cubic Subdivision	Cubic Subdivision	Cubic Subdivision	Grid
Infill Percentage	15	10	20	15

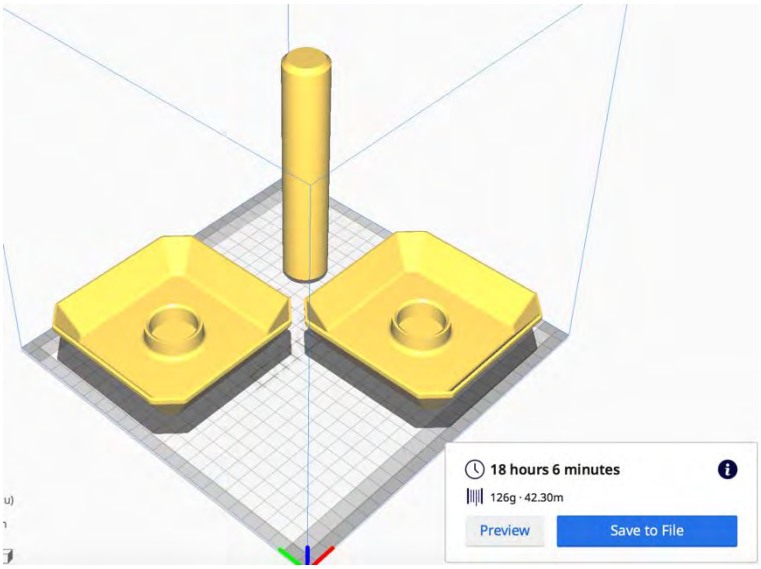

Figure 1: Cura screenshot of Big Bar

Figure 2: Finished prototypes of the Fabricator and the Hedgehog

Figure 3: Finished prototypes of Bartholemew and Big Bar

Concept Selection

To complete the process of determining the best overall design, a final concept selection was conducted for each category. This involved taking the concepts for each that passed through the screening phase and evaluating them with a weighted decision matrix. These matrices contain certain criteria developed based on the established engineering specifications and were specific to each of the four main categories of concepts. The criteria are given a weight percentage based on their priority from the constraints and their perceived importance to the overall design. The group then rated how well each concept met the criteria on a scale of 1 to 5. Finally, the overall score was totaled for each concept by multiplying the rating in each criterion by the weight of said criterion and taking the sum of these products. Evaluating the remaining concepts in this way provided a clear comparison of one concept against another in terms of their capability to meet the design needs. The idea is that concept which received the highest score is the most suitable option.

The sections below further detail the selection process carried out for each of the four main components of the hammer. Each section gives the rationale behind the specific criteria selected, as well as lists the explanations behind each rating. The highest scoring concept was the one selected for each category, provided that the group's instincts agreed that this was the best choice.

I. Casting Method

The method methods were narrowed down to three companies after the concept screening. The group was between either using investment cast or sand casting due to the complex geometries and small production size. Ultimately, sand casting was chosen over investment casting because the group's industry partner was PRL Regal Cast. Although the group had the choice of either doing green sand casting or 3D printed sand casting, the group chose 3D printed sand casting due to the short lead time on mold production and the ability to produce complex geometries for a reasonable cost per part.

Table 13: Criteria and final selection for the connection methods

Industry Contacts	Avalible casting methods	Rationale for failure
Consolidated Precision Products (CPP)	Investment casting, evaporative casting	Only can remelt the steel alloy
Tech Cast	Investment casting, evaporative casting	Only can remelt the steel alloy
PRL Industries	Green sand casting, 3D printed sand casting	Pass

Industry Contact	Casting methods	Rationale for failure
PRL Industries	Green sand casting	Patterns take upwards of 2 months to produce
PRL Industries	3D printed sand casting	Pass

Final Industry Contact	Final Casting methods
PRL Industries	3D printed sand casting

II. Head Structure

At this stage, the last four head structures remained from which to select a final design: The Fabricator, Hedgehog, Big-Bar, and Bartholomew. Though the screening phase passed these four through as designs capable of complying with key specifications, this was a simple pass-fail type of evaluation. It was important to do a more in-depth examination of where each one fell in terms of fulfilling the most relevant design needs. This was particularly true for the head seeing as the overall function of the hammer depends most on this element.

The first criterion the group designated for use in the matrix was Production Feasibility. Aside from casting, nearly all post-processing and finishing operations would be self-performed by the members of the team. As a result, it was important that the design of the head structure be possible for us to post-process ourselves, as well as possible to do with the equipment we had at our disposal. Certain geometries would require very specialized tooling to shape or remove material from and others would require a large amount of material to be removed to get from the minimum required casting dimensions down to the dimensions at which the hammer meets the weight. This would present problems for us completing the operations ourselves given the limited capability of our equipment and the general difficulty of machining this material. Therefore, the ideal selected design would require minimal machining or fixturing in order to reach the conditions needed for competition. The scale for Production Feasibility was established based on this fact, where the highest rating corresponds to the ideal case and the lowest rating corresponds to heavy machining and heavy fixturing.

For the additional criterion for concept selection, the group wanted to directly implement load analysis. Relating back to the fact that the head structure is the most critical component of the hammer, and the one which will be bearing much of the loading during competition, many of our design specifications related to its durability. In order to meet these specifications, the chosen head design had to have the strength and toughness to maintain its structural integrity upon undergoing the anticipated competition testing. Using an FEA analysis, each design could be loaded with the expected force value (6500 lb) based on the design specifications. The second and third criterion were then based directly on the results generated from the software simulations for the Max Von-Mises Stress and the Max Relative Deformation. The quantities of both stress and deformation that each design experienced under the load indicate the level of strength and toughness each offers. Low values of both stress and deformation indicate that the head is not under enough stress to yield and is capable of absorbing a high amount of energy before incurring any permanent damage. This is essential for withstanding impact. The ratings for both Max Stress and Max Deformation were broken up with this idea in mind, where the lowest stress and deformation corresponded to the highest rating and vice versa. Each rating gave a range of stress values or deformation values, and if the head structure's specific FEA result fell within that range, it was given that rating. Using actual stress and deformation values as the bounds for rating each head structure made these criteria less subjective.

The succeeding section gives a detailed description of the process used for running the FEA analysis, including the boundary conditions, supports, and method of solving. Following this description and several FEA diagrams are the tables depicting the criteria breakdown and the decision matrix for the four head designs. Upon rating and scoring each head according to the weights of the criteria, the Hedgehog obtained the highest overall score. The group determined that this was a valid conclusion, and the Hedgehog was selected as the final head design to move forward with in production.

Preliminary FEA

For the analysis conducted on ANSYS workbench, simplified models of all four of the head structures were used. The final model of any of the selected four designs would include external details such as angled flanges extending from the faces and angles cut into the corners, however, any benefit this adds to the structure of the hammer would not be unique to any one design in particular. Therefore, the main purpose of conducting the FEA analysis as part of the concept selection was to specifically examine the effect that the varied internal structure had on the strength of the hammer overall. As such, the models were simplified from the original inventor models discussed previously to include only the main square faces and the internal geometries that connected them: the single round rod, the x-beam, the five square rods, and the four side walls. The faces were kept at the 3.2-inch by 3.2-inch area and 0.25-inch thickness of the initial model and the internal geometry of each was made such that each overall design was approximately the same weight of 3.2lbs. This process was done iteratively.

The models were then saved as Parasolid files and imported as the geometry files in ANSYS Workbench. Based off recommendations from Professional Engineer Jill Johnson and teachings in Penn State Behrend's ME 467, the analysis mode that was selected was static structural. Due to the mesh limitations of the student license of workbench and to save computational resources, each of the models were edited in Space-Claim prior to analysis to one quarter their original size. This was done because each of the four head designs were doubly-symmetric, and symmetry allows the mesh to be refined at areas of interest, while reducing run time. Sharp corner transitions had a fillet of 1mm radius applied to them in order to limit/eliminate singularities in the model and subsequent mesh study divergence. With the model simplified, frictionless boundary conditions were applied to the split faces to allow the model to be solved with symmetry. Mesh revisions were applied at the aforementioned fillet locations to aid in the model accuracy and to allow for proper convergence of the mesh results to be conducted. A fixed support was applied to one of the two hammer faces, and a load of 6,500lbs (see Case Study) applied to the remaining other face. Plots for Equivalent (Von-Mises) Stress, Total deformation, and Structural error were then added to the solution outputs, with figures scoped to properly show their information. Feedback from committee members, also lead to the background of said plots being changed from the default, to a solid white "Presentation" style. With the data collected mesh convergence studies could be conducted iteratively until stress converged to within 5% and deformation to within 1%. Once that had occurred the models were seen to be accurate and were then used in conjunction with the selection matrix. In order to demonstrate the procedures followed, shown below are sample diagrams for the conditions implemented in FEA, the results generated by the loading, and the mesh convergence table to justify model accuracy. This is shown for one of the head structures, The Fabricator, while the remainder are shown in the appendix. However, the following table gives a summary of the stress and deformation results gathered from these diagrams for all four, which were the basis of the selection criteria.

Figure 4: Simplified Fabricator Inventor model

Boundary Conditions:

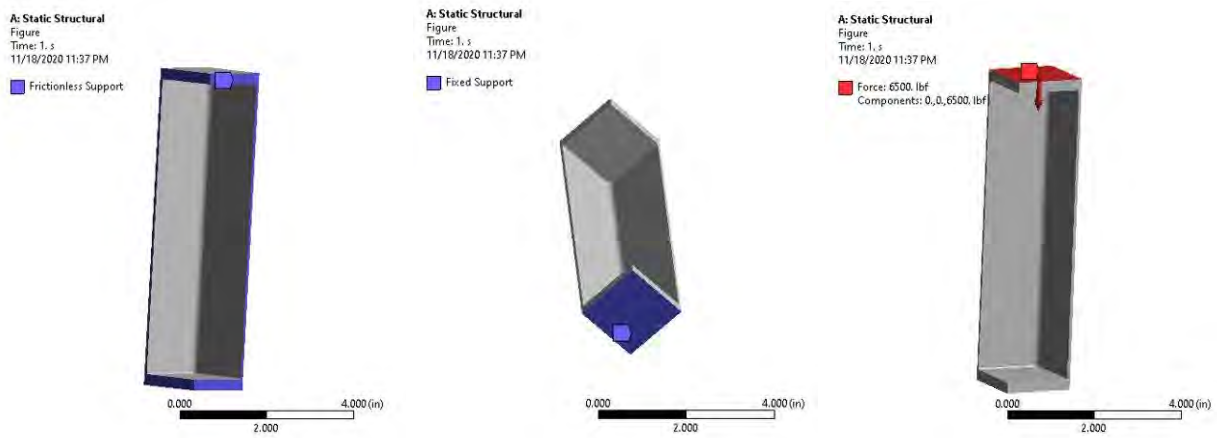

Figure 5: FEA Boundary Conditions, including frictionless support on cut edges, fixed support the bottom face, and a 6500 lbf load distributed on the face respectively.

Results:

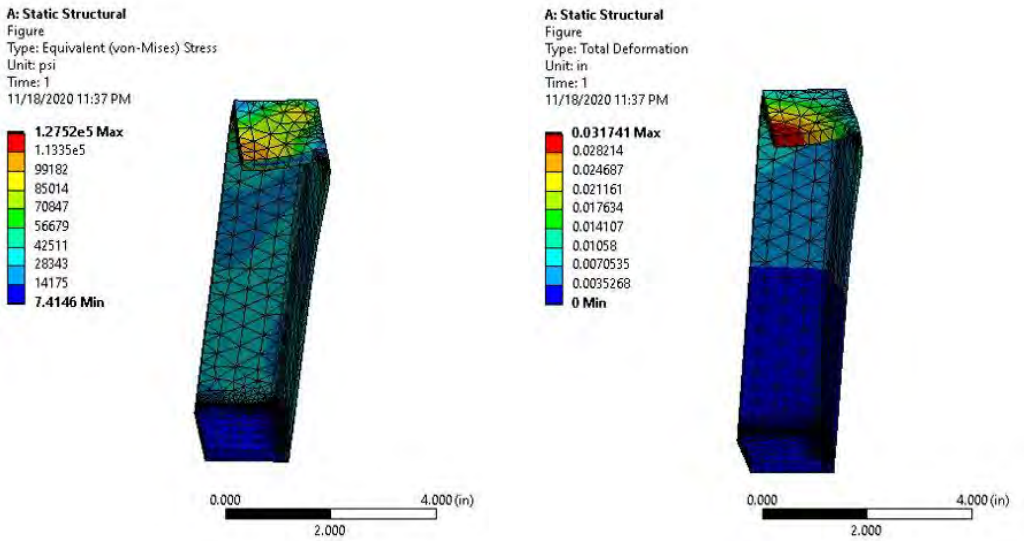

Figure 6: FEA results, including Equivalent Von-Mises Stress and Total Relative Deformation

Table 14: Mesh Convergence table for the Fabricator

	# of Nodes	# of Elements	Total Deformation (in)	Equivalent Stress (psi)	% error (def)	% error (stress)
Bad Mesh						
Default Mesh	1230	6899	0.030695	122380	100.00%	100.00%
	17924	10409	0.030789	145550	0.31%	15.92%
	22553	13737	0.030911	124180	0.39%	17.21%
	25165	14820	0.031059	128610	0.48%	3.44%

Table 15: Summary of FEA results for Max Von-Mises Stress and Max Total Deformation for all four head designs

FEA Results				
	The Fabricator	**The Hedgehog**	**The Bartholemew**	**Big Bar**
Max Von-Mises Stress (ksi)	127.5	90.2	235	529.6
Max Total Deformation (in)	0.0317	0.0116	0.0101	0.0558

Table 16: Criteria and corresponding rating breakdown for the head structures

Head structure			
	FEA Max von-mises stress	FEA Max relative deformation	Production feasibility
5	Has a max von-mises value below 100 ksi	Has a max relative deformation below .010 in	Minimal machining, minimal fixturing
4	Has a max von-mises value between 101 and 200 ksi	Has a max relative deformation between .0101- .020 in	Minimal machining, moderate fixturing
3	Has a max von-mises value between 201 and 300 ksi	Has a max relative deformation between .0201- .030 in	Heavy machining, minimal fixturing
2	Has a max von-mises value between 301 and 400 ksi	Has a max relative deformation between .0301- .040 in	Minimal machining, heavy fixturing
1	Has a max von-mises value above 400 ksi	Has a max relative deformation above .040 in	Heavy machining, Heavy fixturing

Table 17: Weighted decision matrix for the head structures

Material		The Fabricator (2)		Hedgehog (4)		Big bar (9)		Bartholomew (16)	
	Weight	Rating	Score	Rating	Score	Rating	Score	Rating	Score
Von-mises stress	40%	4	1.6	5	2	1	0.4	3	1.2
Relative deformation	30%	2	0.6	4	1.2	1	0.3	5	1.5
Production feasibility	30%	3	0.9	4	1.2	2	0.6	5	1.5
Total		3.1		4.4		1.3		4.2	
Rank		3		1		4		2	

Table 18: Ranking and final selection for head structures

Head structure design	Rank	Rationale for failure
The Fabricator (2)	3	The other head structures are better suited for this task
Hedgehog (4)	1	Pass
Big bar (9)	4	The other head structures are better suited for this task
Bartholomew (16)	2	Pass

Final Head structure design
Hedgehog (4)

III. Handle Materials

The handle material was selected and ranked based on its strength, density, manufacturability, stiffness, and accessibility. Each factor was based on a specific specification or standard that was used to rank each material based on the material's ability to meet the selected criteria. The five screened materials were placed into the weighted matrix and scored based on how they met certain criteria. Based on the scores Hickory, PC/ABS, and Fiberglass were all selected since they scored the three highest and because hammer handles are commonly made out of each of the materials.

Table 19: Criteria and corresponding rating breakdown for the handle materials

Handle Material					
	Strength	Density	Manufacturability	Stiffness	Accessibility
5	Has a yield strength value above 10 ksi	Has a density value below .02 lb/in^3	Can be modified by students on campus	Stiffness below 1*10^6	Off the shelf
4	Has a yield strength value of 9.1-10 ksi	Has a density value of .021-.03 lb/in^3	Can be modified by students off campus	Stiffness of 1*10^6-2*10^6	Catalog order
3	Has a yield strength value of 8.1-9 ksi	Has a density value of .031-.04 lb/in^3	Can be modified with partial outsourcing	Stiffness of 2.1*10^6-3*10^6	Special order
2	Has a yield strength value of 7.1-8 ksi	Has a density value of .041-.05 lb/in^3	Can be modified with complete outsourcing	Stiffness of 3.1*10^6-4*10^6	Completely custom made
1	Has a yield strength value below 7 ksi	Has a density value above .05 lb/in^3	Can not be modified	Stiffness above 4*10^6	Unfeasible

Table 20: Weighted decision matrix for the handle materials

Material		Hickory		PVC		PET		PC/ABS		Fiberglass	
	Weight	Rating	Score	Rating	Score	Rating	Score	Rating	Score	Rating	Score
Strength	25%	3	0.75	1	0.25	2	0.5	3	0.75	5	1.25
Density	30%	4	1.2	2	0.6	2	0.6	2	0.6	1	0.3
Manufacturability	25%	5	1.25	4	1	3	0.75	3	0.75	3	0.75
Usability	10%	3	0.3	5	0.5	5	0.5	5	0.5	1	0.1
Accessibility	10%	5	0.5	3	0.3	3	0.3	3	0.3	4	0.4
Total		4.0		2.7		2.65		2.9		2.8	
Rank		1		5		4		2		3	

Table 21: Ranking and final selection for the handle materials

Material	Rank	Rationale for failure
Hickory	1	Pass
PVC	5	The other materials are better suited for this task
PET	4	The other materials are better suited for this task
PC/ABS	2	Pass
Fiberglass	3	Pass

Final Material
Hickory

IV. Connection Method

The connection method was scored based on the manufacturability, resistance to failure, and estimated completion time. The group was looking for a connection method that would not only work with the head design chosen but also be easy to manufacture. Since the hammer was going to be used in competition, it was crucial that one the connection method was able to be manufactured and two that the connection had more than one failure method. Estimated completion time was also included to help ensure find a connection method that was strong but quick to do since there was such a short timeframe to complete the hammers. As a result, the epoxy along with the tapered sleeve, wedge, and glue connection methods were all considered. Ultimately, the tapered sleeve wedge, and glue were chosen due to the multiple failure methods and easy manufacturability. The selection process can be seen below in table #.

Table 22: Criteria and corresponding rating breakdown for the connection methods

Connection Method			
	Manufacturability	Resistance to failure	Estimated completion time
5	No additional tools required	Five or more components must fail to disconnect handle	One day or less
4	Non-powered hand tools required	Four components must fail to disconnect handle	Two days
3	Powered hand tools required	Three components must fail to disconnect handle	Three days
2	Machinery required	Two components must fail to disconnect handle	Four days
1	Outsourcing required	One component must fail to disconnect handle	Five or more days

Table 23: Weighted decision matrix for the connection methods

Connection		Taper sleeve, wedge, and glue		Threaded, and glue		Epoxy	
	Weight	Rating	Score	Rating	Score	Rating	Score
Manufacturability	40%	4	1.6	2	0.8	5	2
Resistance to failure	30%	3	0.9	2	0.6	1	0.3
Estimated completion time	30%	4	1.2	1	0.3	2	0.6
Total		3.7		1.7		2.9	
Rank		1		3		2	

Table 24: Ranking and final selection for the connection methods

Connection Type	Rank	Rationale for failure
Taper sleeve, wedge, and glue	1	Pass
Threaded, and glue	3	The other connection designs are better suited for this task
Epoxy	2	Pass

Final Connection Type
Taper sleeve, wedge, and glue

Combination Decision Matrix: Final Design

Once each of the designs were screened, it was time to make a final decision matrix to determine the final design combination. Each design aspect of the hammer that passed concept screening was placed into the design matrix and rated based on the specified criterial. After each design combination was determined and rated the total scores for each design were added together. Based on Table #, the two designs that rated the highest were the hedgehog and the Bartholomew with both having a Hickory handle and a Taper sleeve, wedge, and glue connection method. Even though the two designs rated very close to one another the decision was made to use the hedgehog design since it would be easier to connect a handle to and would be able to withstand more force prior to yielding. The decision matrix allowed every option that passed screening to be selected and rated to ensure the best design combination was chosen. Table # shows the final ranking of the two final designs and the rationale for why the final design was ultimately chosen.

Table 25: Decision matrix for the combination of the top-rated concepts in each of the four main categories

Handle material	Handle material concept selection score	Connection Design	Connection design concept selection score	Head structure	Head structure concept selection score	Sum	Rank
Hickory	4	Taper sleeve, wedge, and glue	3.7	Hedgehog (4)	4.4	12.1	1
Hickory	4	Taper sleeve, wedge, and glue	3.7	Bartholomew (16)	4.2	11.9	2
Hickory	4	Epoxy	2.9	Hedgehog (4)	4.4	11.3	3
Hickory	4	Epoxy	2.9	Bartholomew (16)	4.2	11.1	5
PC/ABS	2.9	Taper sleeve, wedge, and glue	3.7	Hedgehog (4)	4.4	11	4
PC/ABS	2.9	Taper sleeve, wedge, and glue	3.7	Bartholomew (16)	4.2	10.8	7
PC/ABS	2.9	Epoxy	2.9	Hedgehog (4)	4.4	10.2	9
PC/ABS	2.9	Epoxy	2.9	Bartholomew (16)	4.2	10	11
Fiberglass	2.8	Taper sleeve, wedge, and glue	3.7	Hedgehog (4)	4.4	10.9	6
Fiberglass	2.8	Taper sleeve, wedge, and glue	3.7	Bartholomew (16)	4.2	10.7	8
Fiberglass	2.8	Epoxy	2.9	Hedgehog (4)	4.4	10.1	10
Fiberglass	2.8	Epoxy	2.9	Bartholomew (16)	4.2	9.9	12

Table 26: Ranking and final selection for the combined head, handle, and connection

Handle material	Connection Design	Head structure	Rationale for Failure
Hickory	Ts, w, g	Hedgehog (4)	Pass
Hickory	Ts, w, g	Bartholomew (16)	More difficult to connect to the selected connection design, can withstand less force before yielding

Final Combination		
Handle material	Connection Design	Head structure
Hickory	Ts, w, g	Hedgehog (4)

CAD Model of Final Design and General Assembly

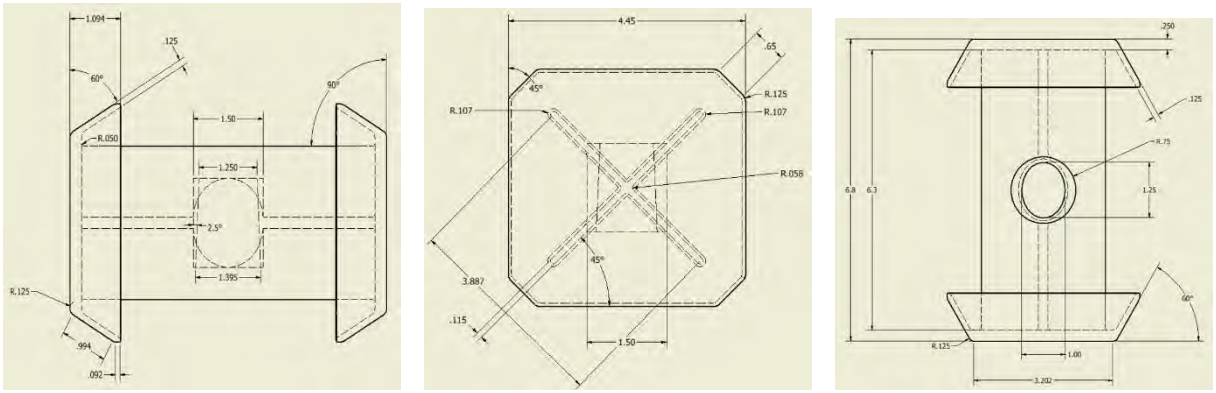

Figure 7: Engineering drawings for final hammer head design

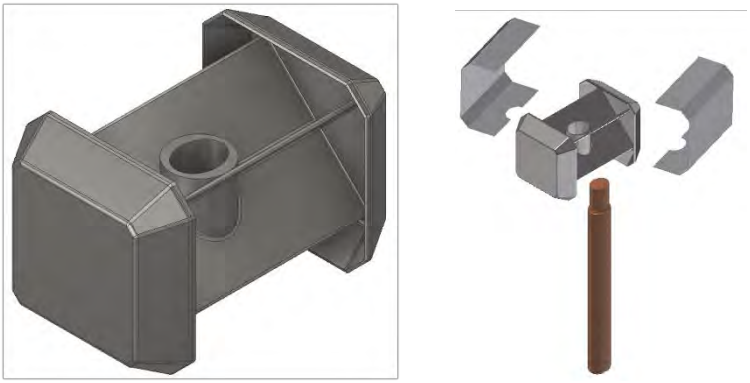

Figure 8: Diagram of the assembly for the final head design

FEA Analysis of Final Design

For the final FEA analysis conducted on the hammer, the same relative steps were taken in conducting the analysis as listed in the Preliminary FEA, with a select few differences. The hammer was modeled as one half of its original size to allow for finer mesh configurations and to abide by the node limits built in to the academic licenses available to the students. Modeling the hammer with symmetry will solve for the stresses and displacements seen by a full hammer and is as accurate a representation. All boundary conditions are set in the same manor to provide loading conditions expected to be seen in use. The inside of the hammer eye was constrained via a 0-displacement condition to account for the additional support placed by the wood being located in it during use (the wood would have to crush for the steel to move). The other difference in test were the scoping of different load scenarios across the face to project what would happen if the load were applied to an arbitrarily small area (perceived as worst case). A final “what if” load time step was added to indicate what load the hemmer could withstand without failure if the entire face were impacted.

I. Boundary Conditions

- Frictionless support on cut edges
- Fixed support on bottom face
- Displacement= 0 in hammer eye

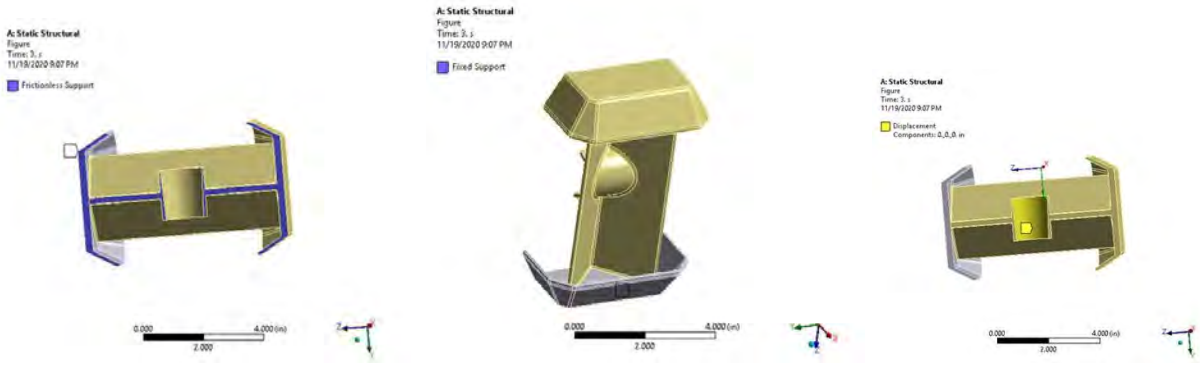

II. Time Stepped Loading conditions

- Max Full face blow to cause material Yielding of (190ksi)- 22,600 lbf t=1s.
- 6,500 lbf applied over a 1mm area t=2s,3s,and 4s

III. Results

Equivalent (von-Mises) Stress
Max: 189.3 ksi

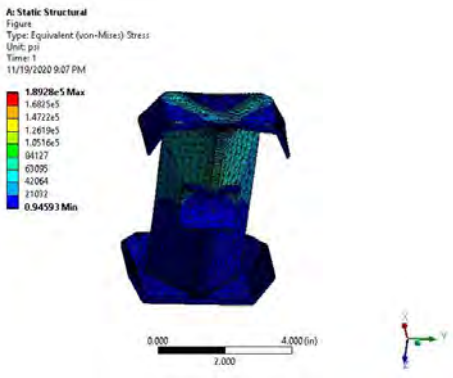

Total Relative Deformation
Max: 0.0087 in

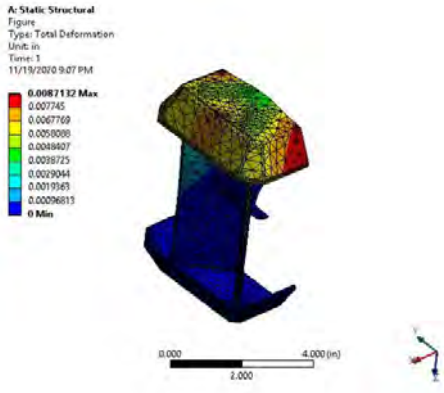

Mesh Convergence Table

# of Nodes	# of Elements	Total Deformation (in)	Equivalent Stress (psi)	% error (def)	% error (stress)
33248	19451	0.0087055	187150	100.00%	100.00%
41186	24393	0.0087132	189280	0.09%	1.13%

Total Deformation

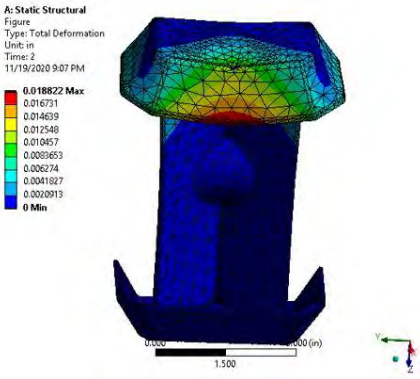

Max Deformation: 0.0188 in

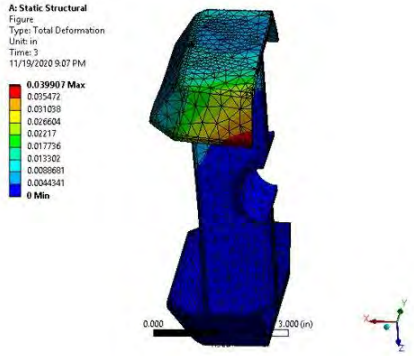

Max Deformation: 0.0391 in

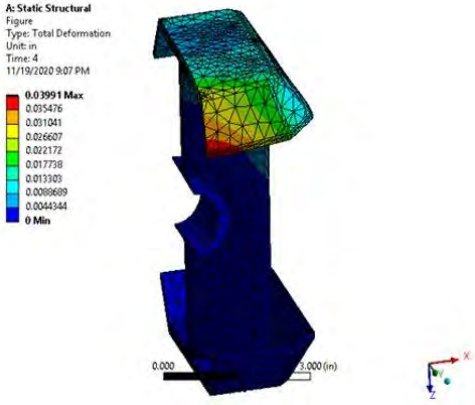

Max Deformation: 0.0399 in

Mold Design

Since the design was pushing the theoretical limits of the sand-casting process, the group decided to design three different size hammers to ensure that the group would receive one completely filled hammer that could be sent into competition. Each size designation states the thickness of every feature of the hammer. The ¼" sized hammer was chosen as the smallest thickness based on recommendations from PRL's Process/Foundry Engineer, Laura Karduck. She was concerned that any smaller of a wall thickness may cause the metal to sinch off and not fill the rest of the mold. Since, the group only had one shot to pour a usable hammer the group also decided to design molds for a 3/8" thick hammer and a 5/8" thick hammer. Although the larger hammers would be way over the weight requirement and would require extensive machining work, the group wanted to have a fail-safe in case the ¼" molds would not fill.

Based on the idea that three different hammer sizes were created, three different molds had to be created for their respective hammer size. To achieve the geometries required a three-part mold was selected. The mold would be split into 3 parts: a cope and a drag to encompass the two hammer faces and a cheek that could house a core box to obtain the x-bar structure. The reason for the 3-part mold with insertable cores is so that the internals of the mold could be coated with Isomol to prevent the hot metal from eroding away the sand. Since the mold were being 3D sand printed, it allowed for a complex mold design to be created since the ExOne 3D sand printers could print with such tight tolerances. Dome shaped connection pins were placed on the cope and the drag to fit into the recessed holes in the cheek. The pins were created to ensure that the cope, the cheek, and the drag fit together and lined up to allow for proper flow with a hole tolerance of 1/32". The molds were also designed in the shape of a rectangular prism to allow for them to be banded down to prevent the mold parts from expanding due to high pressures experienced during the pouring process. Each mold was designed with approximately 3" wall thickness from the casting to the exterior to provide ample mold strength to prevent the likelihood of wall failure. For the internal structural of the mold, each core generates ¼ of the internal x-bar structure. Each core was made with dimensions greater than 1/16" to prevent breakage along with 1/8" fillets were used to provide good material flow. Slots were created in the cheek with a 3-degree taper to provide a snug fit for the core while still providing an accurate alignment. A 1/64" gap was given to each of the cores to allow for a clearance fit within each of the four cores.

The next step in the mold design was coming up with the gating and riser system. Due to the thin wall sizes and complex geometries, it was crucial to get the metal into the mold as quickly as possible. As a result, the group decided to implement a Kalpur instead of a traditional gating and rising system. The Kalpur was beneficial because not only did it act as a riser and a sprue, but it also filtered out the contaminates and slowed down the initial pour velocity. Since difference size hammers were being casted two different size Kalpurs had to be used. For the ¼" and 3/8" size hammer molds a 3" x 6" Kalpur was able to be used where for the ¾" size hammer mold required the 4" x 6" Kalpur since it required a larger riser volume. The final step of the mold design was placing the venting system. The venting system is required to prevent the off gases from getting trapped in the mold and as a result 12 vents were placed around the top and bottom flanges of the hammer. Two vents were placed equally apart on each of the top and bottom flange faces. The bottom vents were then connected into the top vents to allow for a streamlined venting system and so it would allow for gases to be released instead of creating inclusion throughout the casting. It was very important to provide plenty of venting since 3D

sand printing using silica sand and furan binder acts similar to a ceramic mold as compared to a green sand mold.

The figures below show a complete overview of the final mold design components. These include the various sizes of kalpurs and filters corresponding to the various model sizes, the three main mold parts with all relevant details for venting and assembly, and the cores with details for assembly.

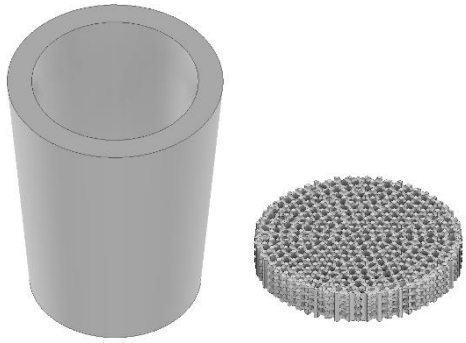

Figure 9: 3x6 inch Kalpur and 3x.5 inch filter used for casting the 1/4-inch and 3/8-inch models

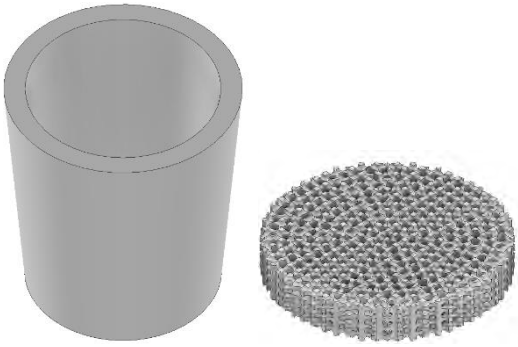

Figure 10: 4x6 inch Kalpur and 4x.5 inch filter used for casting the 5/8-inch models

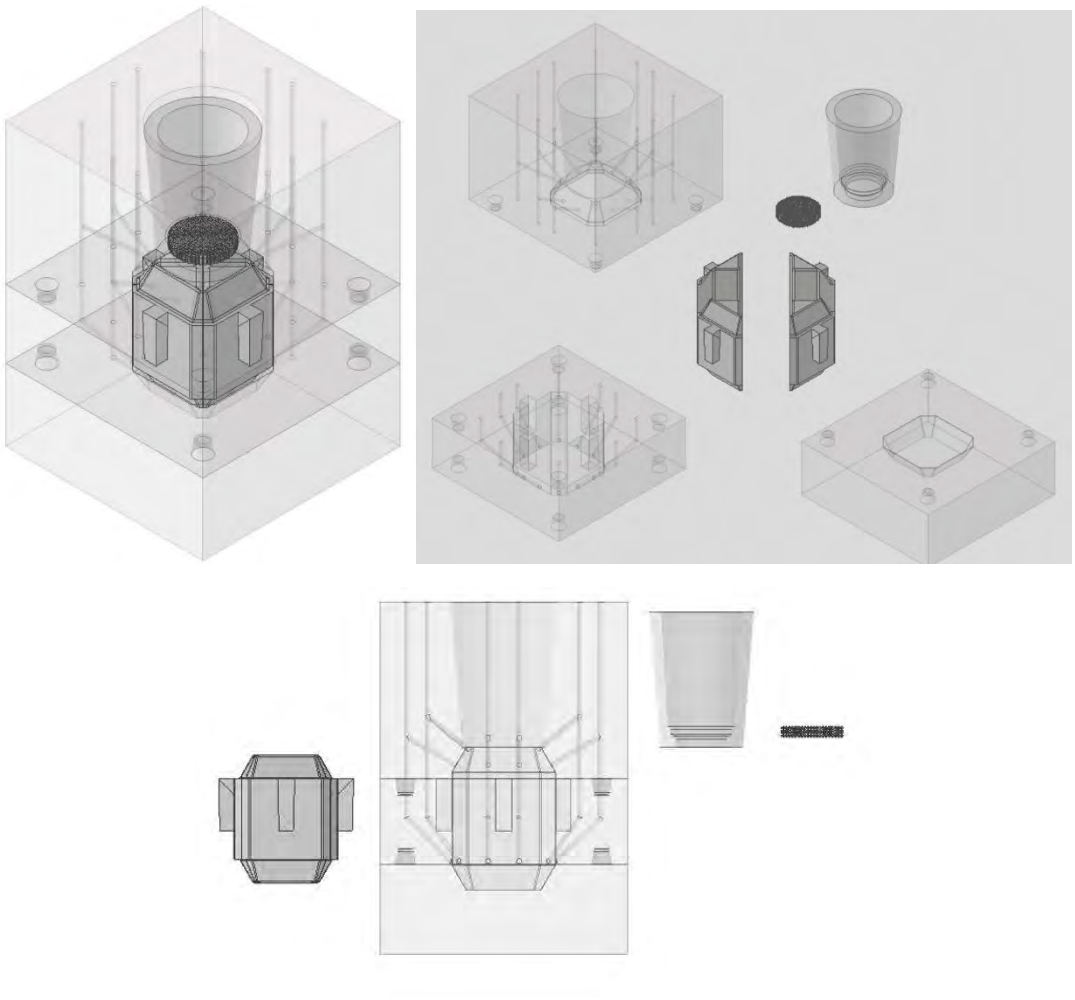

Figure 11: Complete overview of mold components and assemble mold

Flow Simulations

SolidCast

Solidcast is a flow simulation software that simulates what occurs throughout the casting process, from the moment when molten metal is poured into a mold until the metal solidifies. Software such as this that simulates this process allows for predictions of potential defects in the casting and molds design. This can also aid in the redesign process to edit models as necessary to eliminate any defects before making the actual castings.

In order to use the software, elements specific to our design had to be input into the system, including the mold design from inventor, the material, the pour time, and so on. Based on our novice level of experience using this program, recommendations for the simulations came from our industry sponsor at PRL Regal Cast, Foundry Engineer Laura Karduck. Several of the specific input parameters to enter into the software were given to us by her. In terms of material properties, fluid material properties for AF96 were input into the system, which fills in many of

the necessary parameters required by Solidcast for the metal. For the molds, material properties from furan binder 3D printed molds were input, which fills in many of the necessary parameters for the molds. Additional parameters that were set prior to running simulations were a pour temp of 3000 °F based on the anticipated temperature to be used by PRL in the actual casting, a fill time of 5 seconds, and a "well vented" mold. Solidcast does not identify separately modeled vents, so this was one difference from our actual model.

While SolidCast has the capabilities to run a variety of simulations with various outputs, four specific output criteria were carried out with our mold design based on our sponsors recommendations. These four criteria were Critical Fraction Solidification Time, Hot Spot, Niyama, and Material Density. Descriptions of each these four criteria are given in order to demonstrate their relevance to our design process. Following each description are the corresponding results of that simulation for each of the three model sizes.

Critical Fraction Time

The Critical Fraction Time measures the total time it takes in minutes for each part of the casting to reach the point at which the alloy is solid enough that liquid feed metal can no longer flow. In other words, this is the time it takes for each part to become solid. This identifies areas within the model that would become isolated pools of molten metal and would not be able to be fed by a riser if a contraction would occur. In this way, it indicates areas prone to shrinkage. Ideally, the model should solidify at the outside edges of the casting first, then inwards toward where the riser contacts the model, and finally ending with the riser itself.

1/4 Inch Model

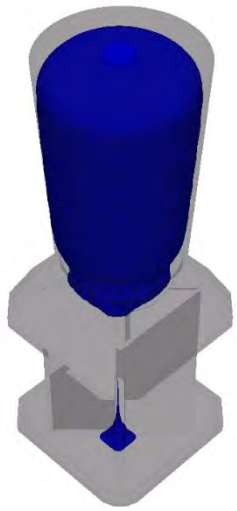

3/8 Inch Model

5/8 Inch Model

Hot Spot

The Hot Spot function locates hot spots within the part by comparing the critical fraction solidification time of each metal node to neighboring nodes. It tracks any differences in time and orders them from greatest isolation to the lowest. A node classifies as a hot spot,

or isolated area, if it froze later than those next to it. All isolated areas are then normalized to a 0-1 range, where 0 means most isolated and 1 means it solidified simultaneously with neighbors.

1/4 Inch Model

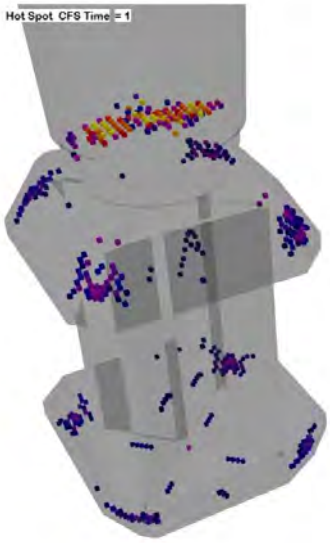

3/8 Inch Model

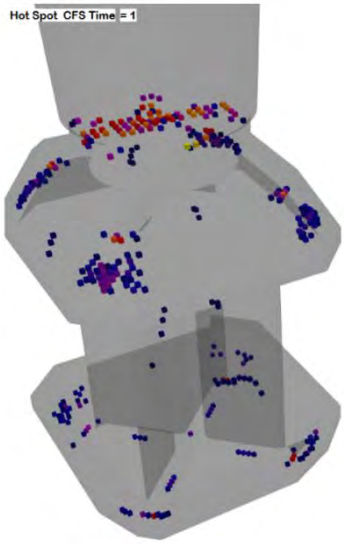

5/8 Inch Model

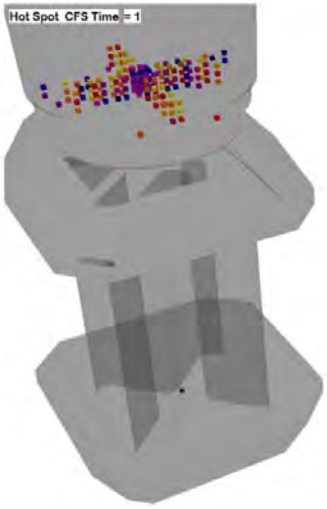

Niyama

Niyama is a function of both the temperature gradient and cooling rate of a casting that corresponds to the presence of shrinkage. In general, it is also a prediction of directional solidification. A value of 0 represents poor directional solidification and the highest probability of shrinkage. Increasing values indicate improved directional solidification, so the severity and probability of porosity decreases.

1/4 Inch Model

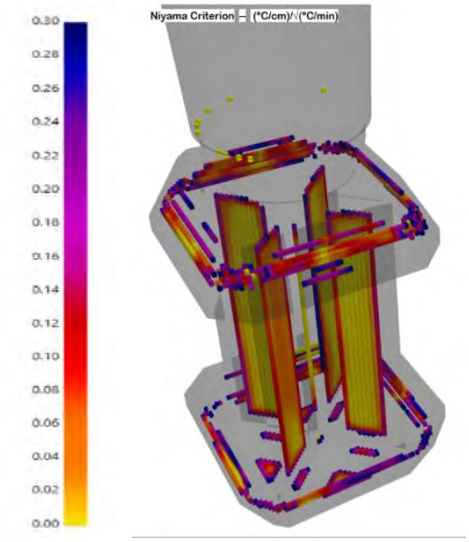

3/8 Inch Model

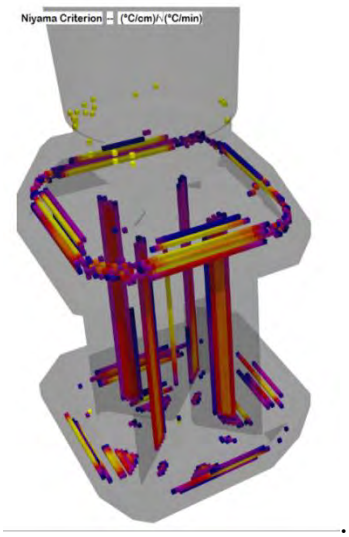

5/8 Inch Model

Material Density

The Material Density criteria examines contractions within the casting during solidification and the resulting flow of liquid feed metal into those contractions. Lower material density numbers are given to areas where metal will be removed due to liquid metal being fed to other areas of the casting. In terms of its value, it is a number that ranges from 0 to 1, specifically measuring how much of the metal remains at each point in the model. A value of 0 indicates that all metal has been removed completely from that area of the casting to feed alternative areas (0% Metal, 100% porosity), while a value of 1 indicates a completely sound area (100% Metal, 0% Porosity). In this way, it is a measure of macro-porosity and a method for predicting potential shrinkage.

1/4 Inch Model

Less than 1 | Less than .99 | Less than .87

3/8 Inch Model

Less than 1 | Less than .99 | Less than .90

5/8 Inch Model

Less than 1 | Less than .99 | Less than .80

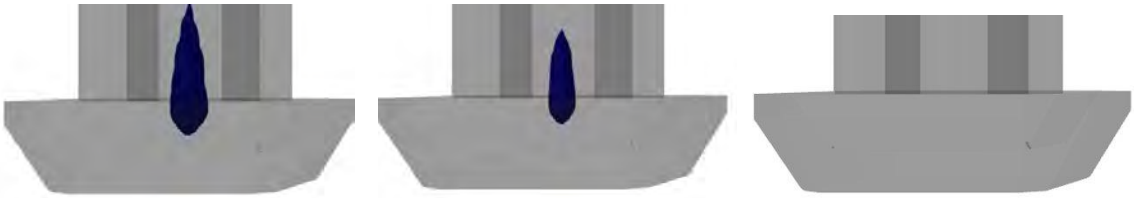

MAGMA- Simulations by Industry Sponsor

Although solidification simulations were ran in SolidCast, it was crucial to verify the results using Magma. Magma is a more powerful software than SolidCast because it simulates a variety of temperature ranges throughout the entire pour cycle where SolidCast requires the user to iteratively change the material temperature as it solidifies. Magma also allows the user to reorient parts and adjust the node count on each part feature to allow for more accurate results. Since the group's sponsor, PRL Regal Cast, had access to Magma it was crucial for the group to

verify their results since there was only one chance to pour competition grade hammers. From an engineering perspective, it is always important to verify the results generated are accurate which was able to be done using both Magma and SolidCast. A comparison was conducted between the Critical Fraction Time, Hot spot, Niyama, and Material density outputted from both Magma and Solidcast to determine not only the validity of the mold design but to also see the differences between software. Having exposure to both software allowed for a great learning experience and showed how each software can display different results. Results from the Magma simulations for the four output criteria are shown below. While comparisons were conducted for all three model sizes, only the Magma results for the ¼-inch model are shown below for the sake of simplicity.

Critical Fraction Time

1/4 Inch Model

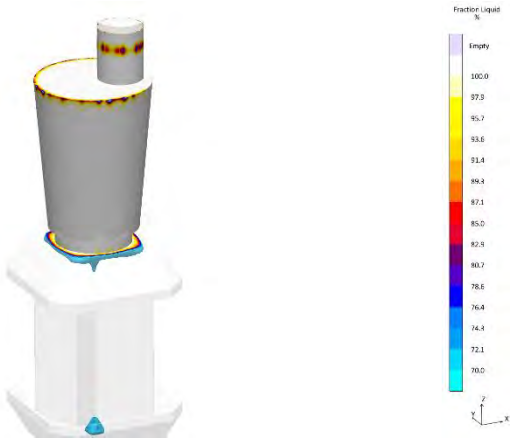

Hot Spot

1/4 Inch Model

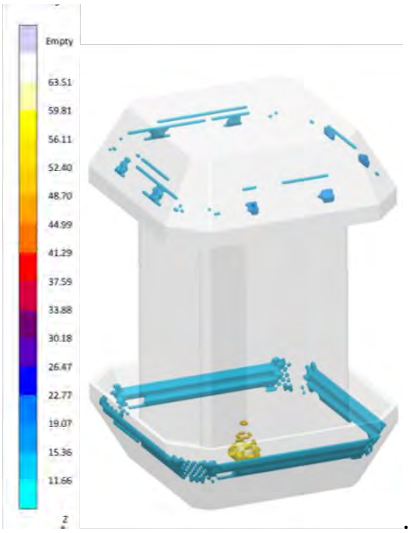

Niyama

1/4 Inch Model

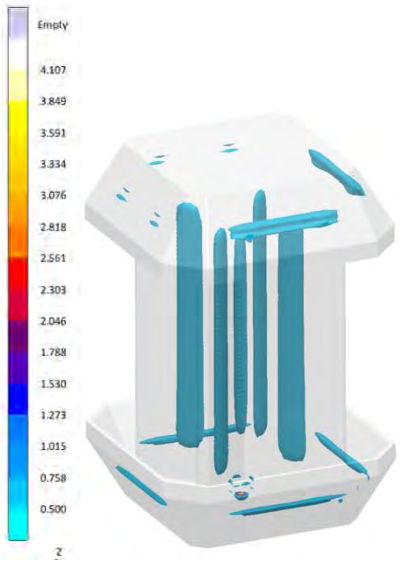

Material Density

1/4 Inch Model

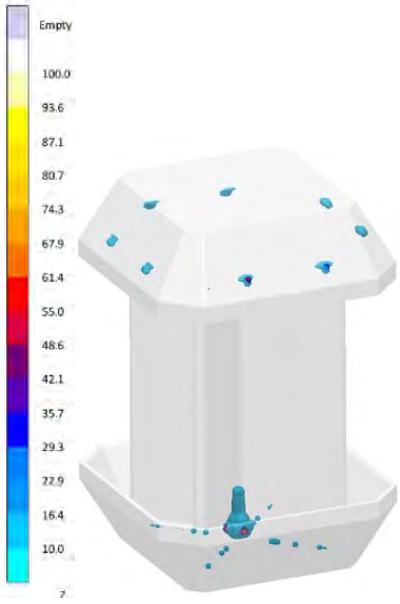

3-D Printed Molds (Hoosier Pattern)

Once the models were created and simulated, the STL files were sent off to be 3D sand printed. Hoosier Pattern became a sponsor because of their past work on previous SFSA competitions, their vast experience with the ExOne 3D sand printing system, and because of recommendations from Kyle Blakeslee at Urick Ductile solutions located in Erie, PA. Hoosier pattern has paved the way for additive manufacturing practices by being one of the first manufacturing facilities in the United States to own an ExOne S-Max Printer. With the ExOne's capabilities to print small production parts with complex geometries up to a 0.02 inch tolerance, it was crucial to partner with them due to the complexity of the final mold design. Along with the complex mold design, 3D sand printing was the only option due to the short timeframe, small production size, and PRL Regal Cast being a sand cast foundry. As a result, Hoosier pattern was able to 3-D print 12 molds, (12in x 12in x 17in mold dimensions) on their ExOne machine in under a week. This allowed for the molds to be printed and shipped to PRL Regal Cast in about a week so the molds could be prepped for pouring.

ExOne S-Max

As a leader in the additive Manufacturing industry, ExOne provides the highest quality sand printing solutions on the market. Throughout this project, ExOne's S-Max was used. The S-Max provides a robust and reliable solution for all cold hardening binder system and is suitable for almost all casting materials. The S-Max is one of ExOne's largest machines with build plate dimensions of 1800 x 1000 x 700mm and a potential build volume of up to 1260 L. These large bed dimensions and a build rate of up to 100 L/h allows for multiple large designs to be printed together thus deceasing the overall production time. The S-Max is designed to print either the Furan or CHP binder system, with most companies opting to use the Furan binder with silica sand combination as an industry standard in the United States. These machines are so accurate that they are able to place a single particle of sand which allows for high dimensional accuracy on complex parts. As a result, these machines allow for complex small-production parts to be produced much more efficiently and accurately without having to go through conventional core making techniques.

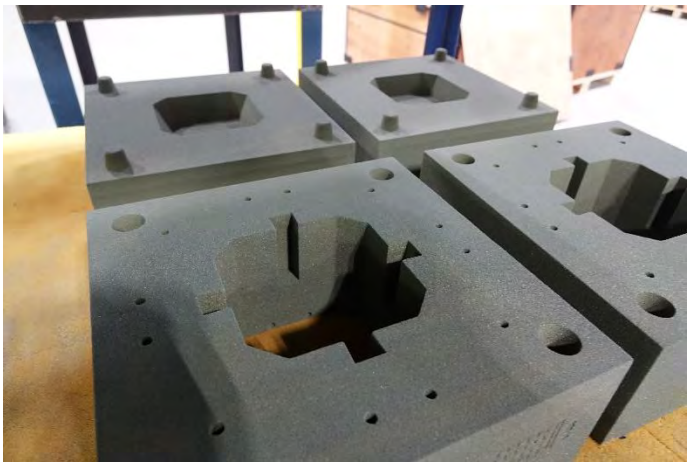

Figure 12: Completed mold prints, the cheek and drag

Pouring Process (PRL Regal Cast)

Once the molds arrived at PRL Regal Cast, located in Lebanon, PA, the group made the 5.5 hr trip to watch the molds be prepped and poured.

Mold Preparation

After arriving, the molds had to be prepped and coated. Prior to coating, the cope, drag, cheek, and 4 cores were all tested fitted to ensure each part of the mold would fit as intended in the mold design. If any adjustments needed to be made, sandpaper was used to remove material to ensure proper fitment. Once the molds were test fitted, they were taken back apart and blown off with air to ensure that any loose sand in the vents and throughout the entirety of the mold would be removed prior to coating the inside of the mold. (not sure if they washed them or not) The inner portions of the mold (areas that come in contact with metal) are coated or painted with a material so a barrier between the sand and the metal are created. This prevents the metal from eating away at eroding the mold and creating inclusions within the cast hammer. This ensures that the parts will have a better surface finish as well. After the various mold parts were coated, they were carefully assembled with glue placed around the cope, drag, and the cheek to prevent the mold from shifting during the pouring process. A Kalpur was also used to feed and filter the material into the mold to allow for an alternative to the conventional sprue and runner design. The Kalpur was inserted into the cope once the rest of the mold had been glued and assembled. The molds were also banded together to ensure the mold sections would not rise or shift from the ferro static head pressure seen reduce the change that the molds would expand to the pressure created during the pouring process.

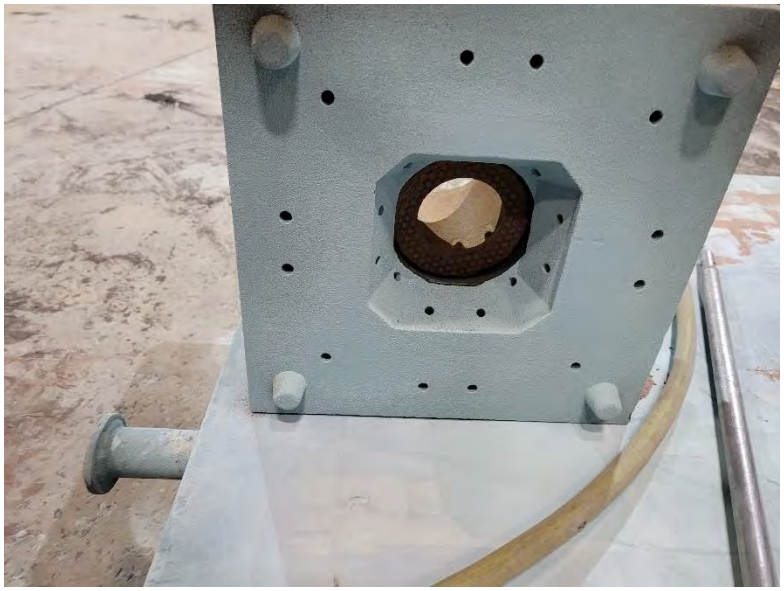

Figure 13: Underside of the printed cope after coating and painting

Steel Alloy and Chemistry

The chemistry of AF96-28 was adjusted prior to the pour process in order to ensure that the material poured at PRL Regal Cast met the standards set by the material patent. A base composition of material was added into the furnace and began to melt. As the material begin to heat up the composition was checked by obtaining a molten puck of metal from the furnace. Once the puck was cooled, it was placed into an Optical emission spectroscopy (OES). An OES is a common form of spectroscopy used to determine elemental components in solid metal samples. Once the machine completed its test, it produced a printout of all the elements found in the sample with their respective percentages. Then PRL's Metallurgists and melt crew made appropriate adjustments to get the metal to its desired composition. This process was repeated until the final composition was achieve based on the composition standards from the patent. For reference, the certificate of the final exact alloy chemistry generated by PRL is given in section I of the Appendix. Additionally, the patent-specific composition ranges can be found in section A of the appendix as a means of comparison to show that the alloy did in fact qualify as AF-96.

Figure 14: Melting of the alloy in the furnace and filling of the ladle

Pouring

Now that the mold was assembled and secured it was time to pour the hammers. With the heat of the material ready a 1000 lb bottom pour ladle was prepared and heated to be used for the pour. The reason a bottom pour ladle was selected was to provide a more accurate pouring procedure. The other reason for a bottom pour ladle was that it reduced the amount of time the metal could encounter the air which increases the purity of the material by reducing the oxides that entered the molten metal. The furnace was heated up until it was tapped at 3108°F and poured into the bottom pour ladle. From there the ladle was moved over to the pour area where the molds were lined up in a row. The pour temperature was approximately at 3000°F when the first mold was poured.

The pour process began by dumping out about 200lbs of material to purge the ladle and get rid of any contaminates that may have been on the end of the ladle stopper. Next, each of the 12 molds were poured in order from smallest to largest thickness to ensure complete filling of each of them. Each of the molds filled in under 1 second which is faster than the estimated fill time of 5 seconds estimated on the solidification models. The quick fill time indicated that the molten metal had more fluidity than anticipated, allowing for no parts of the mold to sinch off and ensuring a complete casting. The molds filled so quick that the entire vent system filled and solidified which was not anticipated based on the solidification simulations. After the molds, two keel block molds were poured producing a total of 8 keel blocks that could be used for material testing. Keel blocks are an industry standard for material testing and provide certification of material properties without having to cut or scrap an entire casting. The keel blocks were poured using hand packed sand molds and were poured directly after the molds were. They consist of a solid base block with two squares or "legs" on top and they are poured in the middle of the mold so that the metal can flow out into each of the four legs which allows for directional solidification and the best material properties. By having a large riser on top, it prevents shrink which allows for property comparison to the actual cast material. After the keel block molds were poured the rest of the material in the ladle, approximately 200lbs, was poured off as scrap material.

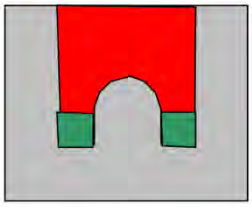

Figure 15: Schematic of overall keel block, with the legs or test blocks indicated in green

Figure 16: Overview of all filled hammer and keel block mold

Breakout

Once the molds were poured, the hammers were left to cool for 5 hours before they broken out of the molds by hand using a hammer. At this point the hammer could be seen with the kalpur and the filled vents still attached. PRL rough cut the vents and the Kalpurs using a torch so that the hammers would be more managable for transport and so that the hammers could be further machined with the tools available to the group. The purpose of only rough cutting the Kalpur and vents was to prevent the faces of the hammer from being heat affected by the torch, which would impact the final material properties of the faces. The remainder of the vents and kalpurs were removed by the group using a bandsaw and grinder upon the return of the hammers to Erie. Shown below is a series of photos depicting the hammer at all three stages. The first shows one casting immediately after breakout, including the vents and kalpur. Next is a picture of all of the hammers after being rough cut, followed by a hammer after the entirety of the excess elements were removed.

Figure 17: Completed casting following breakout, with vents and kalpur included

Figure 18: Collective hammer castings after being rough cut

Figure 19: Hammer after complete removal of vents and kalpur

Finishing Process

I. Hot Isostatic Processing (Hipping) and Full Annealing

To begin the sequence of post-processing and finishing processes, half of the 12 total hammers (two of each size) and half of the test blocks (8 of 16) were sent to Pressure technologies in Painesville, Ohio to undergo hot isostatic process. The purpose for the HIPing process was to homogenize the alloy, thus creating consistent properties throughout the material. Additionally, hipping can reduce any sub-surface voids such as porosity and microshrinkage that may be associated with the casting process. Since the hammer will be used for impact tests it was crucial for the material to have consistent properties, so it can withstand a wide variety of tests and applications without soft or hard spots. The procedure works using a combination of controlled heat and high pressure. The materials were heated up to 1200°C in inert gas at 15,000 psi for 4 hours. This gas applies uniform pressure on the component in all directions, causing the material to become "plastic" and allowing the enclosed voids to collapse under the pressure. The surfaces of the voids then bond together by diffusion as a result of the time and temperature, effectively eliminating defects and bringing the material closer to its theoretical density.

As an alternative to the hipping procedure, the remaining half of the hammers underwent a full anneal. The main purpose for implementing two separate techniques for each half of the hammers was based on the uncertainty in the timeframe needed for the HIPing procedure. In the case that the HIPed hammers were not completed in time based on production delays, the group wanted to have a secondary option that offered some comparable property benefits and could be completed in-house. A full anneal consists of heating the steel above the upper critical austenitic temperature and holding it at temperature for sufficient time to transform the material completely to austenite. Our specific procedure was performed at 1850°F for 1.5 hours. The material is then furnace-cooled such that the furnace and the steel cool to room temperature at the same rate. Due to the length of time is takes for this cooling to occur, it allows for the formation of coarse pearlite. This left the hammers with an increased softness and ductility, which would be useful at this stage prior to machining. In comparison to the HIPing process, the full anneal also leaves the material homogenized and with a uniform grain structure, offering the similar benefit of consistent material properties.

Figure 20: Industry Sponsor for Hipping

II. Designating the "Competition Hammer"

Ultimately, the production time for the hipping was well within the deadline necessary to allow all of the remaining finishing operations to be completed. These hammers were able to outsourced to Pressure Technologies, processed, and returned to Behrend in a matter of two days. As a result, it was decided that the "competition hammer" would be selected from those that were hipped. Though conducting a full anneal did offer improved characteristics relevant to this competition, when the two options are compared, hipping is the superior choice.

Furthermore, within the six hammers that were hipped, there were also three hammers of different dimensions from which to select the competition hammer. Several important factors were considered, and examinations conducted prior to making this decision. The first pertained to the effect that casting at the different dimensions had on the quality of the microstructure. The 1/4-inch casted model was the ideal case given that it was closest to the designed 1/8-inch competition dimensions needed to meet weight. But, because it was at the minimum wall thicknesses required for sand casting, it was also the highest risk in terms of being prone to casting defects. Both the 3/8-inch and the 5/8-inch models were cast with the intent that the increased wall thickness would ensure better fluidity and have a lower risk of porosity and shrinkage, as was indicated by the flow simulations. While there were no major or fatal issues anticipated for any of the three sizes, the simulations for the larger sizes did show slight improvements from the 1/4-inch size. Upon first observation of the hammers after completion of the casting and hipping, there were no major defects detected externally on any. The biggest area of concern, however, was at the base of the x-bar where it was predicted that an area of shrinkage may occur. This required a more detailed examination. On the hammer of smallest dimensions, the location where we expected the shrink to be was checked using a Dremel to "dig" into the area. Instead of porosity, this location contained what seemed to be divots, where it appeared that the wall may have started caving in slightly. This indicated to us that this model was able to pull in external material surrounding this area to fill the void. The affected area was also minor and isolated enough that it would not need to be filled, as material would be removed from this location anyway with the planned machining down to competition size. Given this fact, and the absence of any other unfixable defects in the x-bar or faces, the smallest 1/4-inch model was selected to be the one sent to competition after finishing. As this model was closest to the needed dimensions, it would be the most practical to post-process and would require the least amount of material removal to meet the specifications.

Figure 21: Selected competition casting, 1/4 inch model

III. Machining handle hole/ handles

To produce the hole in the center of the casting to accept the eye/taper sleeve the hammer head had to under-go machining on a Bridgeport mill. Using a 5/8 inch carbide endmill the pilot hole was plunge cut directly through the center of the hammer head. The endmill was then fed 0.4375 in two cardinal directions, making a cross pattern with the same length as diameter needed to input the tapered sleeve. The same procedure was then conducted but feeding along the diagonals, again in an effort to rough in a circular shape. Finally, using a rotary table mounted to the mill the hole could be cut to its final size with the endmill.

Figure 22: Machining the handle hole with carbide endmill

Figure 23: Completed hole for handle, shown with tapered sleeve

IV. Grinding and Machining

Once the hole was cut in the center the bulk of the material removal could take place, grinding and machining to get to the final size parameters needed. This was done using both a Bridgeport milling machine and a 2X72 inch belt grinder. The internal “X-beam” was clamped on one side, mimicking a “plus +” sign, then the material was side milled off until final dimensions were achieved. The hammer was flipped and the process repeated until all sides were machined. To remove the extra steel from the hammer faces and angled flanges 36 grit aluminum oxide belts were used to quickly remove material. The flange thickness was then intermittently checked using a pair of calipers to ensure proper size. Following this step, all sharp corners were broken and all burrs removed.

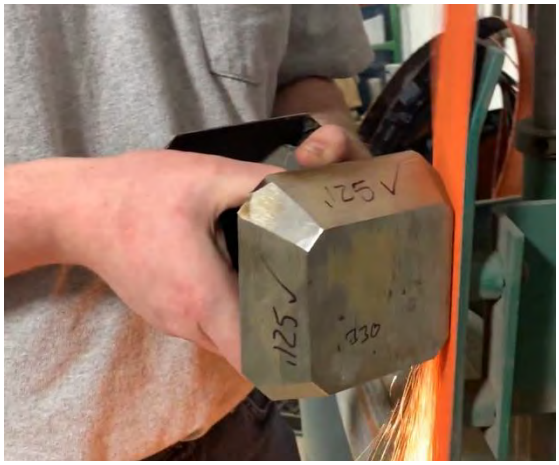

Figure 24: Grinding of the faces and flanges with a slack-belt grinder

V. Welding the Handle Sleeve

To make room for the hammer handle to fit withing the head a 1.5-inch diameter, 2-inch-tall piece of 4130 machined previously to have an oval shaped hole in it, was set to be welded into the machined center hole of the hammer head casting. Both the eye/taper sleeve were preheated using an Oxy Acetylene torch equipped with a rosebud torch tip, until they both surpassed a straw/wheat color and held a deep blue (Light is refracted differently as the oxide layer forms and thickens, with more heat), indicating they were over 400 °F. The preheat was necessary to avoid cracking the weld beads due to the rapid cooling of weld material and possible formation of Martensite. At that point the eye/taper sleeve was welded using a Lincoln Electric MIG Welder with .025-inch wire at 337 in/min, 20.6V. The eye/taper sleeve was welded fully on all points of contact (top, bottom, and sides) to ensure maximum strength of the joint. Post weld heat was then applied to ensure a slow cool time and to limit the potential of weld cracking.

Figure 25: Preheating the weld area and welding in the tapered sleeve

VI. Heat Treatment Process

The process began by sending the samples out for hot isostatic pressing at pressure technologies Following the hipping process, the hammers went through a solution anneal performed at 1200-1250°F for 1.5 hours, followed by an air cool. The solution annealing process allowed for precipitate formation which would thus help to control the grain side during the Austenization phase. Once the solution anneal was completed, an Austenization was performed on the hammers at 1800-1850°F for 1.5 hours, followed by a room temperature water quench. The Austenization allows the phases to change within the hammer from ferrite to Austenite, and then rapidly quench to produce some martensite. The martensite allows for there to be strength in the material through grain boundaries, however if too much martensite is formed the material will become brittle. After the Austenization and quench were performed, a temper was conducted at 400°F for 1.5 hours followed by an air cool. The tempering process allows for the atoms within the material to get to their lowest energy state thus decreasing the internal stresses of the material. This process allows for the material to become more ductile and tough, while still maintaining the hardness desired.

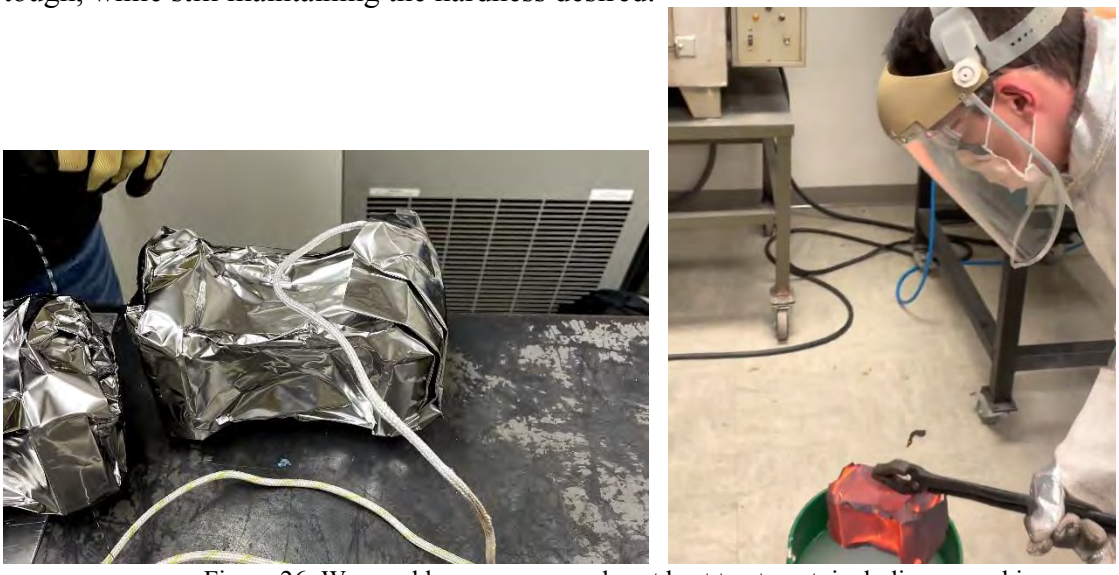
Figure 26: Wrapped hammers pre and post heat treatment, including quenching

VII. Implementing the Outer Shell

With the handle cut and sanded to fit easily into the tapered sleeve or “eye” of the hammer it could be forced into its final position with a 4lb engineer's hammer. Once the handle was seated fully into the sleeve a wooden wedge and 2-part epoxy could be driven into the slot present in the handle, spreading the wood into the taper and forming a mechanical lock holding the handle firmly in place. The outside sheet metal “shell/Skin” made of .050” 4130 was cut to size using a Beverly Shear and then bent using custom fabricated jigs in a bench vise to achieve the angles and radii necessary to cover the hammer flanges accordingly. A hole was then cut through one of the two halves using a step drill bit until the hole was large enough to slip over the handle. Once in place the sheet metal could be clamped in place and tacked to ensure proper fitment. Once the sheet metal was tacked into place and seen to be acceptable, full welds were placed around the perimeter of the angled “flanges” of the hammer. Since the hammers were in their final heat-treated state, cooling time was allotted to ensure that the heat imparted by the welding process disrupted it as little as possible. Also due to the relatively thin sheet metal and the heat-treated state of the hammers no preheat was added.

Figure 27: Bending the sheet metal shell and welding it to the hammer

VIII. Final Finishing

To achieve the final finish for competition, a variety of sanding methods were used. Initially, a Dyna file was used to roughly blend the weld beads to make as seamless a transition as possible between the angled flanges of the hammer face to the sheet metal shell. Once the welds were all roughed in, the tedious task of hand sanding the hammer could begin. Starting with 80 grit sandpaper and continuing to 120 grit, 220 grit, 320 grit, 400 grit, a Muslin Buffing wheel with black buffing compound, and finally ending with polishing compound. This left the hammer with a borderline mirror finish. With the final finish complete, the design etch work could be conducted. Using custom made Vinyl stickers, a pattern could be placed on to the respective sections of the hammer head and be masked off from the rest of the metal surfaces.

Ferric Chloride could then be applied onto the exposed steel surface alloying for an accelerated corrosion to take place. The hammer was then sprayed with an ammonia based cleaner to neutralize the acid and the stickers removed, leaving behind the design pattern. To complete the overall look, the handle was then stained to mimic the “dark leather-like" color seen in the film and the grooves painted over with a metalic-silver marker.

Figure 28: Final finishing steps, including handle staining, buffing, and etching

Material Testing

From the initial design phase of this project, it was determined that certain characteristics, such as strength, hardness, and toughness, were key requirements for the hammer. Various specifications were established that directly correlated to these characteristics, with specific metrics the hammer must provide in order to successfully meet the needs of the competition. Additionally, many criteria throughout the analysis and selection phase were based on the anticipated or simulated strength and resistance to deformation that the design offered. Action was also taken throughout the finishing processes with the hipping and heat treatment procedures to either maintain or increase the base strength and toughness provided by the as-cast AF96. Due to the fact that many decisions throughout this project were made in an effort to contribute to these properties, the group wanted to validate that the intended results were actually achieved. As such, a series of various material tests were conducted both in-house and by an industry partner. These included tensile and charpy bar testing, microhardness and macro-hardness testing, and various microscopy imaging techniques. As discussed previously, all samples to be used for material testing were taken from the keel block bars produced during the casting process. To most accurately represent the properties of the final hammer itself after undergoing the various finishing processes, all keel block bars that were turned into test samples underwent the same hipping and heat treatment procedures that the final hammer did.

Westmoreland Material Testing

The first portion of material tests that were conducted were tensile tests and charpy tests. Not only are these two of the most fundamental types of mechanical testing, but they are the two most applicable to the competition in terms of the information they offer. A tensile test applies axial loads to the sample until failure occurs. From this, we can gather the yield point of our material, or the stress level at which the metal begins to deform and will not go back to its original dimensions. This is an important property to be aware of, as this yield stress of the material should not be surpassed under the predicted competition loading. An impact test, particularly the V-Notch Charpy method, uses a weighted pendulum to strike, deform, and crack a sample. It is designed to predict the fracture behavior of the material by measuring the amount of energy absorbed in the fracture, or the impact energy. This energy measurement is a direct representation of the toughness of the metal. The main type of loading that the hammer is expected to experience throughout the performance testing is impact loading, so it is essential that a high amount of energy be required to fracture the material.

To perform these tests such that they are credible, they must be in compliance with ASTM standards. These testing standards, specifically ASTM E8/E8M − 16aϵ1 for Tensile Testing and ASTM E23 − 18 for Charpy Testing, require that specific specimen sizes, tolerances, machinery, and procedures be utilized. All of the standard-size specimens would have to be produced from the original 1” by 1” by 6” keel block bars. Due to the limitations in equipment available to us at Penn State Behrend, it was not feasible to conduct this portion of testing in-house. In terms of making the specimen, cutting the standard tensile and charpy bars from the original keel block bars required a sufficient amount of machining to tight tolerances. The various manufacturing tools that the group members had access to at home did not have the capabilities to complete the machining. While requesting to have the technicians at Penn State complete the work was an option, it did not fit within the required time frame. In terms of testing the specimen, the load values needed to fracture samples of standard size in either tension or impact are outside or very near the rated load capacity of the university’s test equipment. This is based on the expected yield strength and toughness of the base material. Furthermore, based on prior experience, tests conducted on this equipment tended to produce inaccurate or inconsistent results.

For these reasons, the group decided to outsource this section of both machining and material testing. An outside company would be fully equipped to do the necessary work with a much shorter lead time and produce far more accurate results possible. Our specific partner was Westmoreland Mechanical Testing and Research, selected based on previous collaboration and their expertise in this sector of industry. The hipped and heat-treated keel block bars, five total, were sent out to Westmoreland as the raw material. From these five bars, three tensile bars and four charpy bars were produced overall. The figure below shows the technical machining schematics for the standard size specimen relative to each keel block bar, where one keel block corresponded to two charpy bars or one tensile bar. As mentioned, these specimens were machined to sizes outlined in the ASTM standards for tensile and charpy testing. For the tensile bars specifically, round bars were used as opposed to dog-bone based on ease of machining from the original keel block. Additionally, a sub-size tensile specimen was used as opposed to the full size so that a proper test bar could be generated from the length of the original keel block without including any near-the-surface material that may have defects. Diagrams from the standards

depicting the specific dimensions for these specimens are included below in Figures 29-32, as well as Westmoreland's engineering drawing for the tensile bar which corresponds to a Small-size Specimen 3. All machining was done at room temperature.

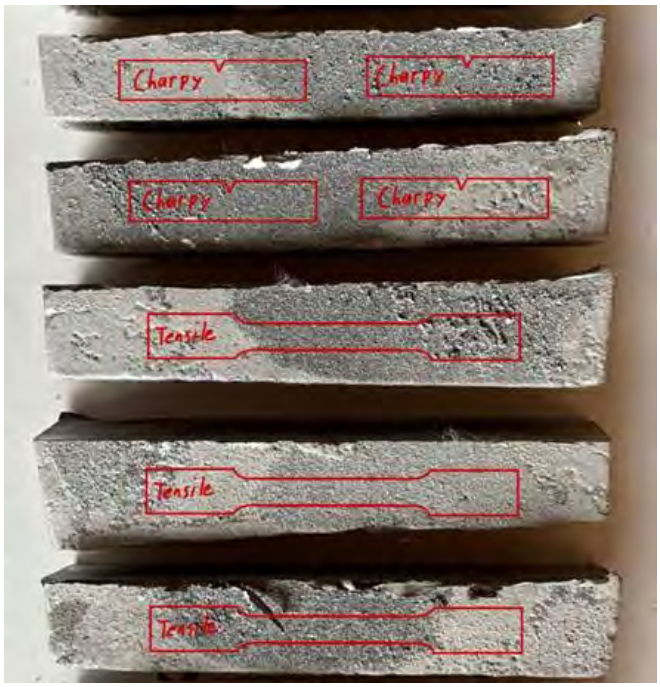

Figure 29: Schematics for machining test specimen from each keel block

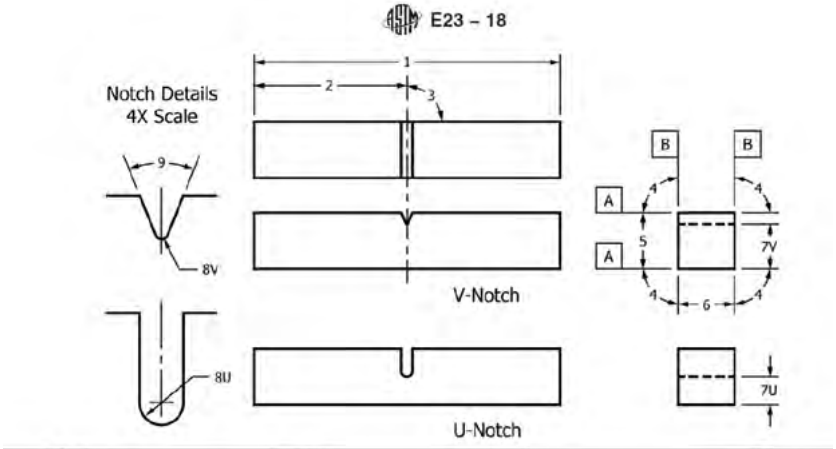

ID Number	Description	Dimension	Tolerance
1	Length of specimen	55 mm	+0/-2.5 mm
2	Centering of notch		±1 mm
3	Notch length to edge	90°	±2°
4	Adjacent sides angle	90°	±0.17°
5	Width	10 mm	±0.075 mm
6	Thickness	10 mm	±0.075 mm
7V	Ligament length, Type V	8 mm	±0.025 mm
7U	Ligament length, Type U	5 mm	±0.075 mm
8V	Radius of notch, Type V	0.25 mm	±0.025 mm
8U	Radius of notch, Type U	1 mm	±0.025 mm
9	Angle of notch	45°	±1°
A	Surface finish requirements	2 µm (Ra)	≤
B	Surface finish requirements	4 µm (Ra)	≤

Figure 30: Diagram for standard V-notch charpy from ASTM E23 − 18

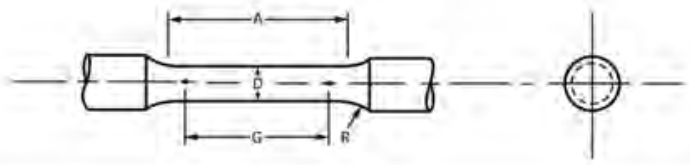

Dimensions, mm [in.]
For Test Specimens with Gauge Length Five times the Diameter [E8M]

	Standard Specimen	Small-Size Specimens Proportional to Standard			
	Specimen 1	Specimen 2	Specimen 3	Specimen 4	Specimen 5
G—Gauge length	62,5 ± 0,1 [2.500 ± 0.005]	45,0 ± 0,1 [1.750 ± 0.005]	30,0 ± 0,1 [1.250 ± 0.005]	20,0 ± 0,1 [0.800 ± 0.005]	12.5 ± 0,1 [0.565 ± 0.005]
D—Diameter (Note 1)	12.5 ± 0.2 [0.500 ± 0.010]	9,0 ± 0,1 [0.350 ± 0.007]	6,0 ± 0,1 [0.250 ± 0.005]	4,0 ± 0,1 [0.160 ± 0.003]	2.5 ± 0,1 [0.113 ± 0.002]
R—Radius of fillet, min	10 [0.375]	8 [0.25]	6 [0.188]	4 [0.156]	2 [0.094]
A—Length of reduced parallel section, min (Note 2)	75 [3.0]	54 [2.0]	36 [1.4]	24 [1.0]	20 [0.75]

Figure 31: Diagram for standard round tensiles from ASTM E8/E8M − 16aϵ1

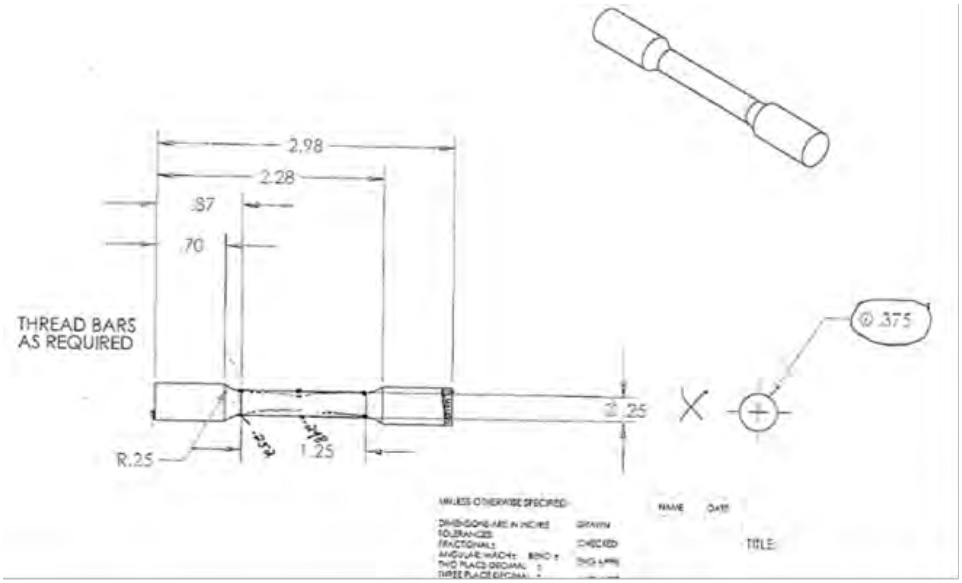

Figure 32: Westmoreland's engineering drawing for the tensile bar

After the machining was completed, all testing was conducted at room temperature in accordance with the procedures outlined in the mentioned ASTM standards. Most notably, this included using an 8 mm striker for charpy testing and a strain rate of .005 in/in/min for tensile testing. The further details of these procedures can be found using the citation information referenced in Appendix C. Upon completion of each charpy test, data was recorded for the amount of energy absorbed by the sample before fracture. For each tensile test, data was recorded for the ultimate tensile strength, the yield strength with 0.2% offset, the modulus of elasticity, and percentages for elongation and area reduction. A summary of these test results for all of the samples are given below in the result reports sent by Westmoreland.

As previously mentioned, the results of most concern were for the yield strength and impact energy. Based on information given in the patent for AF96, we were anticipating a yield strength of around 180 ksi and an impact toughness of around 30 ft-lbs. The patent gives this property data specifically for when the steel is thermally processed according to a patented method. Since we followed a heat treatment consisting of the same general steps of normalization; Austenization with quenching; and tempering, it was inferred that we would achieve roughly similar properties. One important distinction in terms of the impact test is the difference in testing temperatures between ours and those cited in the patent. The patent gave a toughness of 30 ft-lbs for an impact test conducted at a sub-zero temperature of –40 °C while our tests were conducted at room temperature based on ASTM standards for charpy testing. The test results indicated that lower than anticipated impact energy values were achieved, with an average of 14.5 ft-lbs, while higher than anticipated yield strength values were achieved, with an average of about 208 ksi. Theoretically, impacting the material at a higher temperature should have resulted in an improved toughness. Therefore, there had to be an alternative rationale for our low impact energy values. The most likely sources of the low toughness seen in these samples are inclusions generated in the keel block bars during casting and work-hardened material during machining. The high yield strength values can likely be attributed to the additional hipping process of our material as well the aforementioned work hardening that may have occurred.

of 2

IMPACT RESULTS: ASTM E23-18
No Requirements
MATERIAL: Steel
SAMPLE TYPE: Charpy V-Notch **DIS**

SID	TestLog Number	Sample Size	Temp. °F	Energy ft-lbs	Mils Lat Exp	% Shear Fracture	A\U\R
C-1	01-004L4J	Standard	75	16.0	1	15	Report
C-2	01-004L4K	Standard	75	12.0	2	15	Report
C-3	01-004L4L	Standard	75	14.0	1	15	Report
C-4	01-004L4M	Standard	75	16.0	2	15	Report

A\U\R: A=ACCEPTABLE, U=UNACCEPTABLE, R=REPORT

E23 8mm Striker used for testing.

Figure 332Results for four charpy impacts tests conducted according to ASTM E23 − 18

March 8, 2021
Penn State University
217 Advanced Mfg. and Innovation Center
5350 Technology Drive
Erie, PA 16510

WMT&R Report No. 01-210000
P.O. No. Credit Card
WMT&R Quote No. QN210865

Attention: Paul Lynch

Subject: All processes, performed upon the material as received, were conducted at WMT&R, Inc. in accordance with the WMT&R Quality Assurance Manual, Rev.
The following tests were performed on this order: Impact and Tensile

TENSILE RESULTS: ASTM E8-16ae1
SPEED OF TESTING: 0.005 in./in./min.
MATERIAL: AF9628

DISPOSITION: Report

SID	TestLog Number	Temp.	UTS ksi	0.2% YS ksi	Elong %	RA %	Modulus Msi	Ult. Load lbf	0.2% YLD. lbf	Orig. Dia. (in.)	Final Dia. (in.)	4D Orig GL (in.)	4D Final GL (in.)	Orig. Area (sq. in.)	Machine Number	A\U\R
T-2	01-004L4P	Room	262.5	222.2	13	34	35.8	12987	10992	0.2510	0.2046	1.00	1.13	0.04948087	M16	R

A\U\R: A=ACCEPTABLE, U=UNACCEPTABLE, R=REPORT

TENSILE RESULTS: ASTM E8-16ae1
SPEED OF TESTING: 0.005 in./in./min., 0.05 in./min./in.
MATERIAL: AF9628

DISPOSITION: Report

SID	TestLog Number	Temp.	UTS ksi	0.2% YS ksi	Elong %	RA %	Modulus Msi	Ult. Load lbf	0.2% YLD. lbf	Orig. Dia. (in.)	Final Dia. (in.)	4D Orig GL (in.)	4D Final GL (in.)	Orig. Area (sq. in.)	Machine Number	A\U\R
T-1	01-004L4N	Room	258.3	201.2	11	29	28.1	12821	9988	0.2514	0.2125	1.00	1.11	0.04963870	M31	R
T-3	01-004L4Q	Room	262.2	200.7	11	29	28.1	13013	9961	0.2514	0.2118	1.00	1.11	0.04963870	M31	R

A\U\R: A=ACCEPTABLE, U=UNACCEPTABLE, R=REPORT

Figure 34: Results for the three tensile tests conducted according to ASTM E8/E8M − 16aє1

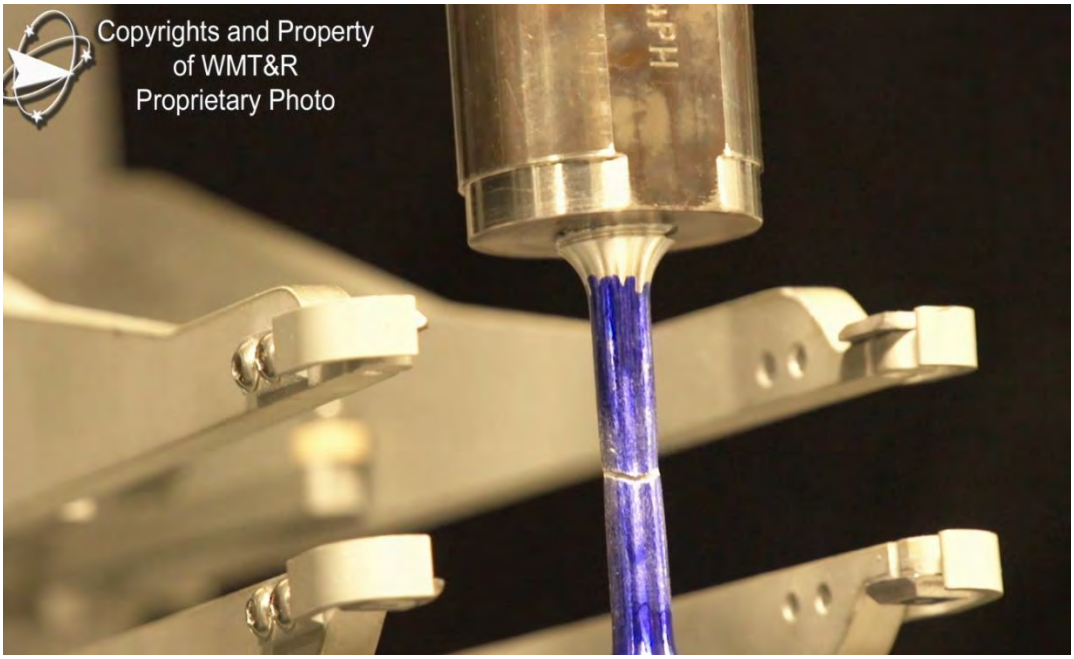

Figure 35: Round bar specimen being fractured during tensile testing

Behrend Material Testing

The second round of material testing included all those that were conducted at Penn State Behrend by the members of the group. Based on the group's research experience in metallography, these tests focused on microstructural examination, including both micro and macro-hardness, etching, and various forms of microscopy. Investigating the structure of the material through these methods offers a great deal of information about the processed material that is otherwise indiscernible. The group felt conducting these tests would be a valuable addition in terms of quality assurance and property validation. Furthermore, because our selected material AF96 has been rarely sand cast, conducting these tests gave our team the opportunity to make new discoveries pertaining to the field of casting. The following sections outline the work involved in conducting each test, including the specific purpose, the equipment needed, the procedures followed, and the obtained results. Similar to the previous round of testing, all samples for these tests were cut from an original 1" by 1" by 6" keel block bar that had been hipped and heat treated. Each sample represented a quarter of the keel block's cross-section. Samples were cut using Penn State Behrend's Allied HiTech Metallography Saw and abrasive cut-off blade (A/O, Rubber Bond) rated for hardened steels and super alloys with hardness between 45-60 HRC. The saw was ran at 3000 rpm with a feed rate of .05 in/min, while high-speed cutting fluid and water flooded the material.

I. Polishing

For any microscopy or microhardness work to be completed, the samples needed to be polished. The polishing was completed using a Struers AbraPol-20 automated polishing machine. After the samples were mounted into a 1 1/4-inch puck, the six samples were placed into a sample holder using a c-clamp to ensure the samples were fasten flat and an allen key was used to ensure the samples were tight and would not move while the polishing process was happening. The polishing step process was determined based on Streurs' recommended polishing procedure for high strength low alloy steels.

This process started with a md piano 120 grinding pad for 3 minutes using water. This step allowed for a rough grind of the samples to get them flat and remove any major imperfections on the surface of the samples. Then, a Piano 220 pad and a Piano 500 pad were used for 2 minutes each using water. These steps helped to get the major scratches out of the material while continuing to ensure the samples were completely flat. After that, a Piano 1200 pad was used with water for 4 minutes followed by a Piano 2000W pad and a Piano 4000W pad each used for 2 minutes with water. After finishing the Piano scale, the samples only had some minor scratches in them which were eliminated with the final two polishing steps. In the second to last polishing step, a Dac polishing pad was used for 5 minutes with a DiaP.Dac 3 substrate to help remove the minor scratches. After this step all the major scratches were taken out of the samples with only a few light scratches remaining. The final polishing pad used was the Nap polishing pad used for 5 minutes with a DiaP.Nap-B1 substrate. This final step removed all the final swirls and light scratches in the sample material, leaving each of the samples with a

mirrored finished polish. In between each of the Piano grinding steps the samples were cleaned using a Struers ultrasonic cleaner to remove any contaminates so that it would not affect the next step in the grinding process. In between the Dac and Nap polishing steps, the samples were cleaned with soapy water in a bucket then sprayed with ethanol and air to prevent the samples from rusting. It was crucial that the samples did not rust so accurate harness and microcopy pictures could be taken.

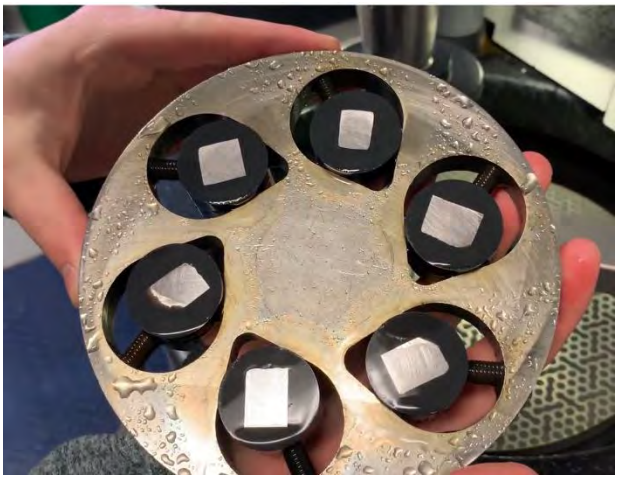

Figure 36: Mounted keel block samples- mid polishing

II. Macrohardness

The keel block samples were tested in accordance with ASTM E18-20 standard for Rockwell Hardness of Metallic Materials. The Rockwell hardness test is an empirical indentation hardness test that can provide useful information about metallic materials. This information may correlate to tensile strength, wear resistance, ductility, and other physical characteristics of metallic materials, and may be useful in verifying theoretically predicted values. For this particular test, the fractured charpy bars from the first round of testing at Westmoreland acted as the test samples. This was done based on the fact that these samples were already machined with precise flat edges as compared to the whole keel block bars. This gave the best chance for accurate results, as there would be no surface inconsistencies to skew the hardness values. Macro-hardness was taken on each of the 4 machined charpy bars from the designated keel blocks with 5 samples taken on each charpy bar for statistical significance. Tests were conducted using a Wilson Rockwell hardness tester with a diamond spheroconical indenter in order to obtain Rockwell C hardness values. The machine was set to a total test force of 150kgf, and each indent was spaced at least 0.1875 in between each indent and 0.1563 in from the edge of the sample to ensure accurate readings. The data obtained from the test block and the respective charpy bars are shown below in tables (#) and (#), respectively.

Table 27: Macrohardness of Calibration Block 62.6 HRC ± 0.08

Test #	Hardness (HRC)
Calibration 1	61.5
Calibration 2	61.0
Calibration 3	61.5
Calibration 4	62.0
Calibration 5	61.5
Average	61.5
St Dev	0.32

Table 28: Macrohardness of Charpy Test Samples

Test #	Hardness (HRC)	Test #	Hardness (HRC)	Test #	Hardness (HRC)	Test #	Hardness (HRC)	Total
C1.1	49.0	C2.1	50.0	C3.1	51.0	C4.1	49.0	
C1.2	49.5	C2.2	49.5	C3.2	51.5	C4.2	49.5	
C1.3	49.5	C2.3	49.0	C3.3	51.0	C4.3	49.5	
C1.4	49.0	C2.4	49.0	C3.4	49.5	C4.4	46.5	
C1.5	49.5	C2.5	48.5	C3.5	51.0	C4.5	48.5	
Average	49.3		49.2		50.8		48.6	49.5
St Dev	0.27		0.57		0.76		1.24	0.35

Figure 37: Fractured charpy bars undergoing macrohardness testing and the 5 locations of indentation

III. Microhardness

In order to determine the hardness of the hammers after heat treatment, microhardness was conducted to determine the bulk hardness. This in particular was an important test to conduct, as the hammer was required to be within a certain range of hardness values (45 to 60 HRC) in order to comply with our design specifications. Traditionally, microhardness is utilized to evaluate and quantify hardness variations that occur over a small distance, such as surface hardening from shotblasting or from carburization. However, based on ASTM standard E384-17, test forces in the upper region of the force range may be used to evaluate bulk hardness. In general, it is suggested that the Vickers indenter as compared to the Knoop indenter is better suited for determining bulk (average) properties. Vickers hardness is better for bulk property exploration since it is not altered by the choice of the test force, from 25 to 1000 gf, because the indent geometry is constant as a function of indent depth. As a result, the Vickers hardness indenter was used with a force of 500 grams force (gf) and a 5 sec dwell time in accordance with the ASTM E384-17 to allow for the Vickers hardness readings to be converted into the Rockwell C hardness scale. It was determined that the hardness values should be converted to Rockwell C because the Rockwell C scale is the most commonly used hardness scale in industry and would allow the results to be more easily quantifiable.

Microhardness was carried out using Penn State Behrend's MMT-X7A Clemex Microhardness Machine. After the mounted samples were polished to mirror finish, they were placed into the microhardness sample holder and slid under the microscope. Once the samples were under the microscope, the Clemex computer software was used to create a 3x3 grid pattern with a 1500 micron x 1500 micron spacing to allow for hardness to be obtained across the entire sample surface and so statistical significance could be achieved on each sample. The reason microhardness was taken from six different samples was to enable a statically significant population mean to be calculated from the sample data. This method allowed for any small deviations throughout the material to average out and gave a representative hardness that is achieved throughout the hammer. Based on the fifty-four samples taken, the material processed an average hardness of 51.60 Rockwell C with a standard deviation of 0.757. This proves that our material, after undergoing our chosen processing, provided the hardness values outlined in the specifications.

Table 29: Average Microhardness of all Samples

Average Hardness	Hardness (HV)	Hardness (HRC)
Average	530	51.6
St Dev	9.3	0.76

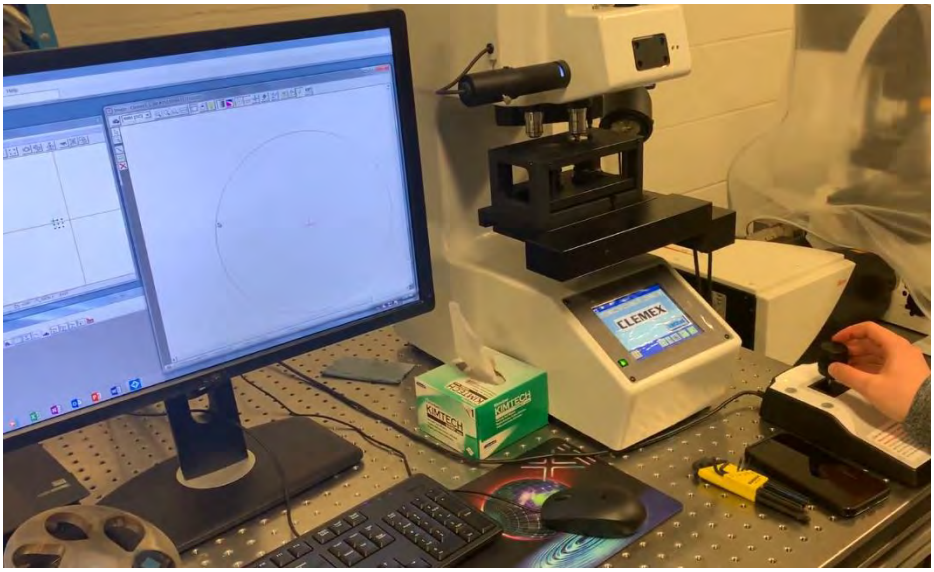

Figure 38: Process of gathering microhardness data

IV. Microstructure Imaging

By examining and quantifying a material's microstructure, its performance can be better understood. Different techniques are used to reveal the microstructural features of metals. Most investigations are carried out with incident light microscopy in brightfield mode, but other less common contrasting techniques, like darkfield or differential interference contrast (DIC), and the use of color (tint) etching are expanding the scope of light microscopy for metallographic applications. The microscopy portion of the material testing was conducted using a Zeiss Inverted microscope system for metallography. The premise of the microscopy work was to analyze the grain structure, dendrites, martensite, and interdendritic regions found within the cast heat-treated samples. By investigating the microstructure allowed for porosities and other defects to be detected and allowed for further analysis of material properties through the measuring of grain size and the distance between the dendrites.

The goal of the microstructure investigation was to obtain images of the grains, martensite, and dendrites within the samples and to measure their relative sizes. In order to study the microstructure, the samples first needed to be etched to bring out the respective microstructure that was being analyzed. Since AF-96 is not normally sand cast the research on etching procedures is very limited. A small etching study was conducted on the material to try and achieve the three different microstructure properties that were trying to be achieved. Although some images were obtained of the microstructure, this is not a conclusive list. More research needs to be done on determining a proper etching process to see the grain structure of the material. The etching procedure used for each chemical is contained below with the respective microstructure picture. To further analyze the effects of HIPing and heat treating, an etching procedure was also done on the wrought material cut off from the casting after they were broken out of the molds.This allowed for a comparison between the microstructure depicted by this

wrought material and that which was depicted by the hipped and heat treated material. Any differences seen would indicate the effect that the post-processing operations had and offer insight into whether or not they truly benefit the material as intended. The etching procedure used is listed below for the wrought material along with the accompanying microstructure pictures.

Table 30: Etching Procedure Used on Hipped/ Heated Treated Samples

Etch	Application Method	Voltage	Duration	Microstructure Seen
Alkaline picrate	Immersion (boiling)	N/A	35 minutes	Dendrite/ Martensite
3% Nital	Swab	N/A	5 seconds	Dendrites / Martensite
Formula LNC1	Electroetch	0.80 V	5 minutes	N/A (burned)
Alkaline Picrate	Immersion (boiling)	N/A	25 minutes	Dendrite/ Martensite
Formula 112A	Electroetch	0.22 V	5 minutes	N/A
Watertown	Electroetch	0.22 V	5 minutes	N/A
Watertown	Immersion (boiling)	N/A	1 minute	N/A
Nitrosulfuric Acid	Swab	N/A	5 seconds	Dendrites
Nitrosulfuric Acid	Swab	N/A	1 second	Dendrites

Table 31: Etching Procedure Used on Non-hipped/ Heat Treated Samples

Etch	Application Method	Voltage	Duration	Microstructure Seen
3% Nital	Swab	N/A	5 Seconds	Grains
Oberhoffer	Immersion	N/A	5 seconds	Dendrite/ Martensite
Formula 2611A	Electroetch	0.1 V	5 minutes	Dendrite/ Martensite

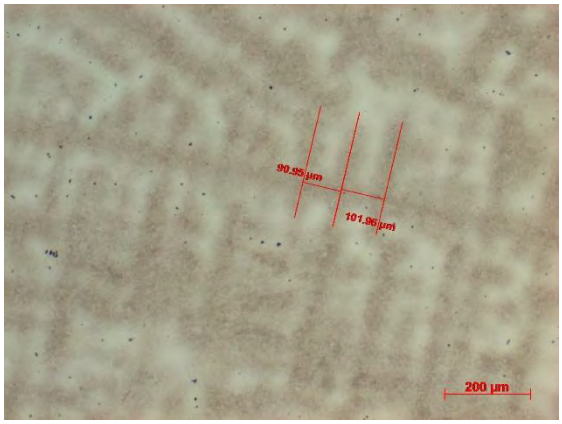

Figure 39: 3% Nital Swab (5X zoom)

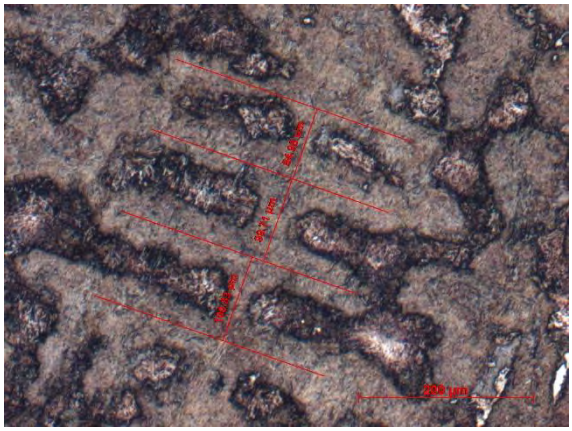
Figure 40: Nitrosulfuric quickswab (10X zoom)

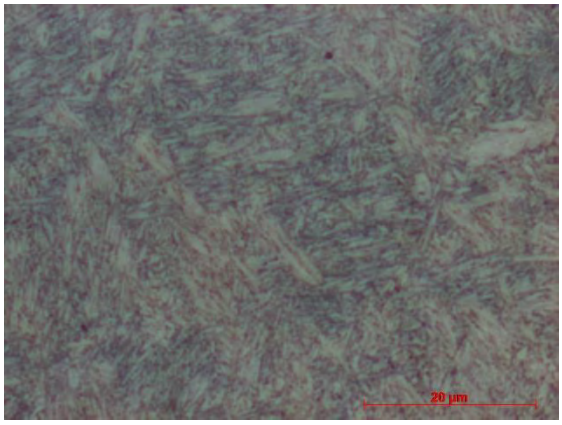

Figure 41: Alkaline Picrate 25 minutes (100x)

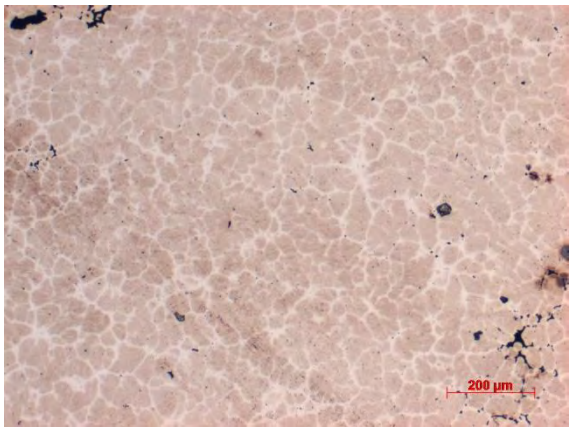

Figure 42: 3% Nital Swab on vent w/ 5x zoom optic

VI. SEM (Scanning Electron Microscope)

Brief overview of SEM/EDS:

A scanning electron microscopy (SEM) scans a focused electron beam over the surface of the sample. Pictures are taken slowly as the beam scans over the sample and the electron beam can only be focused in a vacuum. The beam is emitted from an electron gun with the power source coming from either a thermionic gun (heated tungsten or lanthanum hexaboride, LaB_6, filament) or a field emission gun (FEG, electric field physically pulls electrons from a tungsten crystal).

The SEM used in Penn State Behrend's lab is an Environmental SEM, or ESEM, made by FEI. The model currently in use is a Quanta FEG 650 which means that the field emission gun is the electron source. The FEG is special because it produces the highest intensity electron beam of any power sources and the beam can stay on all the time, as opposed to filament sources that have a working hour life before needing replacement. The "environmental" designation means that gas can be added to the chamber (such as water vapor), which is really useful for biological samples and samples that are non-conductive under the electron beam.

Types of electrons:

Generally, under the SEM, secondary electrons, backscattered electrons, and characteristic x-rays are looked at and analyzed. All these electrons are emitted when the sample is hit with the electron beam. Some electrons are knocked out of the atoms of the sample by the electron beam, called secondary electrons, and come from the sample itself. Secondary Electrons are found closest to the surface of the sample and are useful for showing topology (i.e. classic electron micrograph). Some electrons from the beam interact with the nuclei of the atoms of the sample and are spit back out, called backscatter electrons. These are not from the sample explicitly but from the electron beam, and they interact with the sample when they come back. Backscatter secondary

electrons come from deeper inside the surface of the sample and are useful for showing differences in chemical composition of parts of the sample (heavier elements appear brighter under the backscatter detector as they have a bigger nucleus to interact and diffract more electrons, and lighter elements appear darker).

Energy dispersive x-ray spectroscopy (EDS):

When electrons are knocked out of the atoms of the sample, they are replaced by others and emit a characteristic x-ray. These x-rays are used to determine the composition of the sample. However, there is a second type of x-ray that shows up in the EDS analysis which are Bremsstrahlung x-rays. These are produced when the electrons from the beam lose energy and change direction from interacting with the sample. This phenomenon is also called braking radiation or background radiation and is usually approximated during the EDS analysis by a line.

Types of detectors:

The classic SEM detector is an Everhart-Thornley Detector (ETD) and it is used for secondary and backscatter electron imaging in high vacuum mode which is mainly used on conductive samples like metals. The other detectors used on the SEM are a Large Field Detector (LFD) for imaging in low vacuum/ESEM modes which is mainly for non-conductive samples, and an EDAX detector for x-ray collection.

SEM report:

For this report, SEM pictures were taken from the polished keel block samples and the facture surfaces from the charpie bars. Based on the general data found, there were a lot of small inclusions on the fracture surfaces and in the polished/etched samples. Most of the inclusions were produced during the solidification of the casting. For example, one type of inclusion found was manganese sulfide. These are pretty common in steel castings when the manganese hangs onto the sulfur. It is possible that there was also hydrogen damage as indicted by the pockets of round holes (“fish eyes”) on C-2.

There were also some inclusions of titanium, aluminum, and niobium. Although it is not easy to pinpoint exactly what process caused the inclusions, there are some indications that the inclusions were caused due to potential products that PRL Regal Cast used during the casting process. For example, Ferrotitanium could have been added to steels as a grain refiner in an attempt to clean up the steel by binding to elements not desired but there is a possibility that it could have stayed in the melt. Aluminum also could have been used as a deoxidizer to suck up the oxygen and form a slag, but it can also grab onto the gasses in the melt and form nitrides and oxides. Another possibility is that Niobium could have been used as a ferrite stabilizer to limit the grain growth of austenite.

The best way to prevent a lot of these defects found within the material is with an argon oxygen decarburization (AOD) for the melt. AOD removes dissolved gasses, sulfur, and other non-desired elements and helps eliminate the use of other additives that

may not leave the melt. Unfortunately, due to the furnace used at PRL Regal Cast an AOD was not able to be used on the material thus creating some small inclusions within the material which could have ultimately affected the material properties.

On each of the samples, several spot and area analyses were done to determine the composition at each selected spot. This was done by first etching the three polished samples using 3% Nital solution, Oberhoffer's Reagent, and Vilella's Reagent, respectively. The procedure for etching the samples can be found in table # below. The etched samples and the fractured surfaces were placed into the SCM and analyzed by focusing the SEM's electron beam in selected areas of the samples and picking up all the x-rays that came off of those particular sections. This process generated an EDS report that displayed all the elemental rays that bounced back from the initial electron beam. On some of the samples, the counts on the graphs were somewhat noisy. This is due to some of the elements giving off more x-rays than others, or if the spot was low on the sample, such as a valley, the x-rays have a harder time making their way back to the detector. Based on the EDS spot analyze reports, inclusions can be found in the material from the pouring process, such as MnS, AlN, Nb, Ti, etc. Although the fracture surfaces show higher levels of oxidation, this is pretty typical due to the fracture surface being exposed to air after testing. Further research could also be conducted on the carbides within the microstructure to determine how their size and orientation effect the overall material properties of the material along with which alloying elements grabbed the carbon.

Source:	**For use with:**	**Name:**	**Composition:**	**Method information:**
[1]	Carbon and low-alloy steels	Oberhoffer's Reagent	500 mL H_2O 500 mL alcohol 30 g $FeCl_3$ 0.5 g $SnCl_3$ 1.9 g $CuCl_2$ 40 mL HCl (concentrated)	Macroetch. Use at room temperature and immerse for approximately 20 s.
[2]	Ferrous, most steels, stainless steel	Vilella's Reagent	1 g picric acid 10 mL HCl 100 mL alcohol	Vilella's reagent. Immerse sample at room temperature. Use polished surfaces.
[1]	Carbon and low-alloy steels	2% nital etch	2 mL nitric acid (concentrated) 98 mL ethyl alcohol	Common etchant for carbon and low-alloy steels. Reveals ferrite grain boundaries and constituents

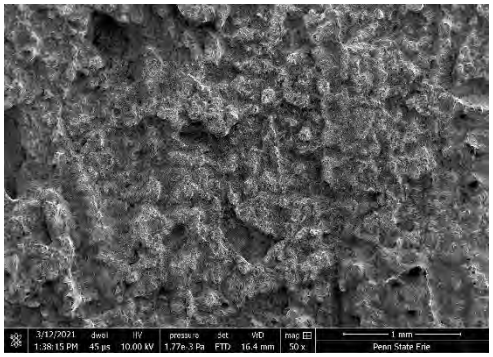

Figure 43: C-1 at 50X magnification

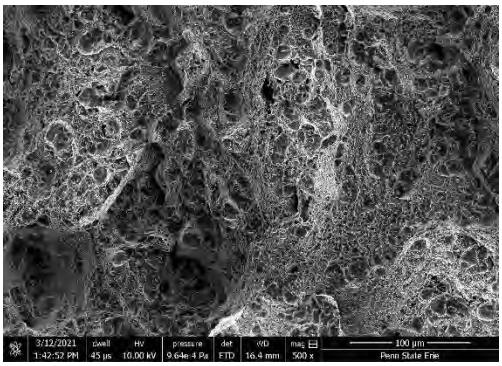

Figure 44: C-1 at 500X magnification

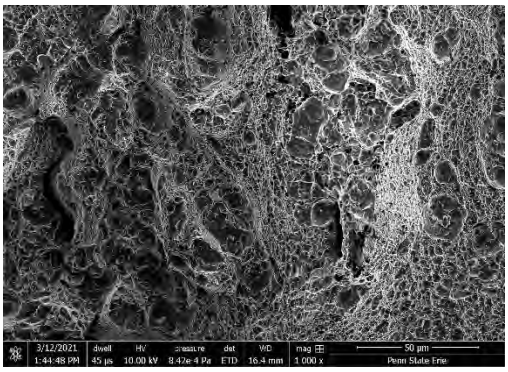

Figure 45: C-1 at 1000X magnification

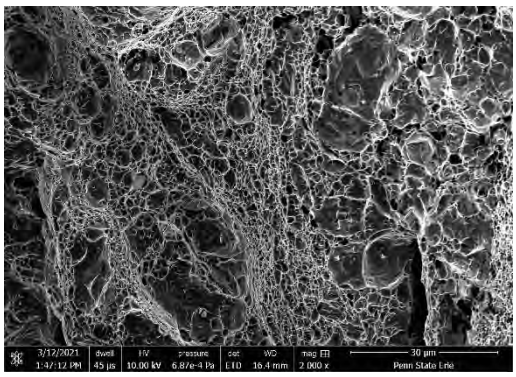

Figure 46: C-1 at 2000X magnification

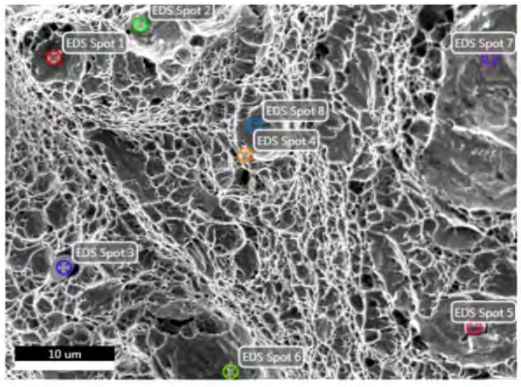

Figure 47: C-1 ESEM Analysis Spots

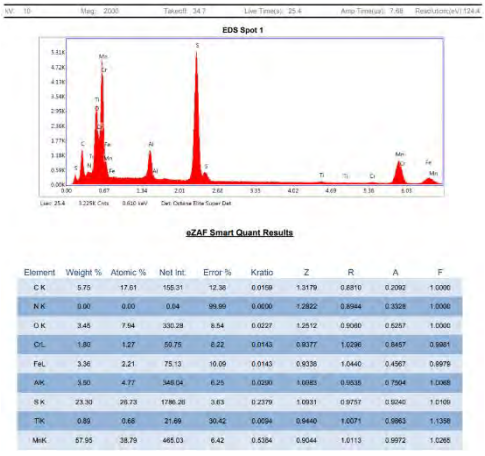

Figure 48: C-1 ESEM Spot 1 Report

Thank You's and Honorable Mentions

The completion of this project would not have been possible without the help our industry partner and sponsors. We would like to take the time to thank each one of them for supporting our group. We would like to thank PRL Regal Cast for being our industry partner and for working so closely with us. We appreciate them allowing us to come and see the hammers being poured. Without them, we would not have been able to get a completed product. Another crucial person who helped us throughout the way was Laura Karduck from PRL Regal Cast. She helped guide us through the mold design process and was a valuable resource when our group had any questions. Another crucial company to our success was Urick Ductile solutions and Hoosier Pattern. The two companies were able to take our design and create it into a 3D sand printed mold using their ExOne 3D printer in under a week. Next, we would like to thank Pressure technologies out of Painesville, Ohio for HIPing our hammers. Their quick turnaround allowed us to reduce the microporosities within the hammer and get the homogeneous composition that we needed for competition. We would also like to thank Oberg Industries out of Sarver, PA for allowing us to use their machining equipment to get the hammers down to competition weight. Another company that was of great help to us was Westmoreland Material testing out of Latrobe, PA. They were able to take our samples, machine them, and test them in under a week so that we would have accurate tensile and charpy data for our report. Now we would like to thank Sam Fillar and FammySillar productions for capturing drone shots of the Penn State Behrend campus. These shots allowed the group to showcase the Penn State Behrend campus during the introduction video with high quality production shots. Another person we would like to thank is Connor Hinton for allowing the group to use his milling equipment along with helping the group when needed. If it was not for him and his equipment the manufacturing portion of this hammer could not be completed. We would also like to thank PhD Candidate Christie Hasbrouck and Dr. Paul Lynch for their assistance throughout the entirety of this project. Their devotion to assisting us allowed our team to produce the highest quality product that we possibility could. Finally, we would like to thank Penn State Behrend for allowing us to use on campus recourses in order to finish this project. We very much appreciate everyone we have worked with throughout this project. This opportunity has allowed us to make industry contacts that we will have for the rest of our lives.

Appendix

Appendix A: Material Selection- AF96 Patent Information

Low alloy high performance steel, by Rachel Abrahams. (2016. Dec. 22). *US20160369362A1*. Accessed on: Mar. 19, 2021. [Online]. Available: https://patents.google.com/patent/US20160369362A1/en#patentCitations

[0025] Table 1 - Alloy Steel Composition Content by Weight (%)

Element	Approximate Percentage by Weight (%)
Carbon (C)	0.24 to 0.32
Chromium (Cr)	2.00 to 3.00
Molybdenum (Mo)	0.50 to 1.50
Vanadium (V)	0.05 to 0.35
Manganese (Mn)	1.00 or less
Nickel (Ni)	3.00 or less
Silicon (Si)	1.25 or less
Copper (Cu)	0.15 or less
Phosphorous (P)	0.015 maximum
Sulfur (S)	0.02 maximum
Calcium (Ca)	0.02 maximum
Nitrogen (N)	0.15 maximum
Aluminum (Al)	0.025 maximum
Iron (Fe)	Balance

Appendix B: Lead-Slug Case Study

Background and Rationale:

As an entry in SFSA's Cast in Steel competition, the designed hammer will subsequently undergo performance evaluation in a series of tasks. However, in accordance with the competition regulations, the task specifications, those more specific than "it will be used as a hammer", are not disclosed to participants prior to the event.

Not only do the typical functions of a hammer vary significantly depending on the style of hammer, but the overall performance of the hammer, as a tool, is also very subjective to the metrics of the user and the surface it contacts. An individual's height, weight, and strength factor into their capability to generate swing velocity, and by consequence, into the force of the strike. Furthermore, depending on the material properties of the surface, such as hardness and toughness, the hammer will experience very different loading conditions upon impact. Due to the variability in conditions, it is difficult to find a standard estimation for the typical load a hammer will experience during usage.

To reduce the number of unknowns in the development of design specifications for the project model, several assumptions were made based both on the structure and uses of Thor's

hammer in the Marvel films and on previous competition participation. The movie interpretation of the Thor's hammer consists of a head with a uniform width and two parallel striking faces. Throughout the film series, the hammer is primarily used for high impact crushing and pounding applications on surfaces ranging from stone to metal. As a result, it is expected that the use of the hammer in competition can most accurately be compared to the functions of heavy striking tools, such as stone or blacksmith sledges. The project model should be designed based on both the ASME regulations for these tools as well as interaction with the surfaces of impact closely associated with these tools. Additionally, based on the evaluation process in competitions of previous years, it is very likely that two adult males will carry out the testing. The load-bearing capacity of the design must also account for the capability of a male user.

In order to obtain values for the loads that would most accurately reflect the loading conditions expected to be induced during the competition, a testing method was developed by building off these previously stated assumptions. The method involved conducting a series of impact tests in which male users of a capability similar or greater to the competition testers struck lead slugs with a 4-lb Engineer's Hammer as the resulting deformation was recorded. Users with a height and weight above that which classifies as average conducted the tests so that the forces generated would likely be larger than the force an average male can generate. This more or less imparts an initial safety factor into the data that will be referenced in the design phase. Tests also utilized a 4 lb hammer because, although the overall weight of the designed hammer will be nearly 6 lbs, its head weight will likely be much closer to 4 lbs to account for the weight of other components.

The goal of the case study was to essentially mimic the impact the hammer will undergo throughout the performance evaluation to produce estimations for the impact loads the judges will be capable of generating. Modeling and analyzing impact is very difficult due to its instantaneous nature and limited manners of measurement. This case study required making several assumptions and simplifications in order to allow for force determination. Because of this, the force values generated are not intended to be used as maximum force values on which to base design criteria. Instead, the purpose of determining these values is to give a reference baseline value of the average force that the hammer may experience, as this was difficult to find through research. This reference can then be used as the minimum force that the hammer must withstand, as a factor of safety will be imparted on this value to ensure that the design can withstand the large loads associated with the competition testing.

Materials:

- 4-lb “Engineer” Hammer
- Steel Anvil
- Machined Steel Mold
- .75” Diameter , 1” tall Soft Lead Cylindrical Slugs with arbitrary 3/8” “tang”
- GoPro Hero 7 camera (Video used at 240 Fames/sec)
- Large Ruler

Procedure:

Machine mold:

1. Select and cut steel barstock to fit the proposed 3/4” casting dimensions of the slugs
2. Face both ends of steel cylinder on a lathe at a speed of roughly 300 rpm
3. Center drill, drill 3/8” through hole (approximately one inch depth) as the pritchel hole
4. Bore a .75” Inner Diameter hole 1” deep to act as the mold for the casting
5. Break all sharp corners.

Casting:

1. Heat lead in ladle with propane torch until liquid (remove slag as needed)
2. Sit mold on flat steel surface and spray inside surfaces with oil based lubricant,
3. Pour molten lead from the ladle into the mold until full and allow to metal solidify.

Casting Removal:

1. Place the mold in an arbor press and force the casting from the mold with a 3/8” punch.

Testing:

1. Measure initial height of samples and record measurements in a notebook
2. Place the aforementioned 3/8” “tang” of the slug into the pritchel hole of an anvil to keep the slug steady during testing
3. Place the reference ruler behind the anvil, ensuring that the intervals are clearly visible

4. Film the user hitting the slug at 240 frames per second (Frame limit for the GoPro Hero 7 Camera)
5. Measure final sample height.

User	Test	Speed (ft/s)	Deformation(in)	Force (lbs)
6' 4" 245	B1	40	0.3125	3809.15
	B2	52.5	0.375	5468.40
	B3	60	0.5	5356.00
6' 3.5" 218	J1	40	0.25	4761.00
	J2	40	0.25	4761.00
	J3	60	0.4375	6122.05
6' 235	T1	45	0.125	12052.80
	T2	47.5	0.125	13429.20
	T3	50	0.25	7440.00

Calculation:

1. Using the video as reference determine the speed of the hammer head at impact
    i. The change in position the hammer makes in one frame is noted based on the ruler that is placed behind the anvil
    ii. Using the fact that the camera records at 240 frames/sec, the time for one frame can be estimated and used with the change in position during one frame to solve for velocity
2. Determine the difference between initial and final height of sample (deformation)
3. Use speed and deformation values in a simplified Work-Energy relation to determine an experimental estimate of force.

Sample Equation to Solve for Force

- y: the distance covered by the hammer during one frame
- t: the camera-designated time increment of one frame (1/240 seconds)
- V: velocity of the hammer at impact (ft/sec)
- m: mass of the hammer head (converted from lbs to slugs)
- D: deformation amount undergone by each slug (inches converted to feet)
- F: force generated by the impact (lbf)

$$V=y*t$$

$$12 * m * V^2 = F * D$$

Assumptions

a. This study looks at the "system" as only the hammer head and lead slug, all other elements are simply external supports and/or loads.

b. All Kinetic energy is halted by the work done by the lead slug opposite direction of motion with no losses.

c. Velocity is an estimated value based off the camera frames and motion blur of the hammer before impact.

d. Any off-center hits were treated the same as centered hits.

e. The anvil was treated as being perfectly rigid.

Appendix C: References for Standards

(1) "Striking Tools," *ASME B107.400-2018*, pp. 1–38, 2019. Retrieved from http://asmestandardscollection.org.ezaccess.libraries.psu.edu/GetDoc.aspx?doc=ASME%20B107.400%202018

(2) Occupational Safety and Health Administration. (1970). *Occupational safety and health standards: Safety and Health Regulations for Construction* (Standard No. 1926.301 (d)). Retrieved from https://www.osha.gov/laws-regs/regulations/standardnumber/1926/1926.301

(3) ASTM Standard E23-18, 2018, " Standard Test Methods for Notched Bar Impact Testing of Metallic Materials," ASTM International, West Conshohocken, PA, 2018, DOI: 10.1520/E0023-18, www.astm.org

(4) ASTM Standard E18-20, 2020, " Standard Test Methods for Rockwell Hardness of Metallic Materials," ASTM International, West Conshohocken, PA, 2020, DOI: 10.1520/E0018-20, www.astm.org

(5) ASTM Standard E384-17, 2017, " Standard Test Method for Microindentation Hardness of Materials1," ASTM International, West Conshohocken, PA, 2017, DOI: 10.1520/E0384-17, www.astm.org

(6) ASTM Standard E8/E8M − 16ae1, 2020, " Standard Test Methods for Tension Testing of Metallic Materials," ASTM International, West Conshohocken, PA, 2020, DOI: 10.1520/E0008_E0008M-16AE01, www.astm.org

Microhardness standard

(7) ASTM International. *E384-17 Standard Test Method for Microindentation Hardness of Materials*. West Conshohocken, PA; ASTM International, 2017. doi: https://doi-org.ezaccess.libraries.psu.edu/10.1520/E0384-17

Appendix D: Concept Generation Process

D1: Head Structure

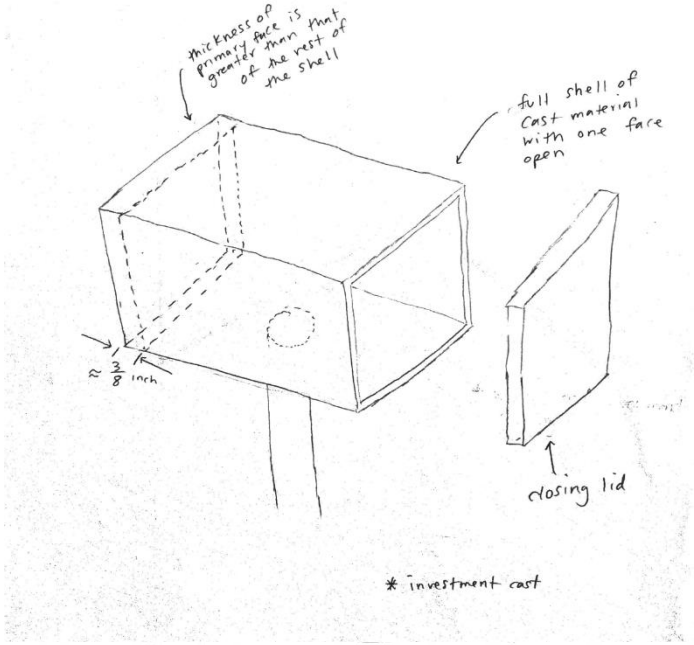

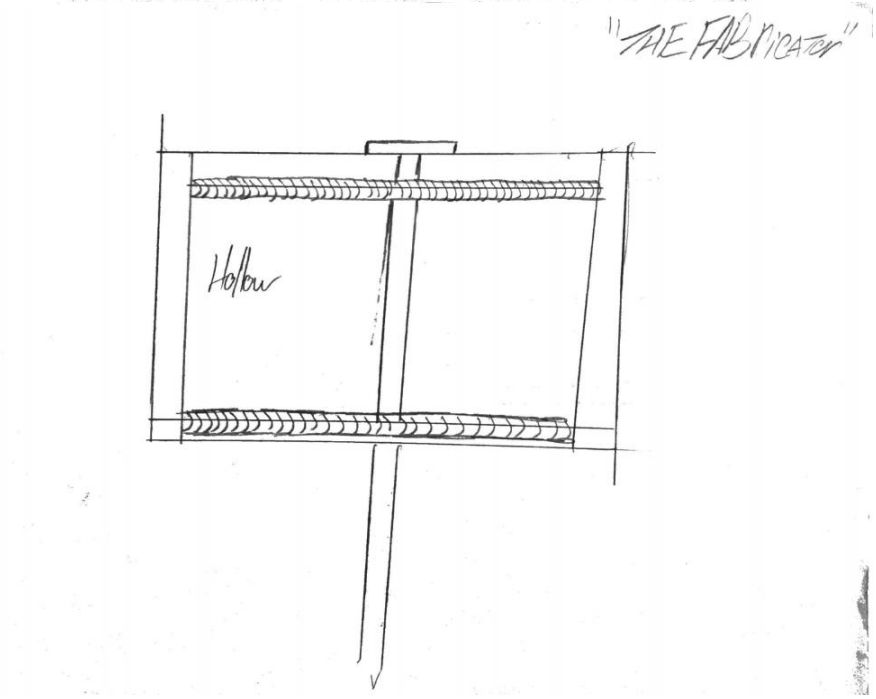

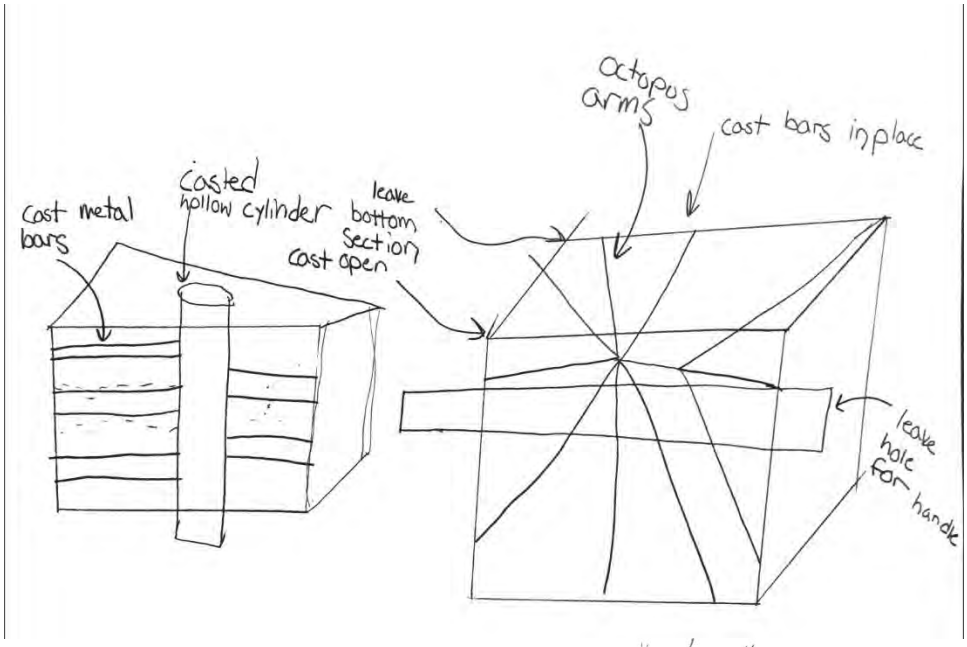
octopus arms
cast bars in place
cast metal bars
casted hollow cylinder
leave bottom section cast open
leave hole for handle

"Hedge Hog"

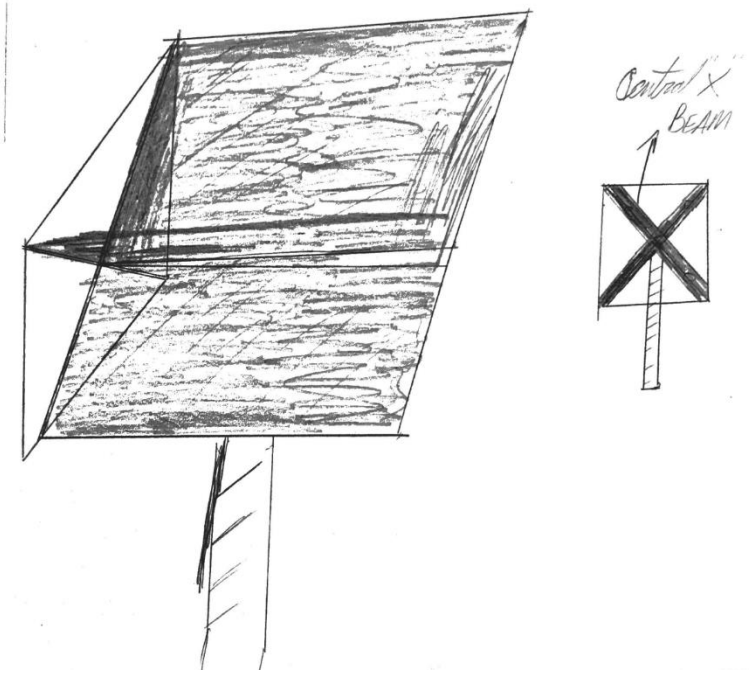
Central "X" BEAM

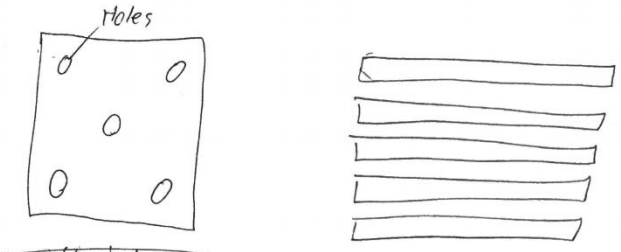

~~weld into holes~~

- wrap and weld outside shell
- put in 3D printed part
- crush ends to hold together — or thread ends in (don't forget lock tight) or both

- have shell fitted and crushed into main plates
- or stick shell into the main plates, then bend the shell to shape

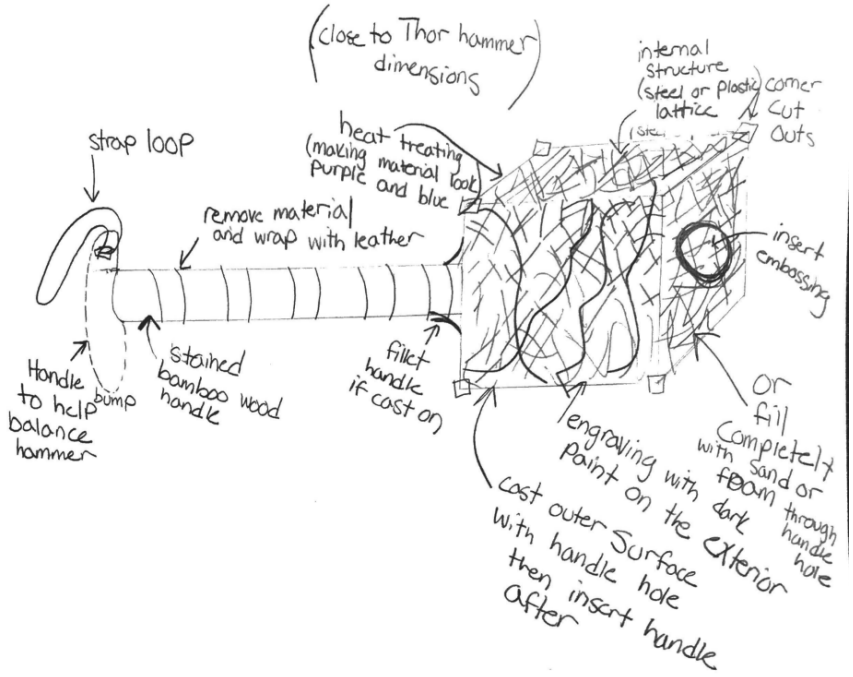

"THE Composite ONE"

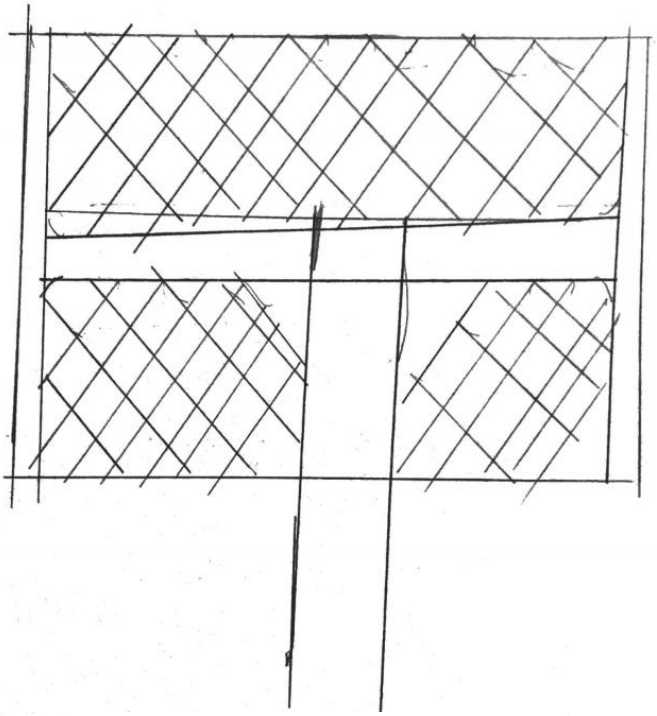

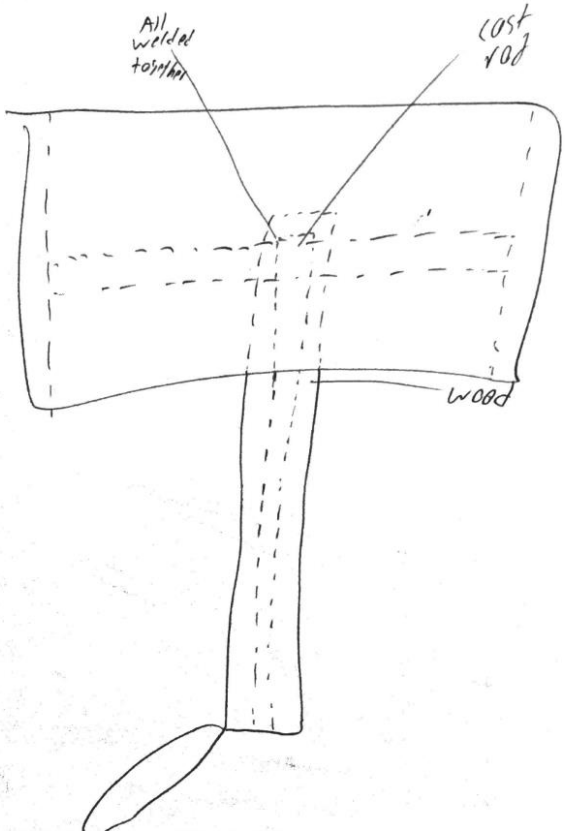

"Big Bar"

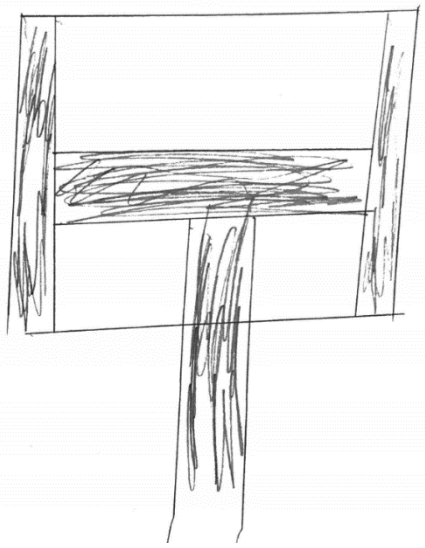

"The Solid Boy"

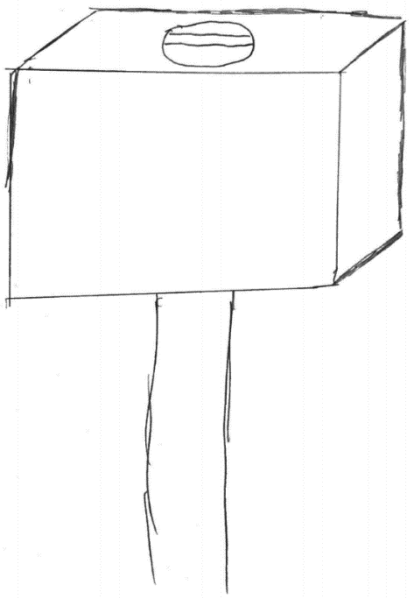

"THE Solid Boy"
Round Edition

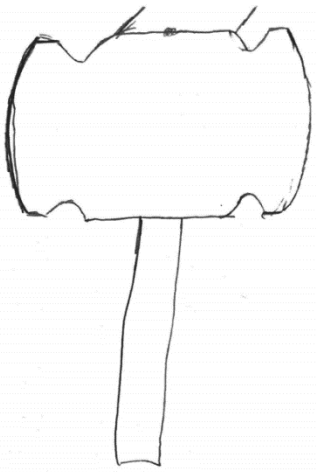

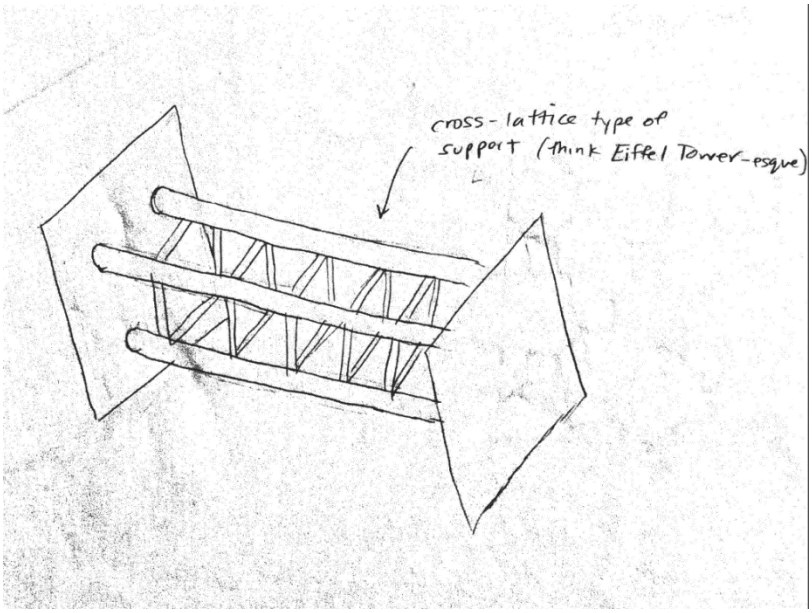

Internal Structure

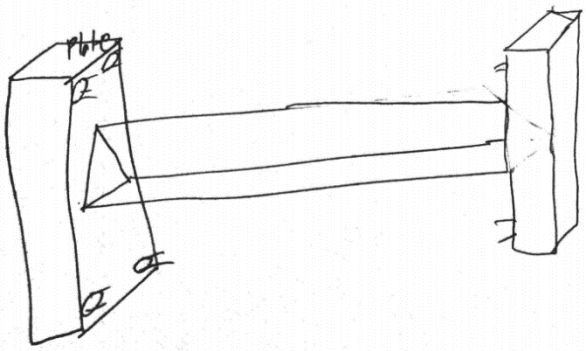

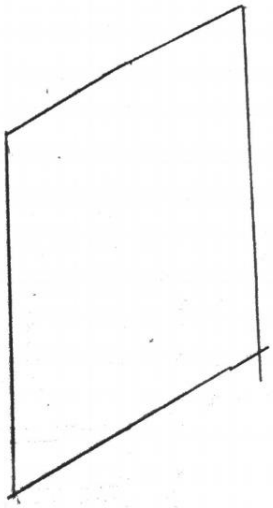

"The Honeycomb"

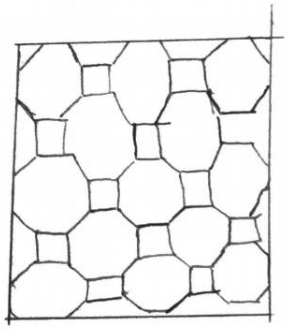

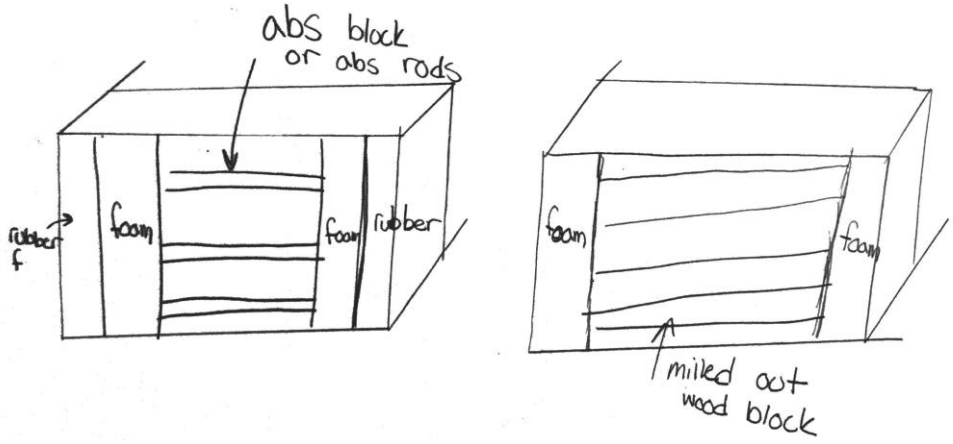
abs block
or abs rods
rubber
f
foam
foam
rubber
foam
foam
milled out
wood block

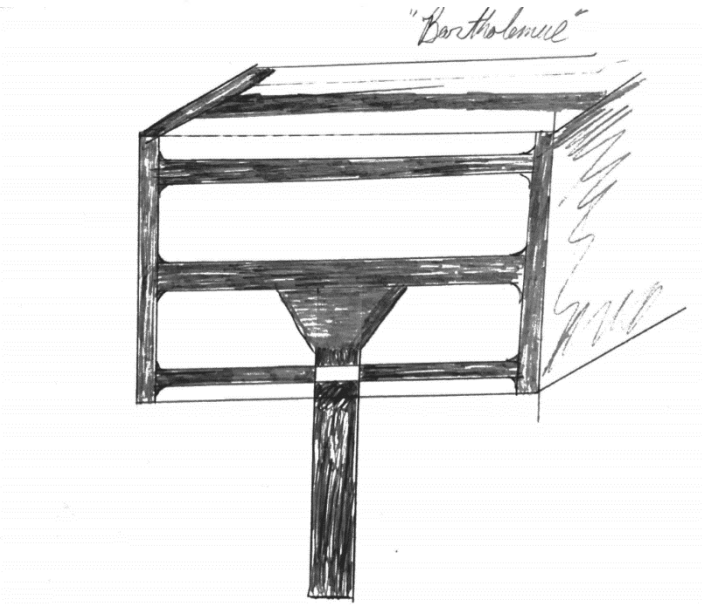
"Bartholomew"

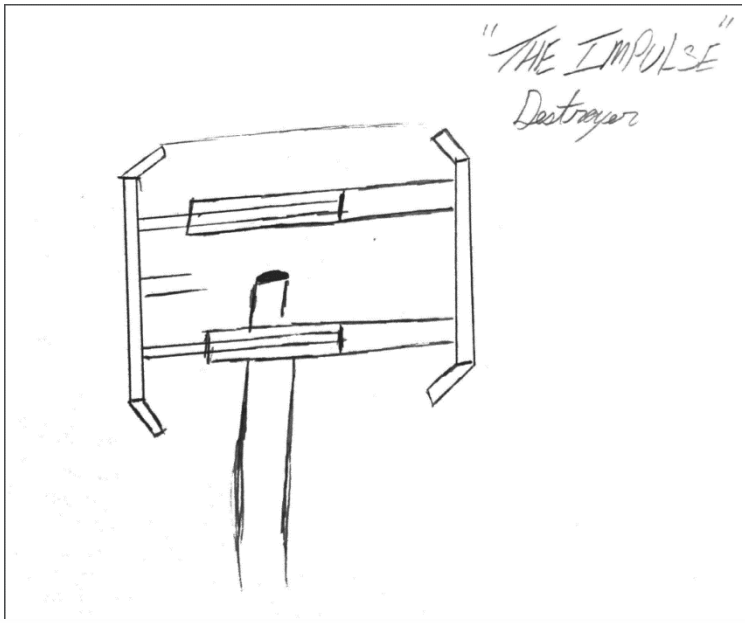
"THE IMPULSE"
Destroyer

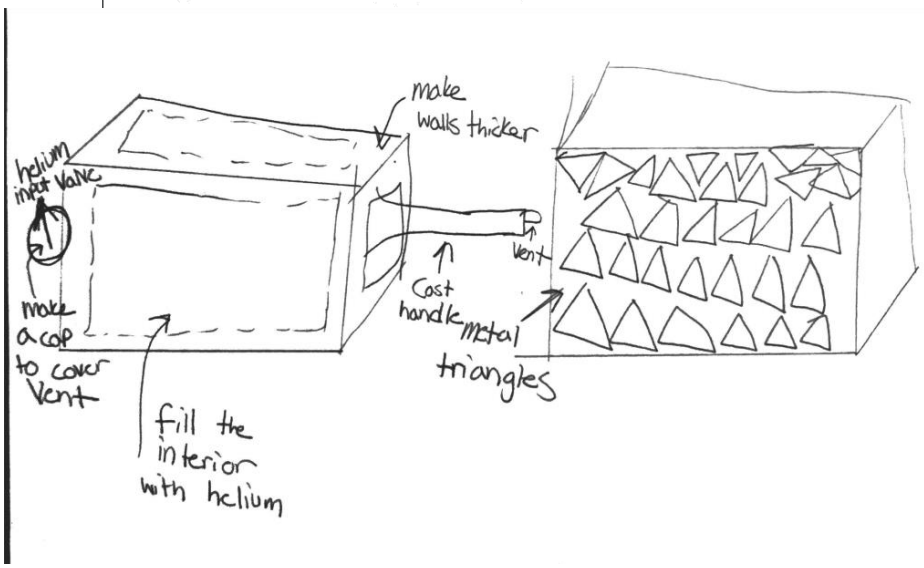
make walls thicker
helium input valve
make a cap to cover vent
fill the interior with helium
vent
cast handle
metal triangles

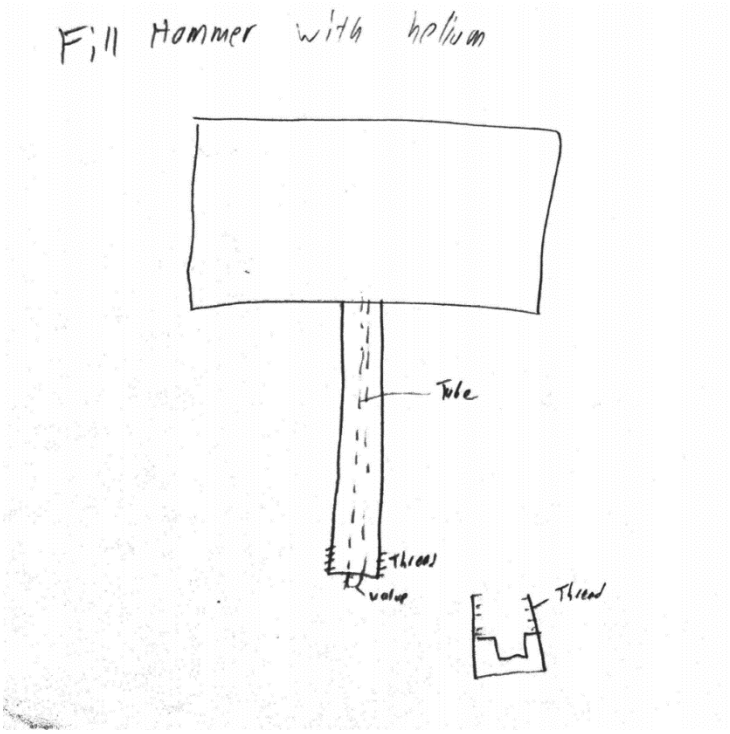

D2: Handle Materials

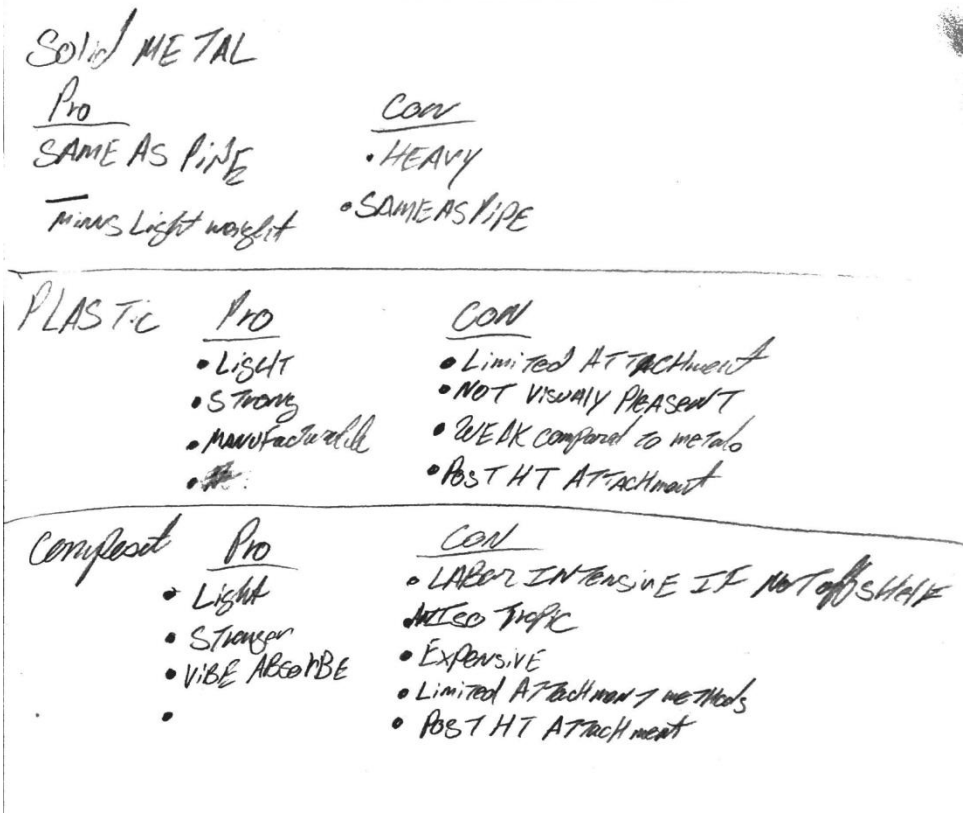

Wood → Hickory

Pro

- Low Density
- Workable
  Easy
- "Standardized"
- Vibe → Absorb
- Accesable
- Cheap
- Strong
- Pretty/Aesthetic

Con

- Anisotropy
- Natural mat
- Split
- Weak compared to metal
- Limited connection methods

Pipe/Tube

Pro

- Light
- Stronger than wood
- Connection possibilities
- Isotropic
- Ens. needed mat
- Polish/Etch
- Pre Heat Treat
  Attachment

Con

- No vibe absorption
- Weak compared to solid
- Metals only
- Bend/crush
-

D3: Connection Method

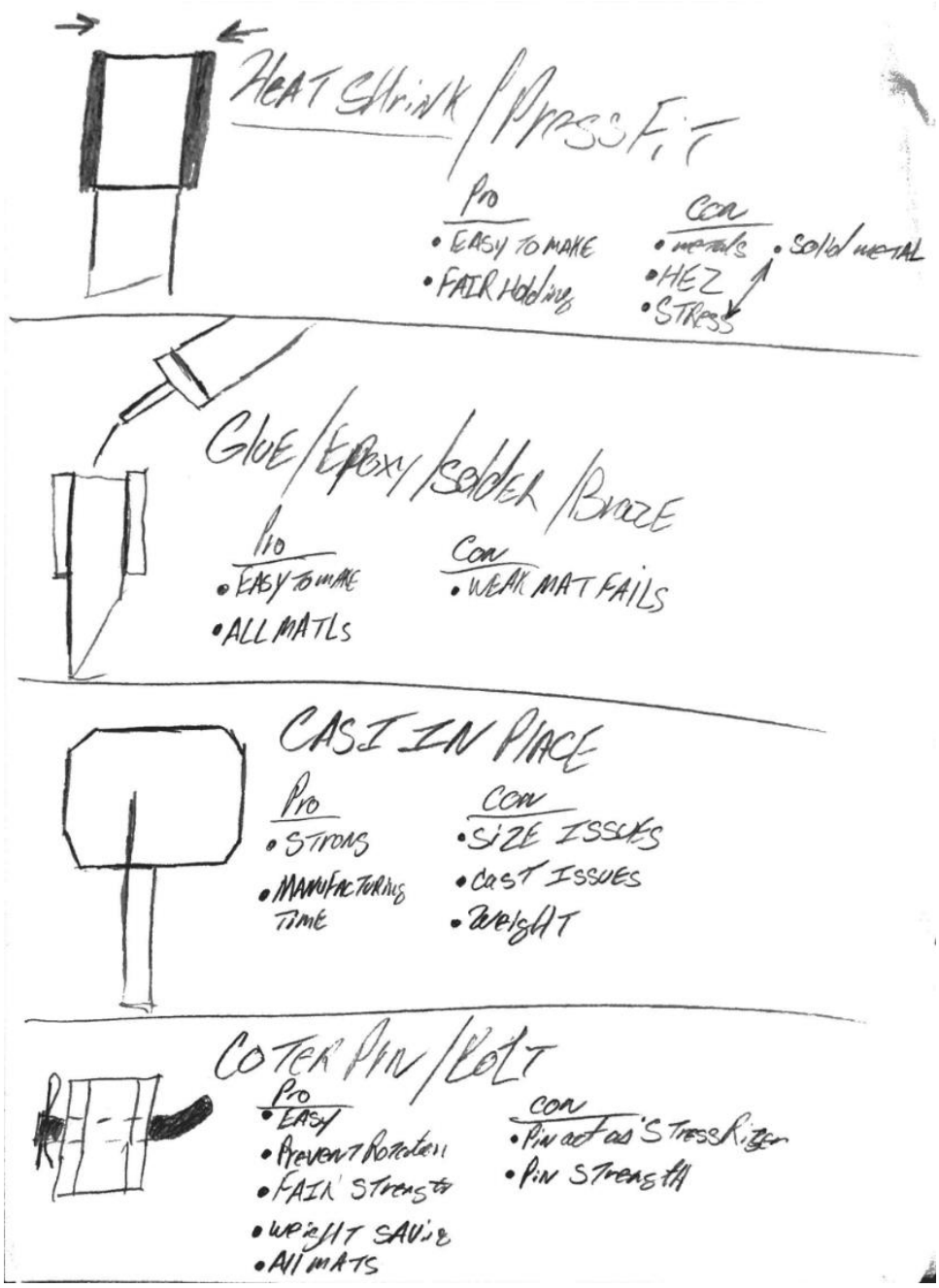

Handle Attachment

Tapered Sleeve w/ wedge

Pro
- All mats
- Mano

Con
- Directional
- Split Hazard
- Loosen

Threaded

Pro
- Easy to make
- Strong

Con
- Only metal
- Loosen

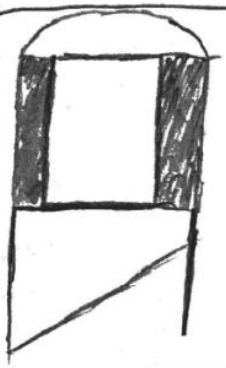

Hot Rivet

Pro
- Easy to make
- Strong

Con
- Directional
- Metals only
- H.E.Z

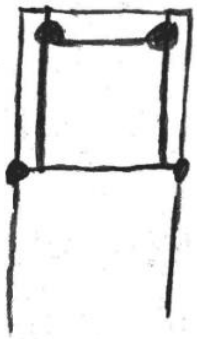

Welded

Pro
- Strong
- Easy to make

Con
- Only Steel
- HEZ
- Porosity/weld failure
- Weight

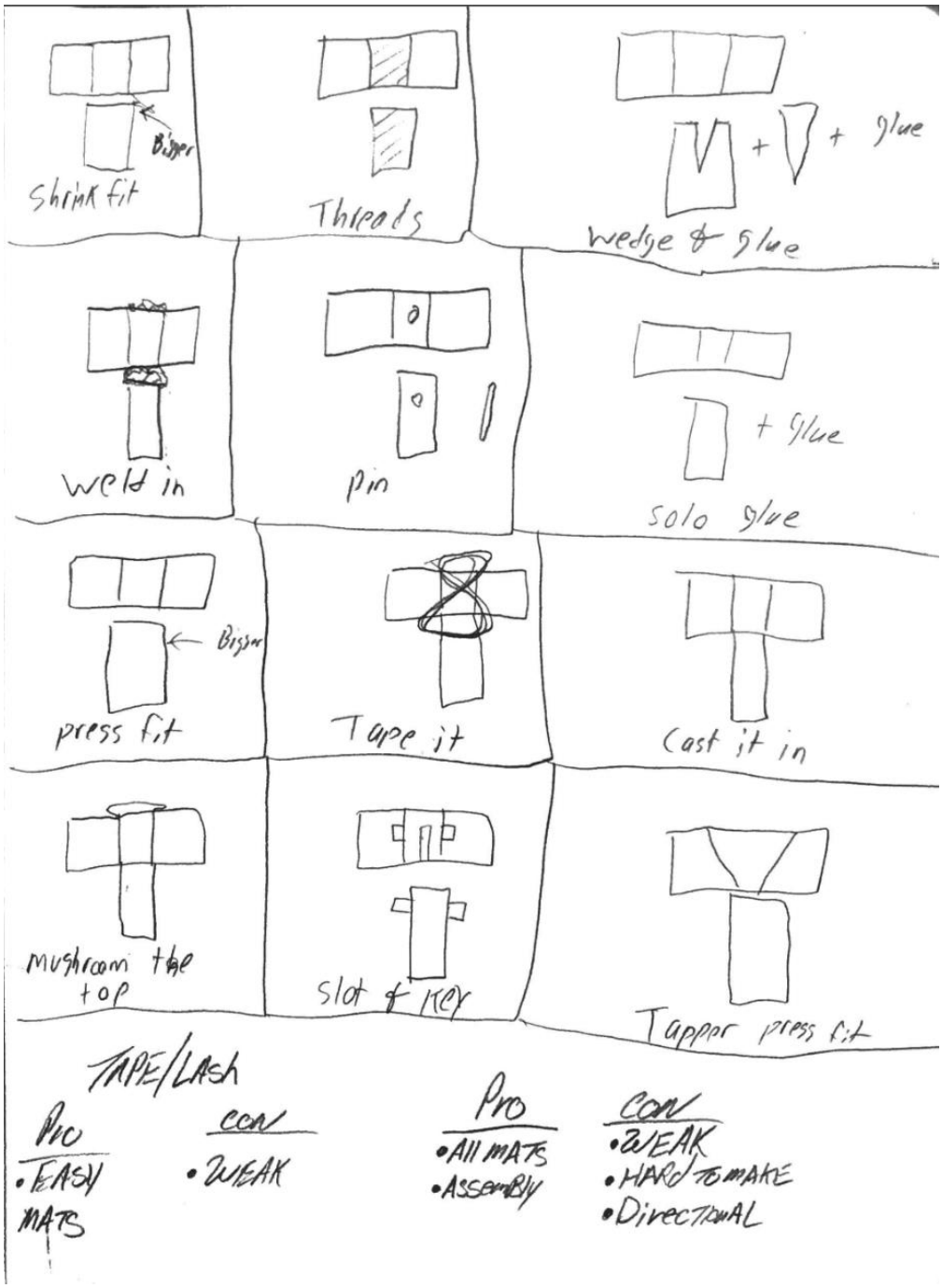
Bisque
Shrink fit
Threads
+
+ Glue
Wedge & Glue
Weld in
Pin
+ Glue
Solo Glue
Bisque
press fit
Tape it
Cast it in
mushroom the top
Slot & Key
Tapper press fit
TAPE/LASH
Pro
• EASY MATS
con
• WEAK
Pro
• All MATS
• ASSEMBLY
con
• WEAK
• HARD TO MAKE
• DIRECTIONAL

Wedge

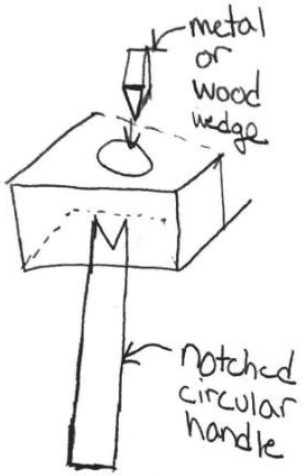

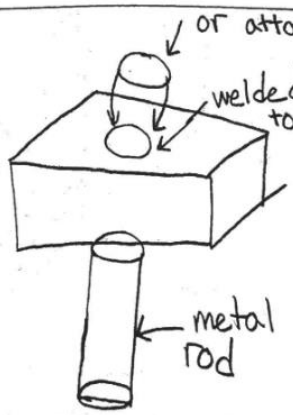

Welded
TUBE

"Welded"

Pro	Con
• EASY	• HEZ
• STRUCTURAL INTEGRITY	• WEIGHT
	• STRENGTH
	• STEEL COST

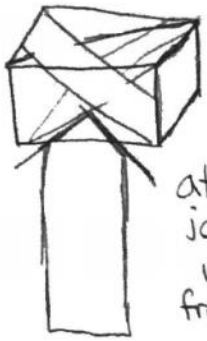

attach handle into triangle joint would have to either weld if metal or secure by a friction fit

---

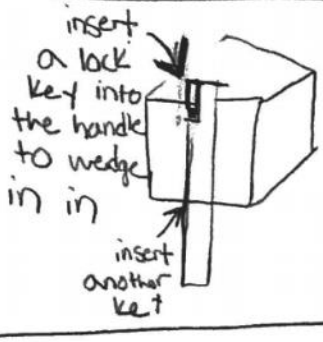

KEY

Pro	Con
• EASY → ISH	• STRENGTH
• MAKCOST	• DIRECTIONAL

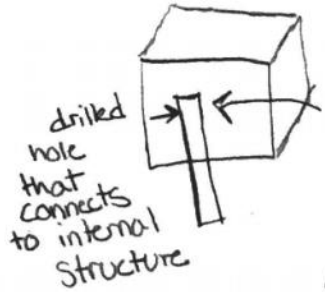

or bond the material to the internal plastic or metal

Pin

Connection Methods

1. 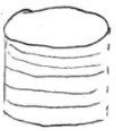

threaded interior of the hole so that handle would essentially screw into head

2. 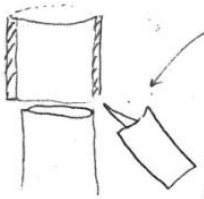

3. 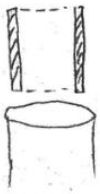

shrink fitting → heat to expand then it will contract when cool

4. 

weld it

5. 

lock pins I guess you could call it

Appendix E: Preliminary FEA- Boundary Conditions and Results

E1: The Hedgehog

Figure #: Simplified Hedgehog Inventor model

Boundary Conditions:

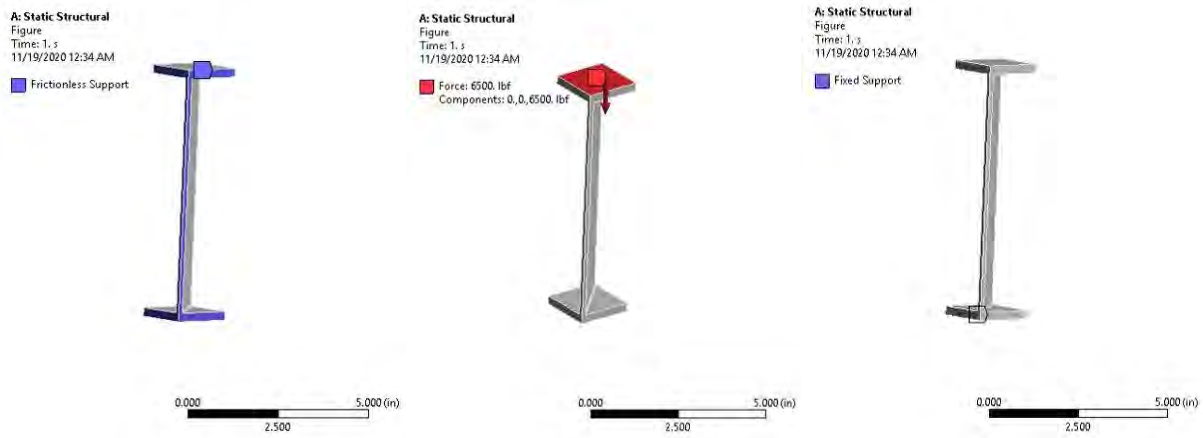

Figure #: FEA Boundary Conditions, including frictionless support on cut edges, fixed support the bottom face, and a 6500 lbf load distributed on the face respectively.

Results:

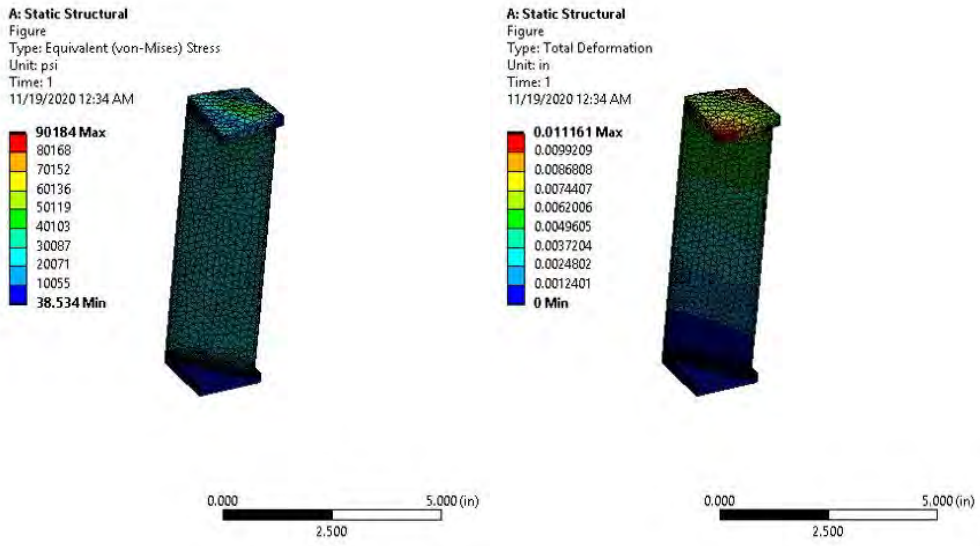

Figure #: FEA results, including Equivalent Von-Mises Stress and Total Relative Deformation

Table #: Mesh Convergence table for the Hedgehog

# of Nodes	# of Elements	Total Deformation (in)	Equivalent Stress (psi)	% error (def)	% error (stress)
29656	18288	1.11E-02	89626	100.00%	100.00%
43418	27098	0.011161	90184	0.32%	0.62%

E1: The Bartholemew

Figure #: Simplified Bartholemew Inventor model

Boundary Conditions:

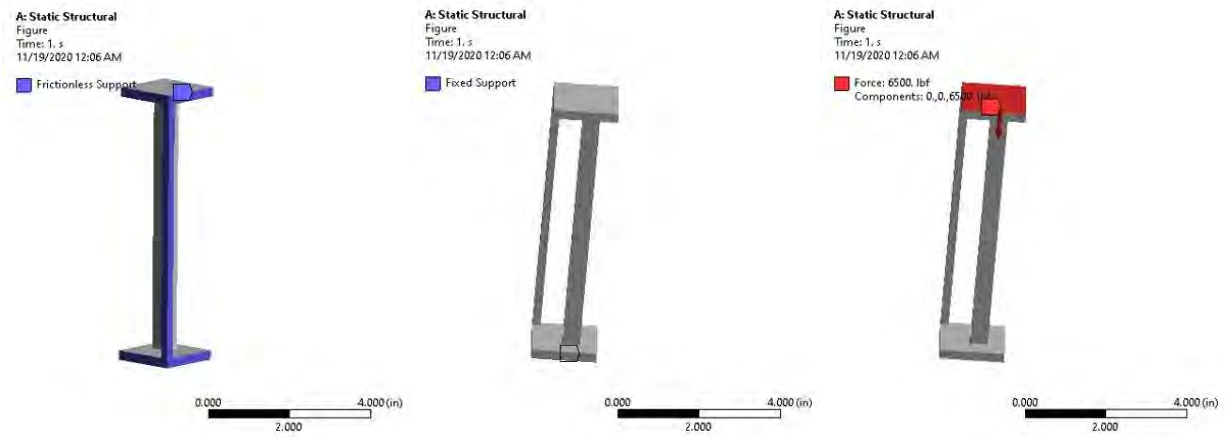

Figure #: FEA Boundary Conditions, including frictionless support on cut edges, fixed support the bottom face, and a 6500 lbf load distributed on the face respectively.

Results:

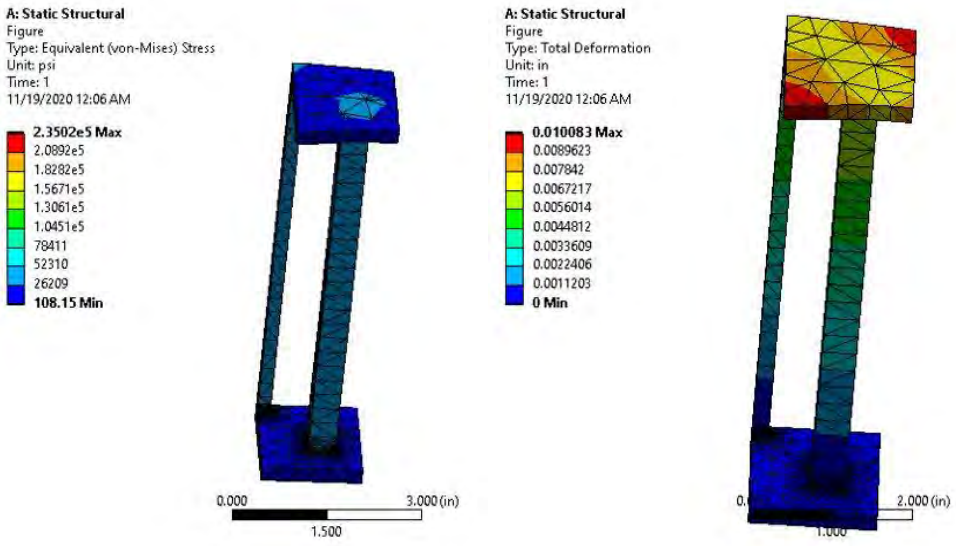

Figure #: FEA results, including Equivalent Von-Mises Stress and Total Relative Deformation

Table #: Mesh Convergence table for the Bartholemew

# of Nodes	# of Elements	Total Deformation (in)	Equivalent Stress (psi)	% error (def)	% error (stress)
12774	7444	1.01E-02	2.30E+05	100.00%	100.00%
16919	10564	1.01E-02	2.35E+05	0.03%	2.22%

E1: The Big Bar

Figure #: Simplified Big Bar Inventor model

Boundary Conditions:

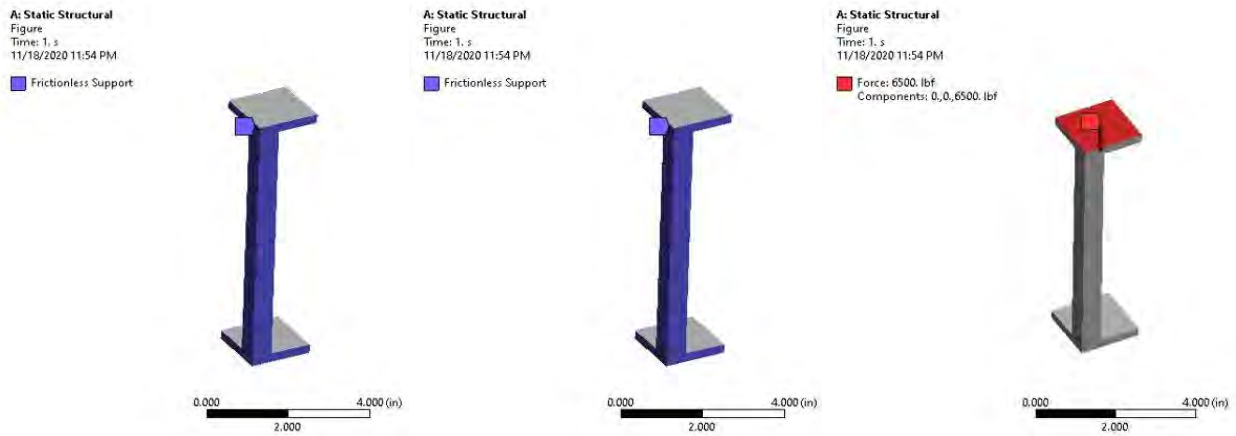

Figure #: FEA Boundary Conditions, including frictionless support on cut edges, fixed support the bottom face, and a 6500 lbf load distributed on the face respectively.

Results:

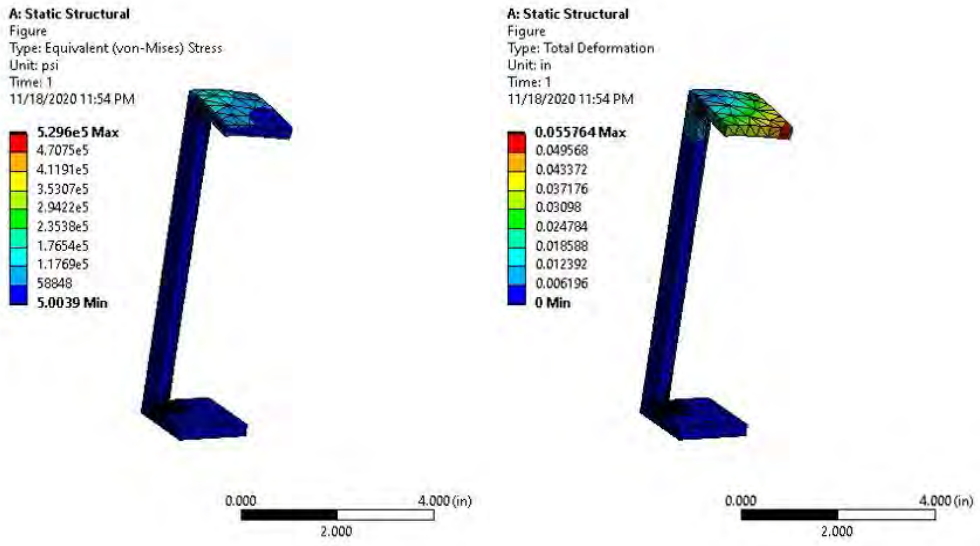

Figure #: FEA results, including Equivalent Von-Mises Stress and Total Relative Deformation

Table #: Mesh Convergence table for the Fabricator

# of Nodes	# of Elements	Total Deformation (in)	Equivalent Stress (psi)	% error (def)	% error (stress)
5270	3027	0.055809	540000	100.00%	100.00%
7782	4697	5.58E-02	5.30E+05	0.08%	1.96%

Appendix F: CAD Models of Final Design- Size Variations for Casting

F1: 1/4 Inch Model

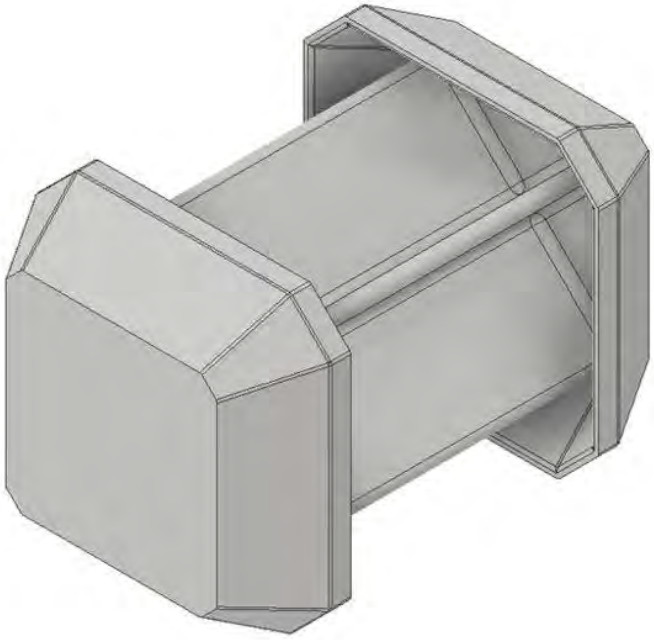

E2: 3/8 Inch Model

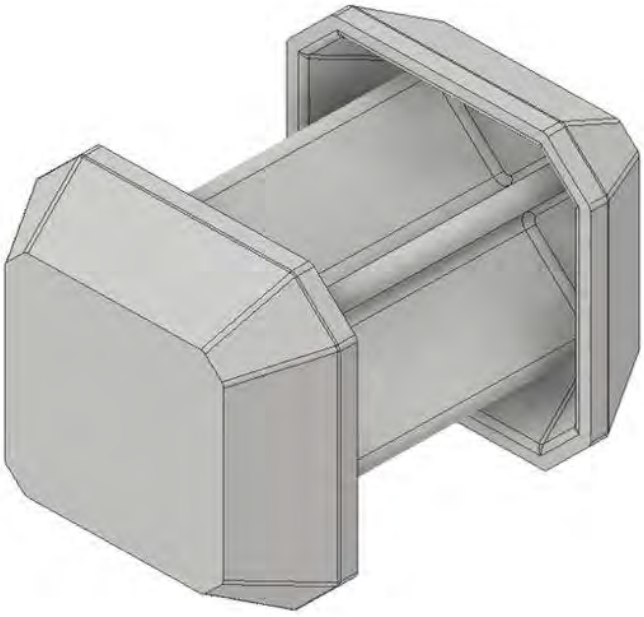

E3: 5/8 Inch Model

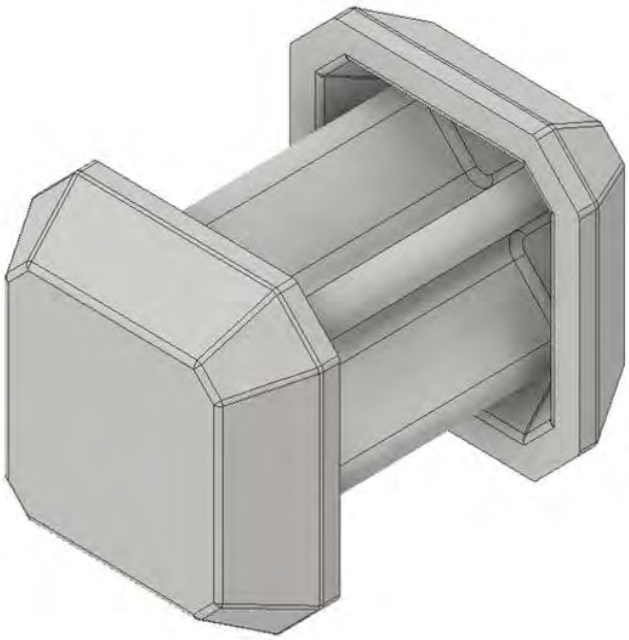

Appendix G: FEA Analysis of Final Design- Result Reports

First Saved	Saturday, November 7, 2020
Last Saved	Saturday, November 7, 2020
Product Version	2020 R2
Save Project Before Solution	No
Save Project After Solution	No

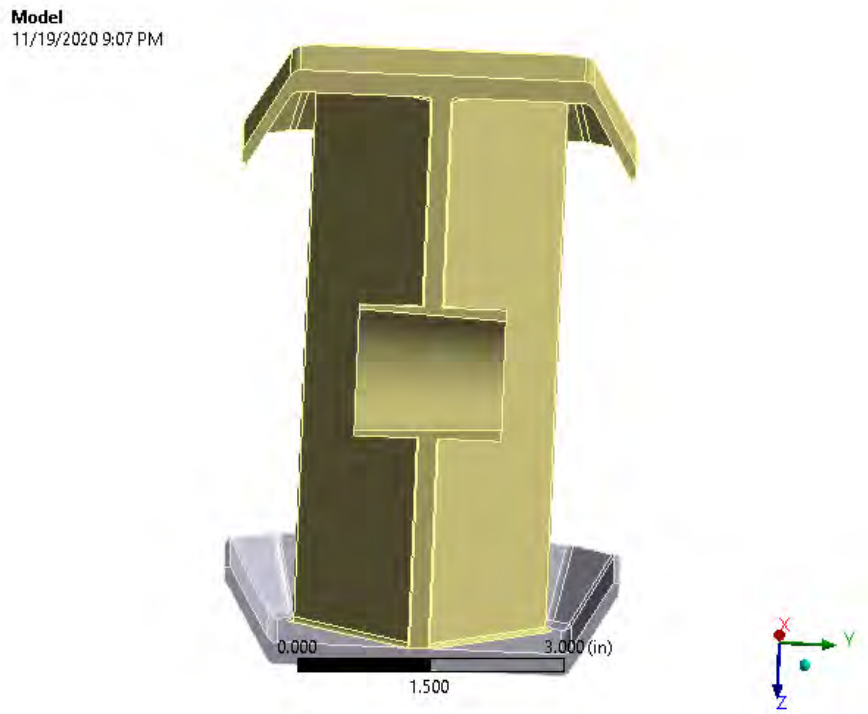

Contents

Units

TABLE 1

Unit System	U.S. Customary (in, lbm, lbf, s, V, A) Degrees rad/s Fahrenheit
Angle	Degrees
Rotational Velocity	rad/s
Temperature	Fahrenheit

Model (A4)

Geometry

TABLE 2
Model (A4) > Geometry

Object Name	*Geometry*
State	Fully Defined
Definition	
Source	C:\Users\jtc5495\AppData\Local\Temp\FINAL_Model_For_Thors_Hammer..tmp\FINAL_Model_For_Thors_Hammer._files\dp0\SYS\DM\SYS.scdoc
Type	SpaceClaim
Length Unit	Meters
Element Control	Program Controlled
Display Style	Body Color
Bounding Box	
Length X	2.2233 in
Length Y	4.446 in
Length Z	6.8 in
Properties	
Volume	7.8536 in³
Mass	2.2273 lbm
Scale Factor Value	1.
Statistics	
Bodies	2
Active Bodies	2

Nodes	41186
Elements	24393
Mesh Metric	None
Update Options	
Assign Default Material	No
Basic Geometry Options	
Solid Bodies	Yes
Surface Bodies	Yes
Line Bodies	Yes
Parameters	Independent
Parameter Key	
Attributes	Yes
Attribute Key	
Named Selections	Yes
Named Selection Key	
Material Properties	Yes
Advanced Geometry Options	
Use Associativity	Yes
Coordinate Systems	Yes
Coordinate System Key	
Reader Mode Saves Updated File	No
Use Instances	Yes
Smart CAD Update	Yes
Compare Parts On Update	No
Analysis Type	3-D
Mixed Import Resolution	None
Clean Bodies On Import	No
Stitch Surfaces On Import	None
Decompose Disjoint Geometry	Yes
Enclosure and Symmetry Processing	Yes

TABLE 3
Model (A4) > Geometry > Parts

Object Name	*Component1\Solid21*	*Component2\Solid11*
State	Meshed	
Graphics Properties		
Visible	Yes	
Transparency	1	
Definition		
Suppressed	No	
Stiffness Behavior	Flexible	
Coordinate System	Default Coordinate System	
Reference Temperature	By Environment	
Treatment	None	

Material		
Assignment	AF-96	
Nonlinear Effects	Yes	
Thermal Strain Effects	Yes	
Bounding Box		
Length X	2.2233 in	2.223 in
Length Y	4.446 in	
Length Z	6.5501 in	1.0963 in
Properties		
Volume	5.4873 in³	2.3662 in³
Mass	1.5562 lbm	0.67106 lbm
Centroid X	2.4404 in	2.6524 in
Centroid Y	2.0152 in	2.0095 in
Centroid Z	-0.60247 in	3.8 in
Moment of Inertia Ip1	8.0169 lbm·in²	1.0865 lbm·in²
Moment of Inertia Ip2	6.8339 lbm·in²	0.32262 lbm·in²
Moment of Inertia Ip3	2.0256 lbm·in²	1.3164 lbm·in²
Statistics		
Nodes	35383	5803
Elements	21519	2874
Mesh Metric	None	
CAD Attributes		
PartTolerance:	0.00000001	
Color:175.159.143		

TABLE 4
Model (A4) > Materials

Object Name	*Materials*
State	Fully Defined
Statistics	
Materials	3
Material Assignments	0

Coordinate Systems

TABLE 5
Model (A4) > Coordinate Systems > Coordinate System

Object Name	*Global Coordinate System*
State	Fully Defined
Definition	
Type	Cartesian
Coordinate System ID	0.
Origin	
Origin X	0. in
Origin Y	0. in
Origin Z	0. in

Directional Vectors	
X Axis Data	[1. 0. 0.]
Y Axis Data	[0. 1. 0.]
Z Axis Data	[0. 0. 1.]

Connections

TABLE 6
Model (A4) > Connections

Object Name	*Connections*
State	Fully Defined
Auto Detection	
Generate Automatic Connection On Refresh	Yes
Transparency	
Enabled	Yes

TABLE 7
Model (A4) > Connections > Contacts

Object Name	*Contacts*
State	Fully Defined
Definition	
Connection Type	Contact
Scope	
Scoping Method	Geometry Selection
Geometry	All Bodies
Auto Detection	
Tolerance Type	Slider
Tolerance Slider	0.
Tolerance Value	2.1058e-002 in
Use Range	No
Face/Face	Yes
Face-Face Angle Tolerance	75. °
Face Overlap Tolerance	Off
Cylindrical Faces	Include
Face/Edge	No
Edge/Edge	No
Priority	Include All
Group By	Bodies
Search Across	Bodies
Statistics	
Connections	1
Active Connections	1

TABLE 8
Model (A4) > Connections > Contacts > Contact Regions

Object Name	*Contact Region 4*

State	Fully Defined
Scope	
Scoping Method	Geometry Selection
Contact	1 Face
Target	1 Face
Contact Bodies	Component1\Solid21
Target Bodies	Component2\Solid11
Protected	No
Definition	
Type	Bonded
Scope Mode	Automatic
Behavior	Program Controlled
Trim Contact	Program Controlled
Trim Tolerance	2.1058e-002 in
Suppressed	No
Advanced	
Formulation	Program Controlled
Small Sliding	Program Controlled
Detection Method	Program Controlled
Penetration Tolerance	Program Controlled
Elastic Slip Tolerance	Program Controlled
Normal Stiffness	Program Controlled
Update Stiffness	Program Controlled
Pinball Region	Program Controlled
Geometric Modification	
Contact Geometry Correction	None
Target Geometry Correction	None

Mesh

TABLE 9
Model (A4) > Mesh

Object Name	*Mesh*
State	Solved
Display	
Display Style	Use Geometry Setting
Defaults	
Physics Preference	Mechanical
Element Order	Program Controlled
Element Size	Default
Sizing	
Use Adaptive Sizing	Yes

Resolution	4
Mesh Defeaturing	Yes
Defeature Size	Default
Transition	Fast
Span Angle Center	Coarse
Initial Size Seed	Assembly
Bounding Box Diagonal	8.4232 in
Average Surface Area	0.63741 in²
Minimum Edge Length	2.1822e-003 in
Quality	
Check Mesh Quality	Yes, Errors
Error Limits	Aggressive Mechanical
Target Quality	Default (0.050000)
Smoothing	Medium
Mesh Metric	None
Inflation	
Use Automatic Inflation	None
Inflation Option	Smooth Transition
Transition Ratio	0.272
Maximum Layers	5
Growth Rate	1.2
Inflation Algorithm	Pre
View Advanced Options	No
Advanced	
Number of CPUs for Parallel Part Meshing	Program Controlled
Straight Sided Elements	No
Rigid Body Behavior	Dimensionally Reduced
Triangle Surface Mesher	Program Controlled
Topology Checking	Yes
Pinch Tolerance	Please Define
Generate Pinch on Refresh	No
Statistics	
Nodes	41186
Elements	24393

TABLE 10
Model (A4) > Mesh > Mesh Controls

Object Name	*Refinement*
State	Fully Defined
Scope	
Scoping Method	Geometry Selection
Geometry	9 Faces

Definition	
Suppressed	No
Refinement	1

FIGURE 1
Model (A4) > Mesh > Figure

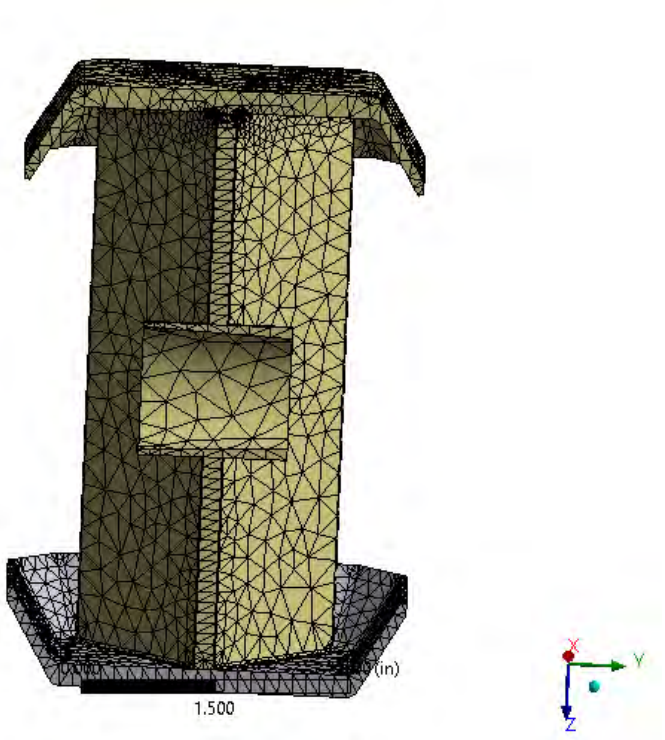

Static Structural (A5)

TABLE 11
Model (A4) > Analysis

Object Name	*Static Structural (A5)*
State	Solved
Definition	
Physics Type	Structural
Analysis Type	Static Structural
Solver Target	Mechanical APDL
Options	
Environment Temperature	71.6 °F
Generate Input Only	No

TABLE 12
Model (A4) > Static Structural (A5) > Analysis Settings

Object Name	*Analysis Settings*
State	Fully Defined
Step Controls	
Number Of Steps	4.
Current Step Number	3.
Step End Time	3. s
Auto Time Stepping	Program Controlled
Solver Controls	
Solver Type	Program Controlled
Weak Springs	Off
Solver Pivot Checking	Program Controlled
Large Deflection	Off
Inertia Relief	Off
Quasi-Static Solution	Off
Rotordynamics Controls	
Coriolis Effect	Off
Restart Controls	
Generate Restart Points	Program Controlled
Retain Files After Full Solve	No
Combine Restart Files	Program Controlled
Nonlinear Controls	
Newton-Raphson Option	Program Controlled
Force Convergence	Program Controlled
Moment Convergence	Program Controlled
Displacement Convergence	Program Controlled
Rotation Convergence	Program Controlled
Line Search	Program Controlled
Stabilization	Program Controlled
Advanced	
Inverse Option	No
Contact Split (DMP)	Off
Output Controls	
Stress	Yes
Surface Stress	No
Back Stress	No
Strain	Yes
Contact Data	Yes
Nonlinear Data	No
Nodal Forces	No
Volume and Energy	Yes
Euler Angles	Yes
General Miscellaneous	No
Contact Miscellaneous	No
Store Results At	All Time Points
Result File Compression	Program Controlled

Analysis Data Management	
Solver Files Directory	C:\Users\jtc5495\AppData\Local\Temp\FINAL_Model_For_Thors_Hammer ..tmp\FINAL_Model_For_Thors_Hammer._files\dp0\SYS\MECH\
Future Analysis	None
Scratch Solver Files Directory	
Save MAPDL db	No
Contact Summary	Program Controlled
Delete Unneeded Files	Yes
Nonlinear Solution	No
Solver Units	Active System
Solver Unit System	Bin

TABLE 13
Model (A4) > Static Structural (A5) > Analysis Settings
Step-Specific "Step Controls"

Step	Step End Time
1	1. s
2	2. s
3	3. s
4	4. s

TABLE 14
Model (A4) > Static Structural (A5) > Loads

Object Name	*Fixed Support*	*Full Face Blow MAX To Yeild*	*POINT at Top*	*POINT at Bottom*	*POINT at Side*	*Displacement*	*Frictionless Support*
State	Fully Defined						
Scope							
Scoping Method	Geometry Selection						
Geometry	1 Face						3 Faces
Definition							
Type	Fixed Support	Force				Displacement	Frictionless Support
Suppressed	No						
Define By		Components					
Applied By		Surface Effect					
Coordinate System		Global Coordinate System					
X Component		Tabular Data			0. lbf (ramped)	0. in (ramped)	
Y Component		Tabular Data			0. lbf (ramped)	0. in (ramped)	
Z Component		Tabular Data				0. in (ramped)	
Tabular Data							
Independent Variable		Time					

FIGURE 2
Model (A4) > Static Structural (A5) > Fixed Support > Figure

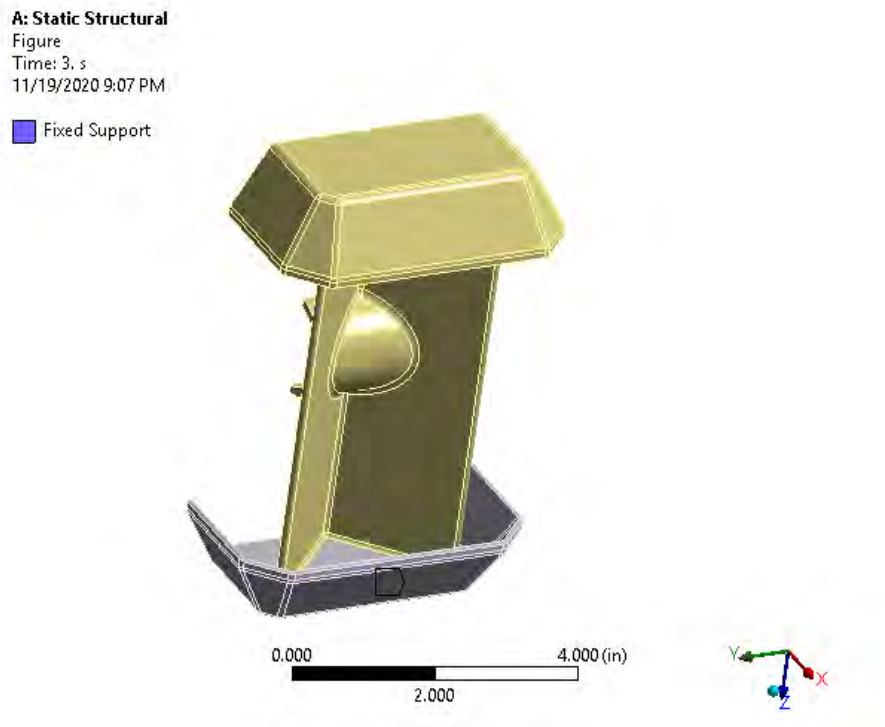

FIGURE 3
Model (A4) > Static Structural (A5) > Full Face Blow MAX To Yeild

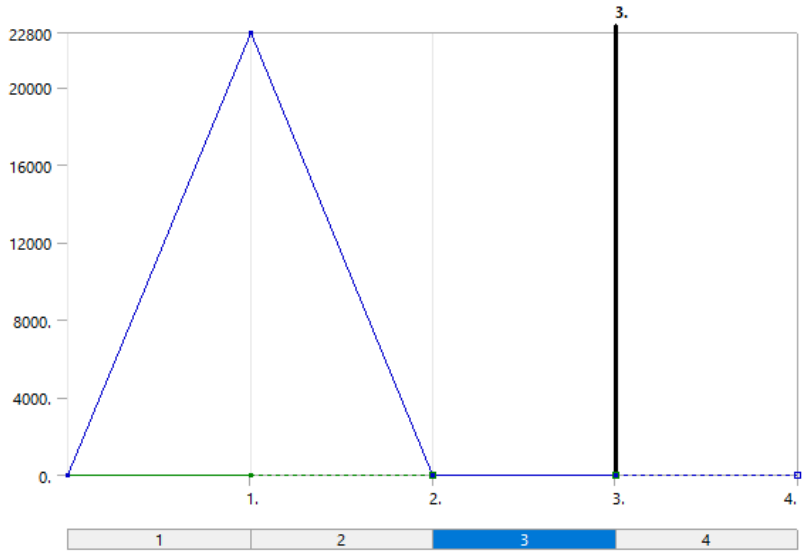

TABLE 15
Model (A4) > Static Structural (A5) > Full Face Blow MAX To Yeild

Steps	Time [s]	X [lbf]	Y [lbf]	Z [lbf]
1	0.	0.	0.	0.
	1.			22800
2	2.	= 0.	= 0.	0.
3	3.			
4	4.			= 0.

FIGURE 4
Model (A4) > Static Structural (A5) > Full Face Blow MAX To Yeild > Figure

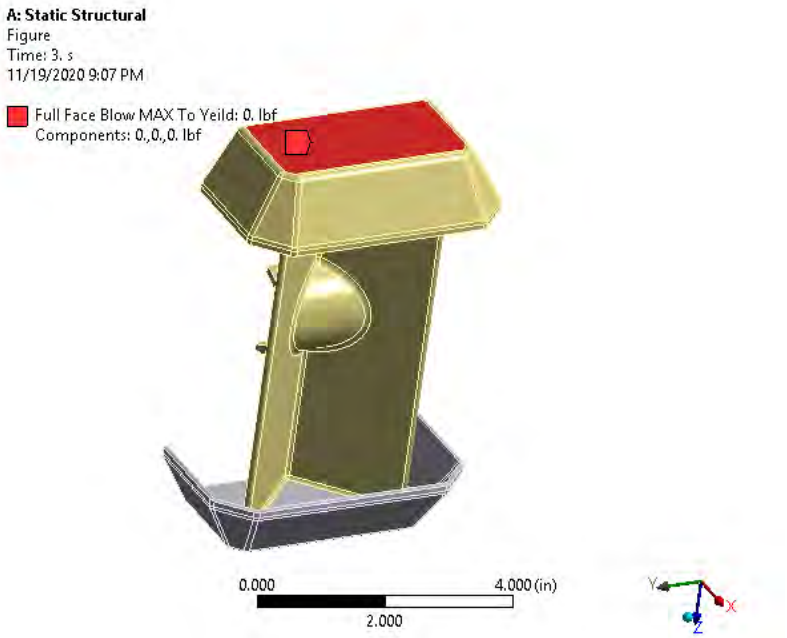

FIGURE 5
Model (A4) > Static Structural (A5) > POINT at Top

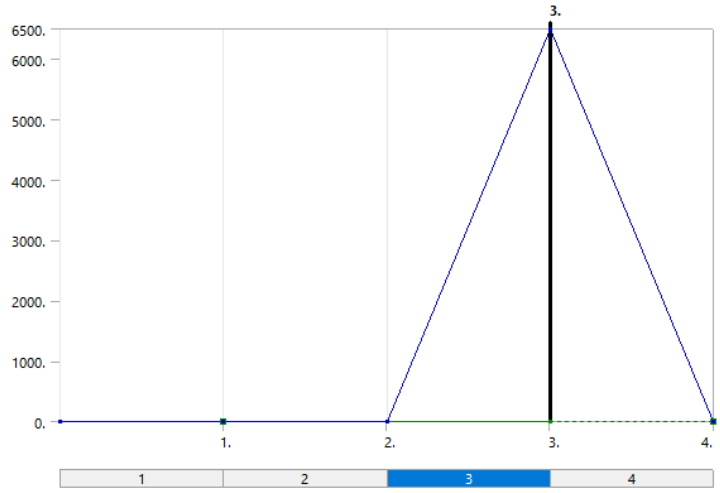

TABLE 16
Model (A4) > Static Structural (A5) > POINT at Top

Steps	Time [s]	X [lbf]	Y [lbf]	Z [lbf]
1	0.	0.	0.	0.
	1.	= 0.	= 0.	
2	2.	0.	0.	
3	3.			6500.
4	4.	= 0.	= 0.	0.

FIGURE 6
Model (A4) > Static Structural (A5) > POINT at Top > Figure

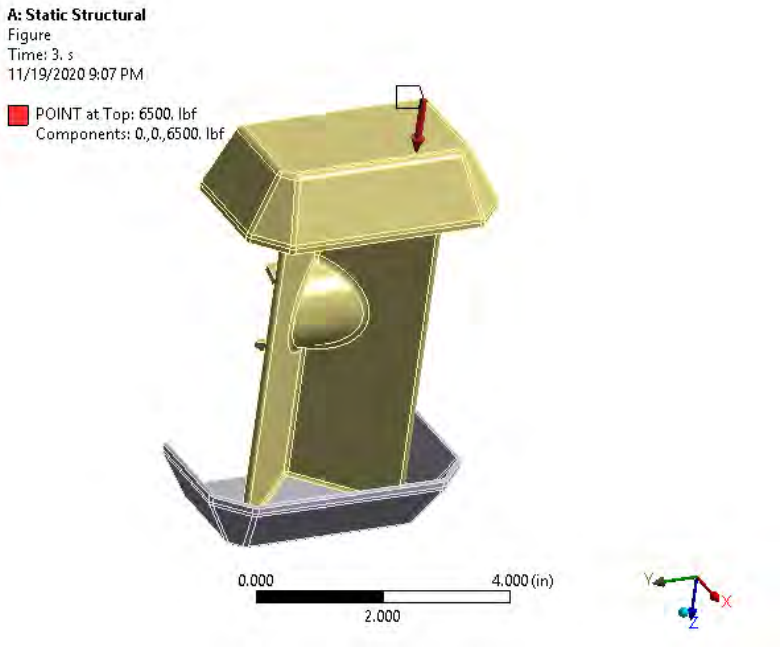

FIGURE 7
Model (A4) > Static Structural (A5) > POINT at Bottom

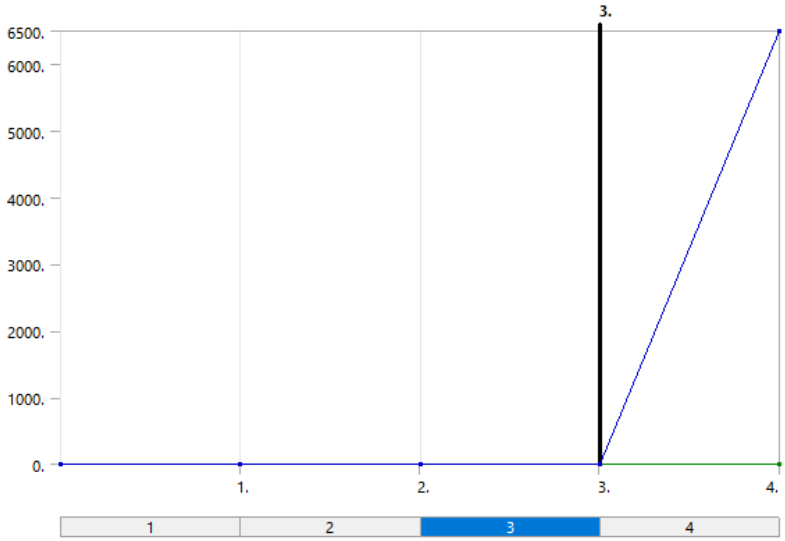

TABLE 17
Model (A4) > Static Structural (A5) > POINT at Bottom

Steps	Time [s]	X [lbf]	Y [lbf]	Z [lbf]
1	0.	0.	0.	0.
	1.			
2	2.			
3	3.			
4	4.			6500.

FIGURE 8
Model (A4) > Static Structural (A5) > POINT at Bottom > Figure

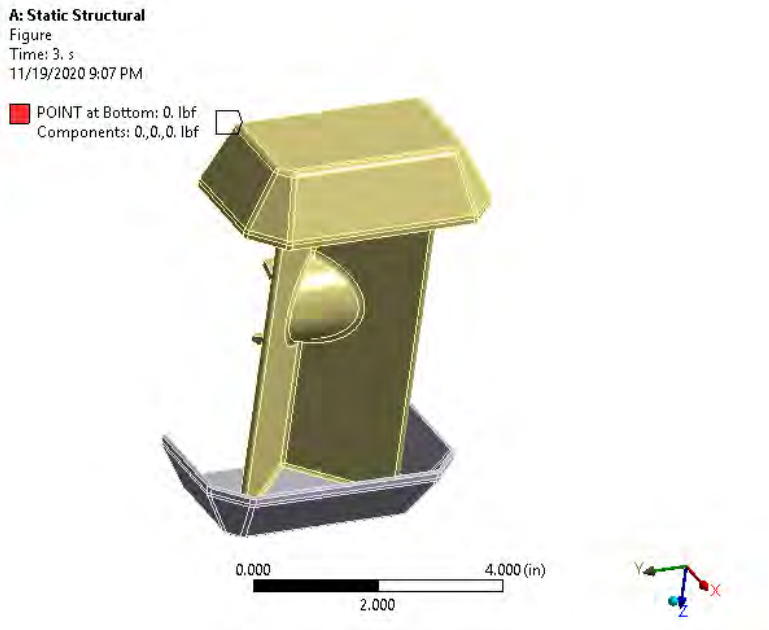

FIGURE 9
Model (A4) > Static Structural (A5) > POINT at Side

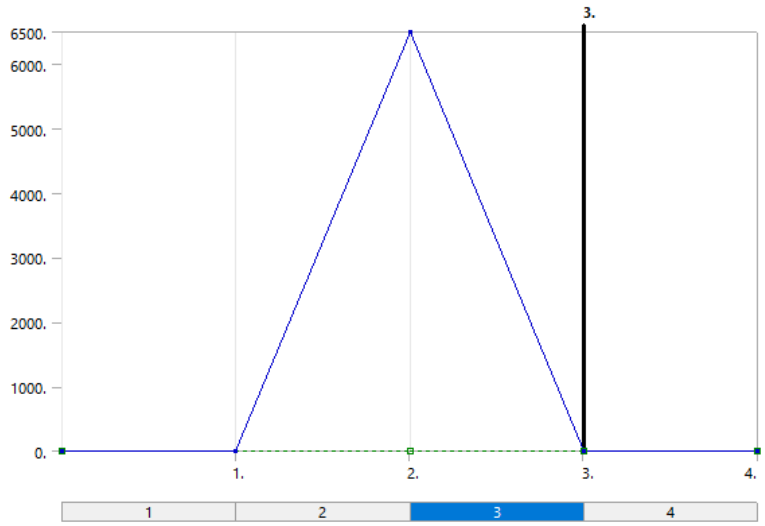

TABLE 18
Model (A4) > Static Structural (A5) > POINT at Side

Steps	Time [s]	X [lbf]	Y [lbf]	Z [lbf]
1	0.	= 0.	= 0.	0.
	1.	0.	0.	
2	2.	= 0.	= 0.	6500.
3	3.			0.
4	4.			

FIGURE 10
Model (A4) > Static Structural (A5) > POINT at Side > Figure

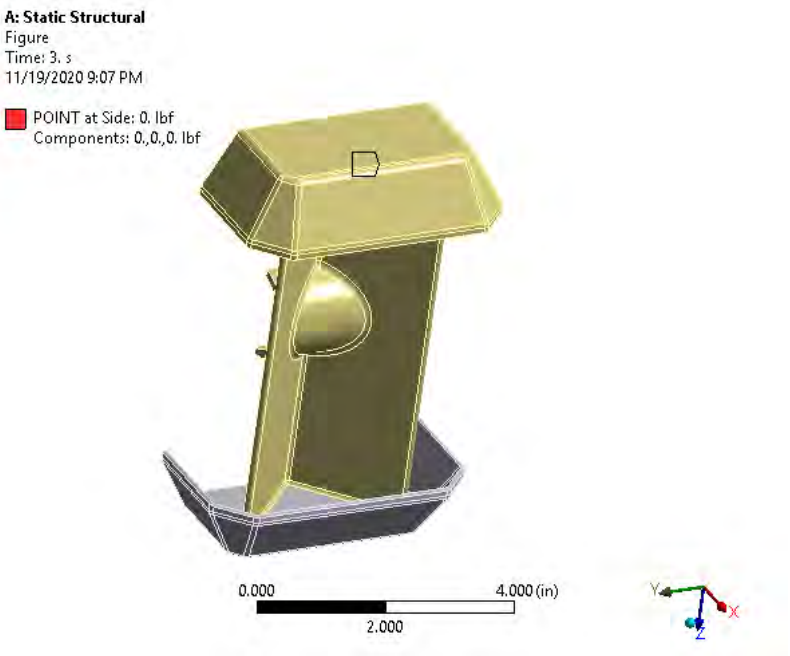

FIGURE 11
Model (A4) > Static Structural (A5) > Displacement

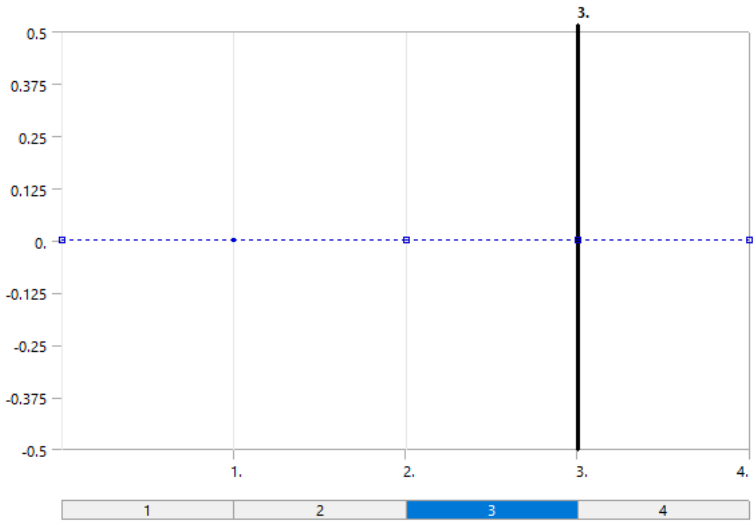

FIGURE 12
Model (A4) > Static Structural (A5) > Displacement > Figure

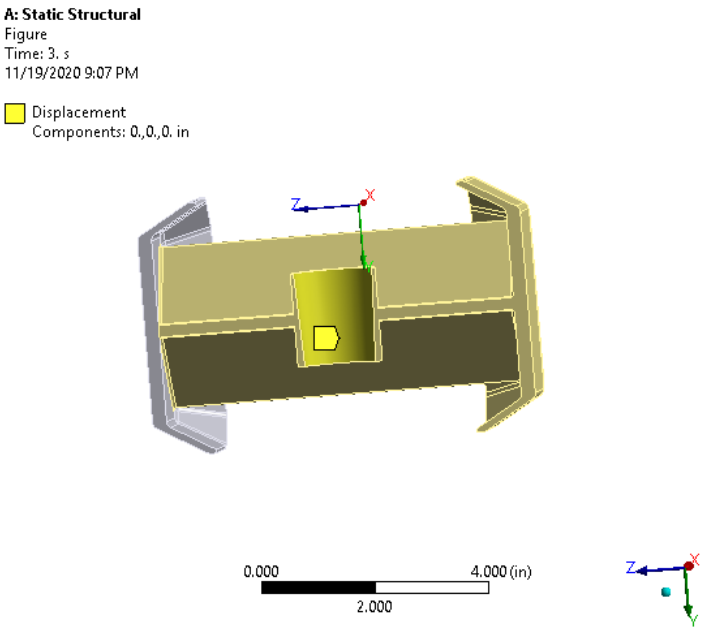

FIGURE 13
Model (A4) > Static Structural (A5) > Frictionless Support > Figure

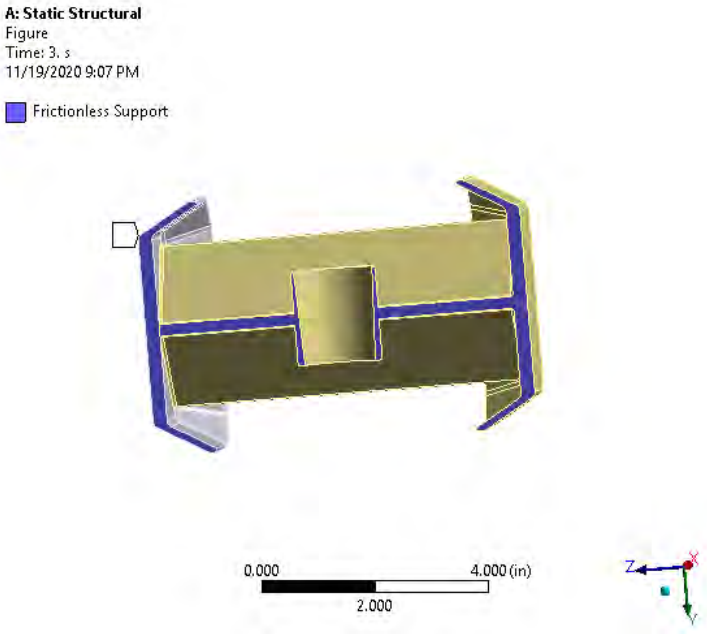

Solution (A6)

TABLE 19
Model (A4) > Static Structural (A5) > Solution

Object Name	*Solution (A6)*
State	Solved

Adaptive Mesh Refinement	
Max Refinement Loops	1.
Refinement Depth	2.
Information	
Status	Done
MAPDL Elapsed Time	9. s
MAPDL Memory Used	733. MB
MAPDL Result File Size	43.813 MB
Post Processing	
Beam Section Results	No
On Demand Stress/Strain	No

TABLE 20
Model (A4) > Static Structural (A5) > Solution (A6) > Solution Information

Object Name	*Solution Information*
State	Solved
Solution Information	
Solution Output	Solver Output
Newton-Raphson Residuals	0
Identify Element Violations	0
Update Interval	2.5 s
Display Points	All
FE Connection Visibility	
Activate Visibility	Yes
Display	All FE Connectors
Draw Connections Attached To	All Nodes
Line Color	Connection Type
Visible on Results	No
Line Thickness	Single
Display Type	Lines

TABLE 21
Model (A4) > Static Structural (A5) > Solution (A6) > Results

Object Name	*Equivalent (von-Mises) Stress - 1. s*	*Total Deformation - 1. s*	*Equivalent (von-Mises) Stress - 2. s*	*Equivalent (von-Mises) Stress - 3. s*	*Equivalent (von-Mises) Stress - 4. s*	*Total Deformation - 2. s*	*Total Deformation - 3. s*	*Total Deformation - 4. s*	*Structural Error*
State	Solved								
Scope									
Scoping Method	Geometry Selection								
Geometry	All Bodies								
Definition									
Type	Equivalent	Total Deformation	Equivalent (von-Mises) Stress			Total Deformation			Structural Error

	(von-Mises) Stress								
By	Time								
Display Time	1. s		2. s	3. s	4. s	2. s	3. s	4. s	1. s
Calculate Time History	Yes								
Identifier									
Suppressed	No								
Integration Point Results									
Display Option	Averaged		Averaged						
Average Across Bodies	No		No						
Results									
Minimum	0.94593 psi	0. in	0.27811 psi	5.2075e-002 psi	2.6784e-002 psi	0. in			9.029e-018 BTU
Maximum	1.8928e+005 psi	8.7132e-003 in	1.8725e+006 psi	2.1121e+006 psi	2.2985e+006 psi	1.8822e-002 in	3.9907e-002 in	3.991e-002 in	2.6808e-006 BTU
Average	22943 psi	3.7045e-003 in	22689 psi	26746 psi	25307 psi	1.7109e-003 in	6.4547e-003 in	6.4562e-003 in	
Minimum Occurs On	Component2\Solid11	Component1\Solid21	Component2\Solid11			Component1\Solid21			Component2\Solid11
Maximum Occurs On	Component1\Solid21								
Total									1.723e-004 BTU
Minimum Value Over Time									
Minimum	2.6784e-002 psi	0. in	2.6784e-002 psi			0. in			5.9989e-020 BTU
Maximum	0.94593 psi	0. in	0.94593 psi			0. in			9.029e-018 BTU
Maximum Value Over Time									
Minimum	1.8928e+005 psi	8.7132e-003 in	1.8928e+005 psi			8.7132e-003 in			2.6808e-006 BTU
Maximum	2.2985e+006 psi	3.991e-002 in	2.2985e+006 psi			3.991e-002 in			7.0153e-005 BTU
Information									
Time	1. s		2. s	3. s	4. s	2. s	3. s	4. s	1. s
Load Step	1		2	3	4	2	3	4	1
Substep	1								
Iteration Number	1		2	3	4	2	3	4	1

FIGURE 14
Model (A4) > Static Structural (A5) > Solution (A6) > Equivalent (von-Mises) Stress - 1. s

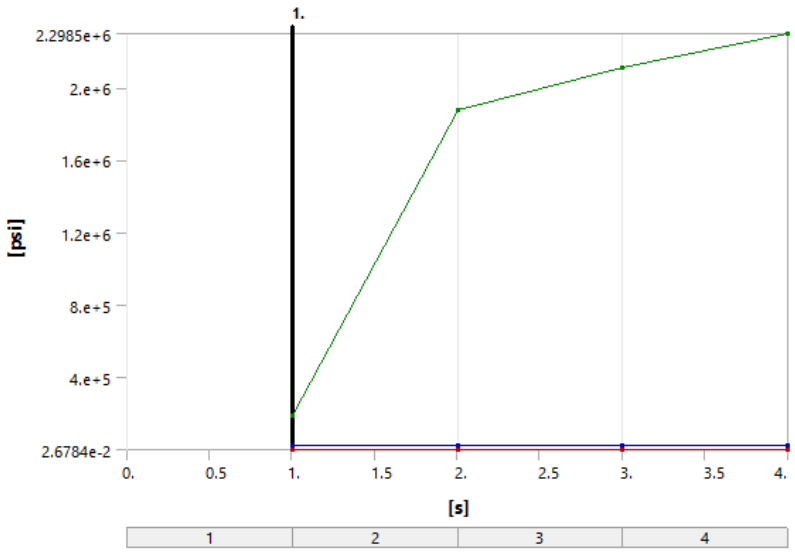

TABLE 22
Model (A4) > Static Structural (A5) > Solution (A6) > Equivalent (von-Mises) Stress - 1. s

Time [s]	Minimum [psi]	Maximum [psi]	Average [psi]
1.	0.94593	1.8928e+005	22943
2.	0.27811	1.8725e+006	22689
3.	5.2075e-002	2.1121e+006	26746
4.	2.6784e-002	2.2985e+006	25307

FIGURE 15
Model (A4) > Static Structural (A5) > Solution (A6) > Equivalent (von-Mises) Stress - 1. s > Figure

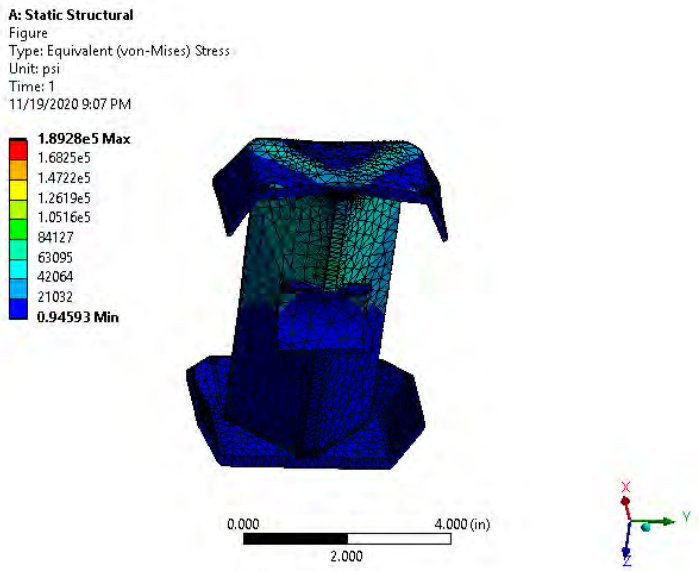

FIGURE 16
Model (A4) > Static Structural (A5) > Solution (A6) > Total Deformation - 1. s

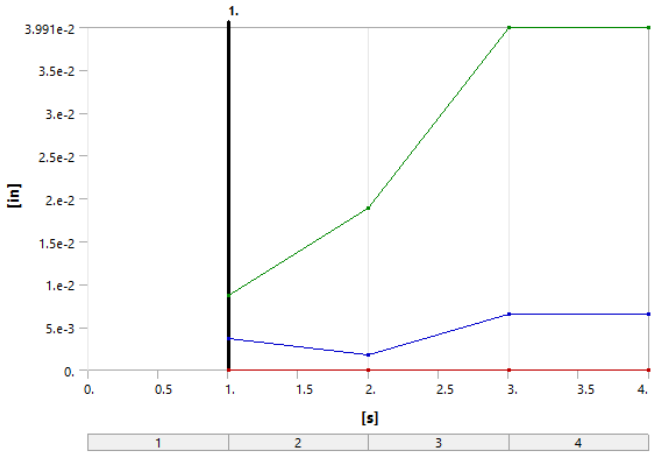

TABLE 23
Model (A4) > Static Structural (A5) > Solution (A6) > Total Deformation - 1. s

Time [s]	Minimum [in]	Maximum [in]	Average [in]
1.	0.	8.7132e-003	3.7045e-003
2.		1.8822e-002	1.7109e-003
3.		3.9907e-002	6.4547e-003
4.		3.991e-002	6.4562e-003

FIGURE 17
Model (A4) > Static Structural (A5) > Solution (A6) > Total Deformation - 1. s > Figure

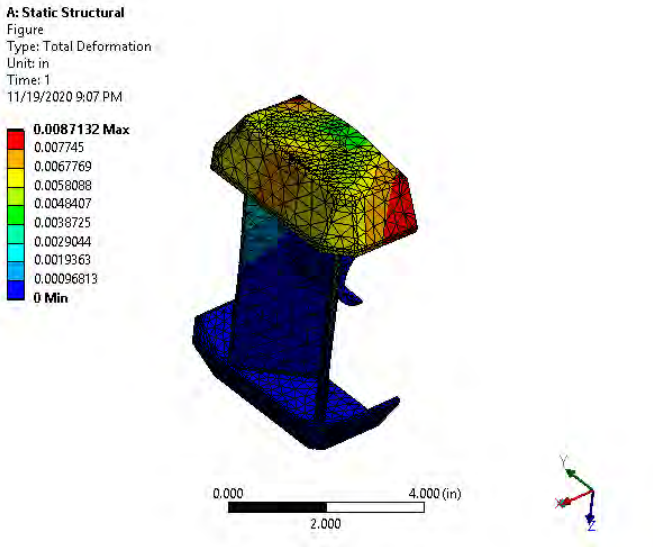

FIGURE 18
Model (A4) > Static Structural (A5) > Solution (A6) > Equivalent (von-Mises) Stress - 2. s

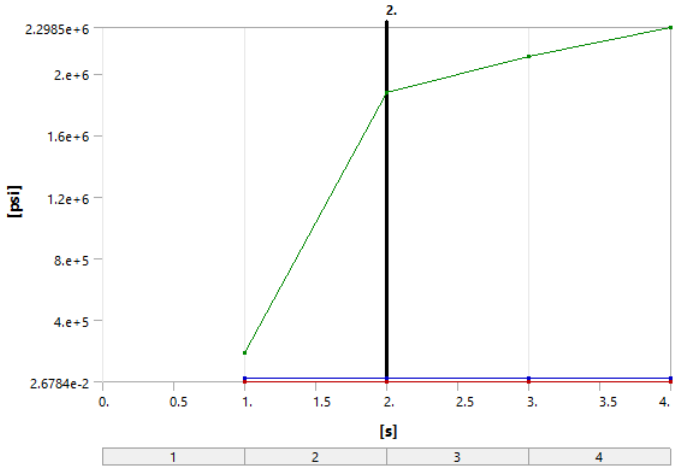

TABLE 24
Model (A4) > Static Structural (A5) > Solution (A6) > Equivalent (von-Mises) Stress - 2. s

Time [s]	Minimum [psi]	Maximum [psi]	Average [psi]
1.	0.94593	1.8928e+005	22943
2.	0.27811	1.8725e+006	22689
3.	5.2075e-002	2.1121e+006	26746
4.	2.6784e-002	2.2985e+006	25307

FIGURE 19
Model (A4) > Static Structural (A5) > Solution (A6) > Equivalent (von-Mises) Stress - 2. s > Figure

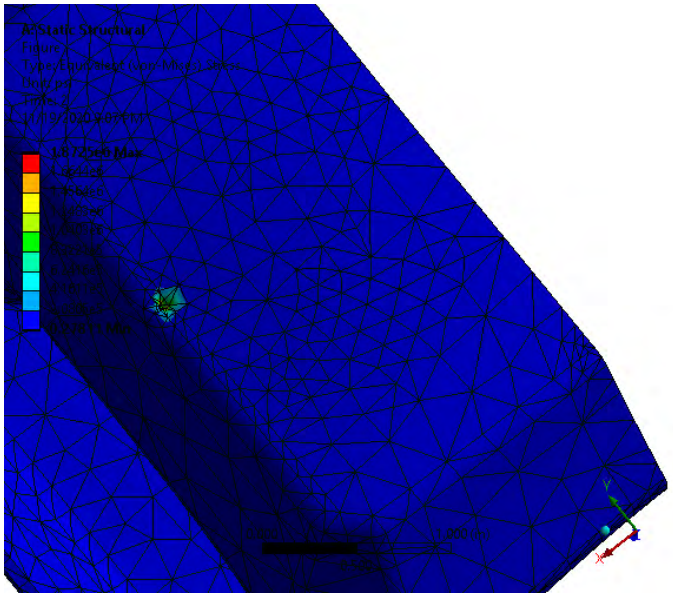

FIGURE 20
Model (A4) > Static Structural (A5) > Solution (A6) > Equivalent (von-Mises) Stress - 3. s

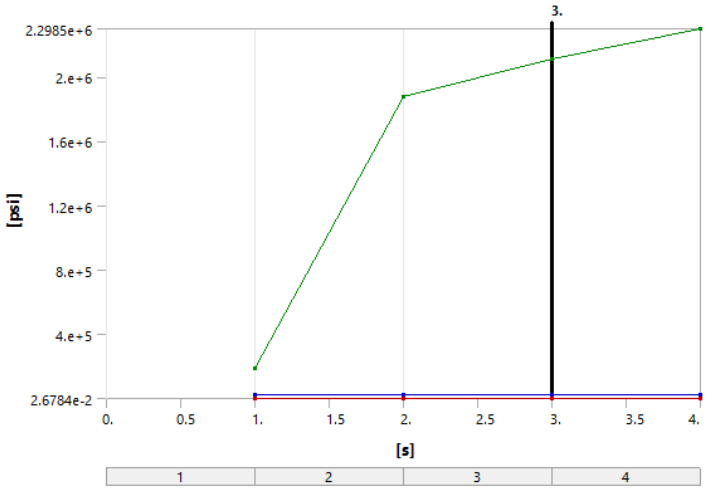

TABLE 25
Model (A4) > Static Structural (A5) > Solution (A6) > Equivalent (von-Mises) Stress - 3. s

Time [s]	Minimum [psi]	Maximum [psi]	Average [psi]
1.	0.94593	1.8928e+005	22943
2.	0.27811	1.8725e+006	22689
3.	5.2075e-002	2.1121e+006	26746
4.	2.6784e-002	2.2985e+006	25307

FIGURE 21
Model (A4) > Static Structural (A5) > Solution (A6) > Equivalent (von-Mises) Stress - 3. s > Figure

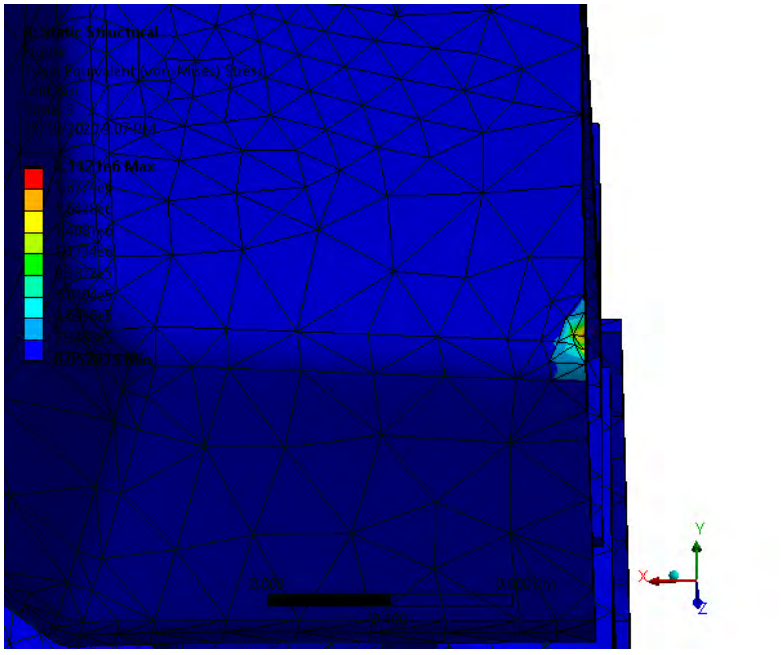

FIGURE 22
Model (A4) > Static Structural (A5) > Solution (A6) > Equivalent (von-Mises) Stress - 4. s

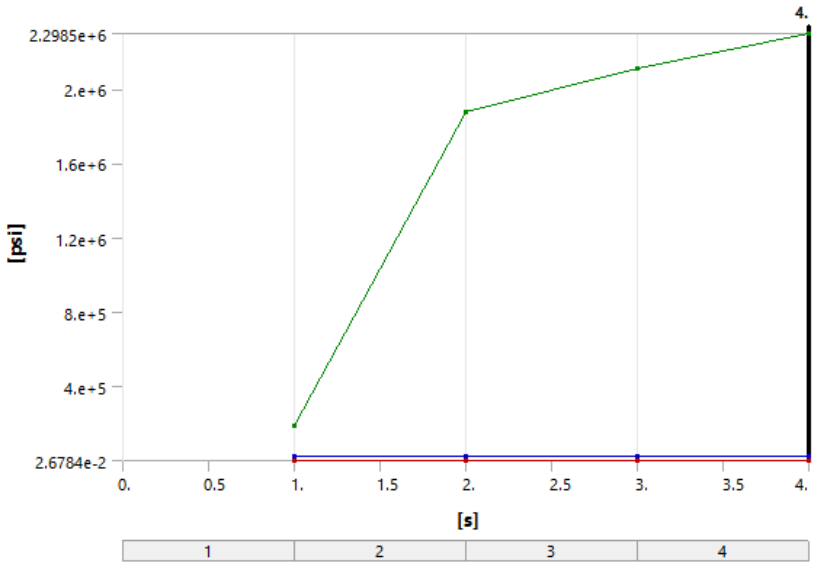

TABLE 26
Model (A4) > Static Structural (A5) > Solution (A6) > Equivalent (von-Mises) Stress - 4. s

Time [s]	Minimum [psi]	Maximum [psi]	Average [psi]
1.	0.94593	1.8928e+005	22943
2.	0.27811	1.8725e+006	22689
3.	5.2075e-002	2.1121e+006	26746
4.	2.6784e-002	2.2985e+006	25307

FIGURE 23
Model (A4) > Static Structural (A5) > Solution (A6) > Equivalent (von-Mises) Stress - 4. s > Figure

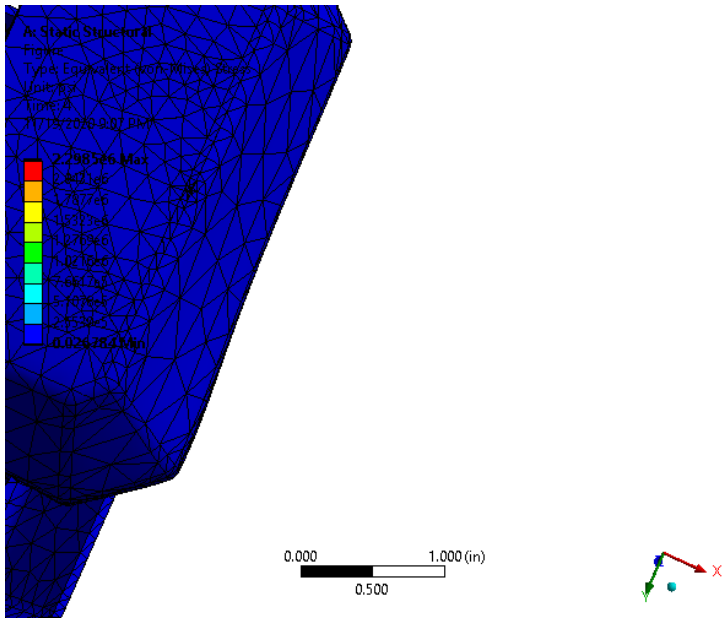

FIGURE 24
Model (A4) > Static Structural (A5) > Solution (A6) > Total Deformation - 2. s

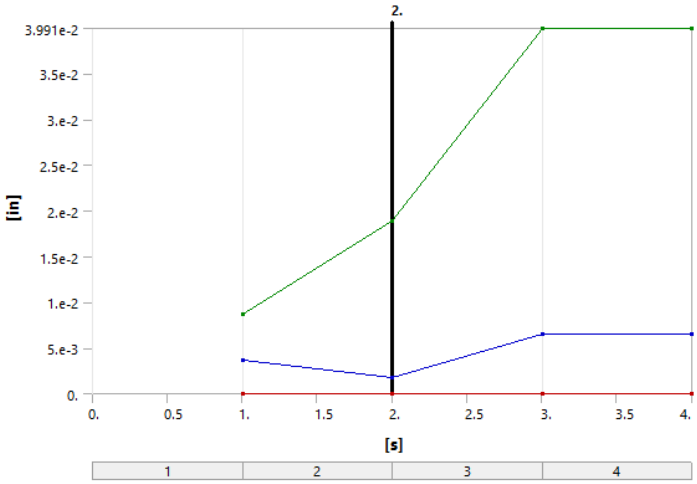

TABLE 27
Model (A4) > Static Structural (A5) > Solution (A6) > Total Deformation - 2. s

Time [s]	Minimum [in]	Maximum [in]	Average [in]
1.	0.	8.7132e-003	3.7045e-003
2.		1.8822e-002	1.7109e-003
3.		3.9907e-002	6.4547e-003
4.		3.991e-002	6.4562e-003

FIGURE 25
Model (A4) > Static Structural (A5) > Solution (A6) > Total Deformation - 2. s > Figure

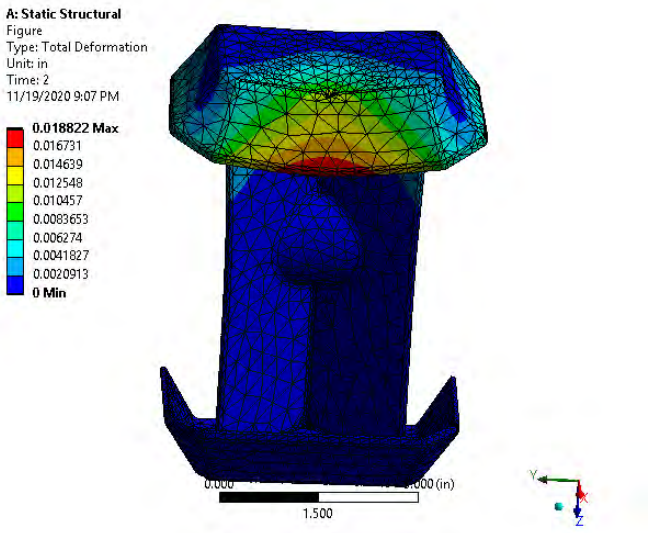

FIGURE 26
Model (A4) > Static Structural (A5) > Solution (A6) > Total Deformation - 3. s

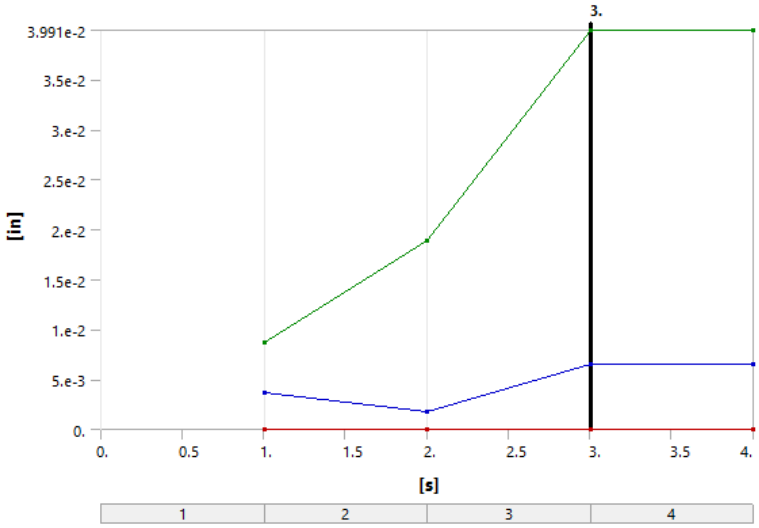

TABLE 28
Model (A4) > Static Structural (A5) > Solution (A6) > Total Deformation - 3. s

Time [s]	Minimum [in]	Maximum [in]	Average [in]
1.	0.	8.7132e-003	3.7045e-003
2.		1.8822e-002	1.7109e-003
3.		3.9907e-002	6.4547e-003
4.		3.991e-002	6.4562e-003

FIGURE 27
Model (A4) > Static Structural (A5) > Solution (A6) > Total Deformation - 3. s > Figure

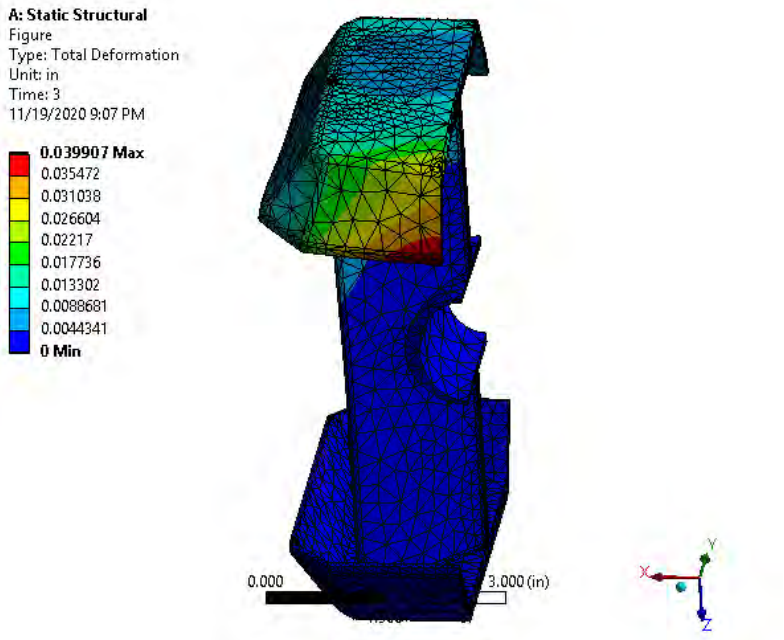

FIGURE 28
Model (A4) > Static Structural (A5) > Solution (A6) > Total Deformation - 4. s

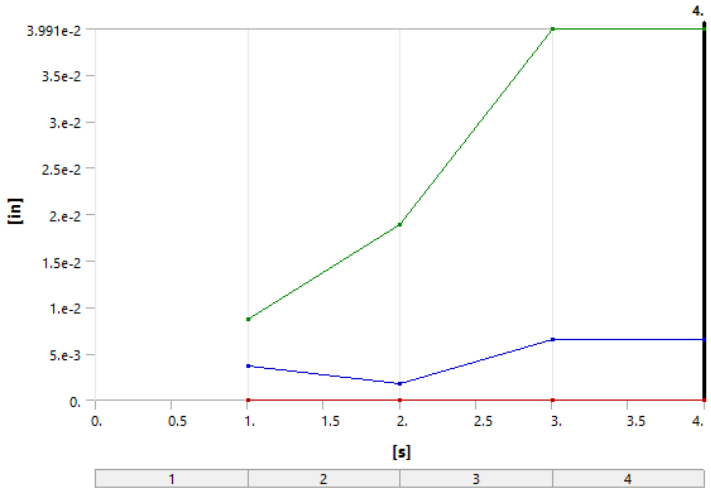

TABLE 29
Model (A4) > Static Structural (A5) > Solution (A6) > Total Deformation - 4. s

Time [s]	Minimum [in]	Maximum [in]	Average [in]
1.	0.	8.7132e-003	3.7045e-003
2.		1.8822e-002	1.7109e-003
3.		3.9907e-002	6.4547e-003
4.		3.991e-002	6.4562e-003

FIGURE 29
Model (A4) > Static Structural (A5) > Solution (A6) > Total Deformation - 4. s > Figure

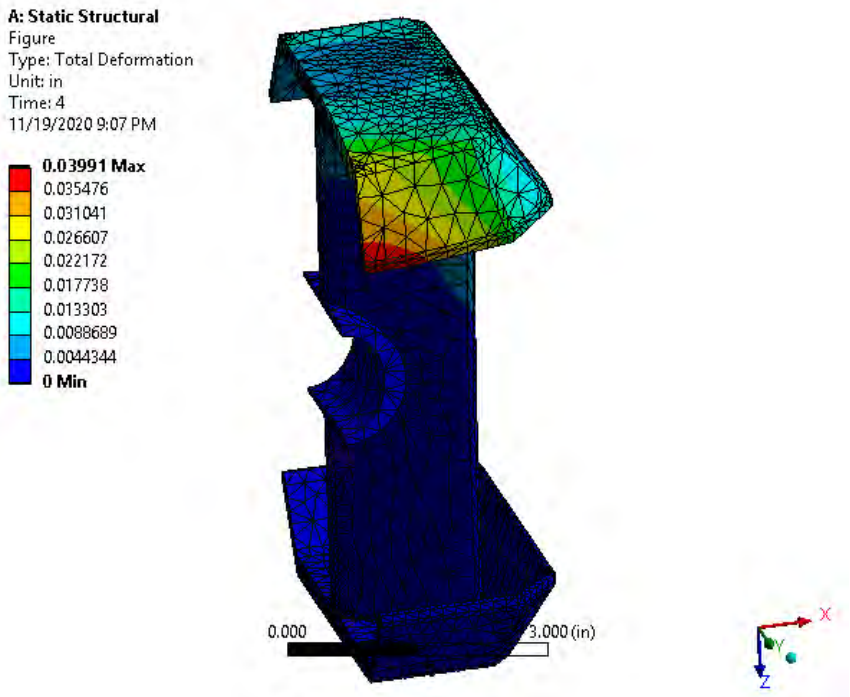

FIGURE 30
Model (A4) > Static Structural (A5) > Solution (A6) > Structural Error

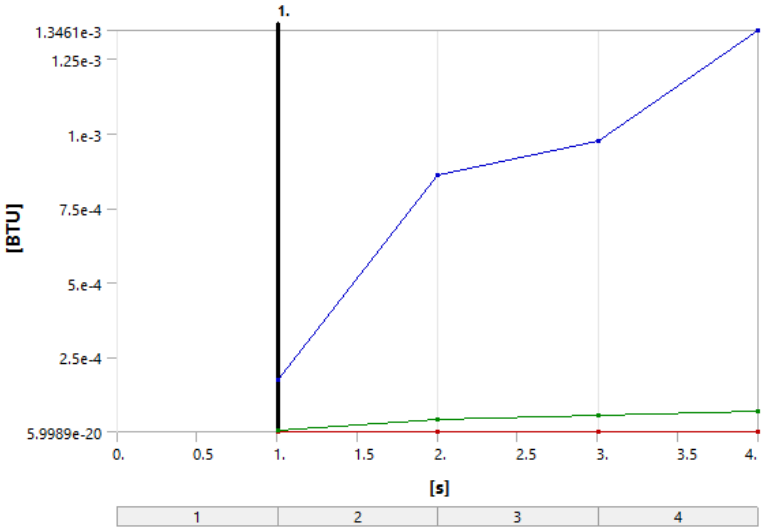

TABLE 30
Model (A4) > Static Structural (A5) > Solution (A6) > Structural Error

Time [s]	Minimum [BTU]	Maximum [BTU]	Total [BTU]
1.	9.029e-018	2.6808e-006	1.723e-004
2.	7.9256e-019	3.9678e-005	8.5872e-004
3.	6.545e-020	5.4662e-005	9.7397e-004
4.	5.9989e-020	7.0153e-005	1.3461e-003

Material Data

AF-96

TABLE 31
AF-96 > Constants

Density	0.2836 lbm in^-3
Coefficient of Thermal Expansion	6.6667e-006 F^-1
Specific Heat	0.10366 BTU lbm^-1 F^-1
Thermal Conductivity	8.0917e-004 BTU s^-1 in^-1 F^-1
Resistivity	8.5235 ohm cmil in^-1

TABLE 32
AF-96 > Color

Red	Green	Blue
132	139	179

TABLE 33
AF-96 > Compressive Ultimate Strength

Compressive Ultimate Strength psi
0

TABLE 34
AF-96 > Compressive Yield Strength

Compressive Yield Strength psi
36259

TABLE 35
AF-96 > Tensile Yield Strength

Tensile Yield Strength psi
36259

TABLE 36
AF-96 > Tensile Ultimate Strength

Tensile Ultimate Strength psi
66717

TABLE 37
AF-96 > Isotropic Secant Coefficient of Thermal Expansion

Zero-Thermal-Strain Reference Temperature F
71.6

TABLE 38
AF-96 > S-N Curve

Alternating Stress psi	Cycles	Mean Stress psi
5.8001e+005	10	0
4.1002e+005	20	0
2.7499e+005	50	0
2.0494e+005	100	0
1.5505e+005	200	0
63962	2000	0
38000	10000	0
31038	20000	0
20015	1.e+005	0
16534	2.e+005	0
12502	1.e+006	0

TABLE 39
AF-96 > Strain-Life Parameters

Strength Coefficient psi	Strength Exponent	Ductility Coefficient	Ductility Exponent	Cyclic Strength Coefficient psi	Cyclic Strain Hardening Exponent
1.3343e+005	-0.106	0.213	-0.47	1.4504e+005	0.2

TABLE 40
AF-96 > Isotropic Elasticity

Young's Modulus psi	Poisson's Ratio	Bulk Modulus psi	Shear Modulus psi	Temperature F
3.e+007	0.423	6.4935e+007	1.0541e+007	

TABLE 41
AF-96 > Isotropic Relative Permeability

Relative Permeability
10000

Mesh Convergence

	# of Nodes	# of Elements	Total Deformation (in)	Equivalent Stress (psi)	% error (def)	% error (stress)
Bad Mesh						
Default Mesh	33248	19451	0.0087055	187150	100.00%	100.00%
	41186	24393	0.0087132	189280	0.09%	1.13%

Appendix H: Mold Design-Additional Views

H1: Side Views

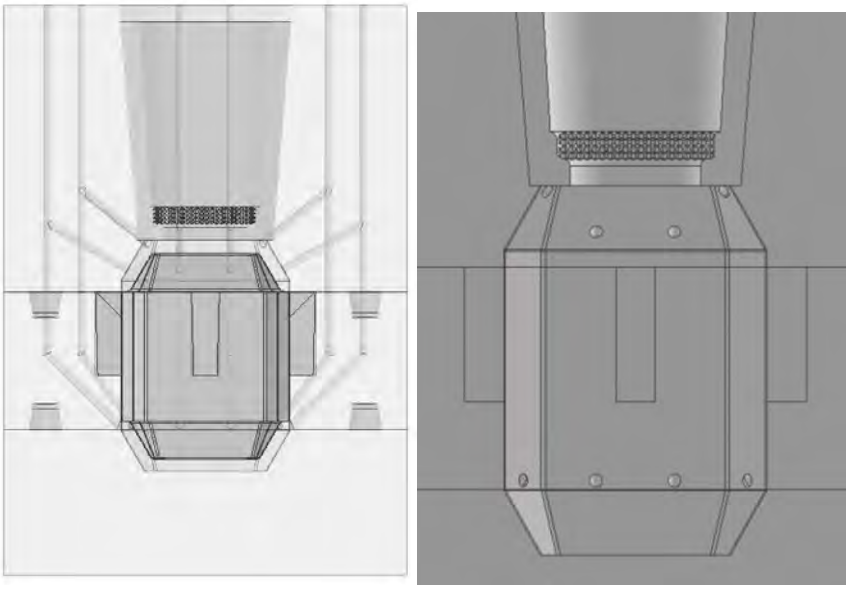

H2: Top View

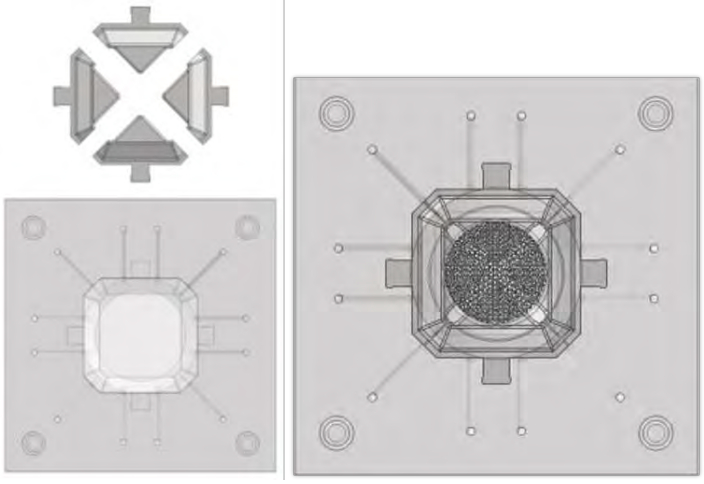

H3: Cross-Section View

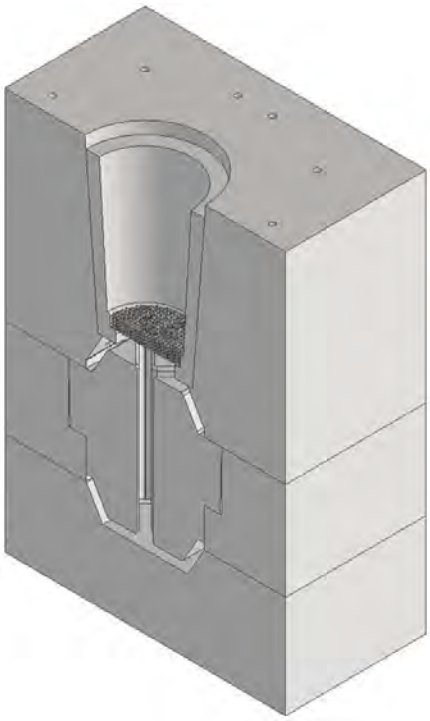

Appendix I: Pouring Process- Certificate of Exact Alloy Chemistry

PRL METALLURGICAL LABORATORY
PO BOX 1170
307 N. NINTH AVENUE
LEBANON, PA 17046
TELEPHONE: (717) 270-1888 FAX: (717) 270-2868

MATERIAL TEST REPORT

CUSTOMER: REGAL CAST, INC.

MATERIAL GRADE(S): X2015A2KCPA02(AF9628)

CHEMICAL ANALYSIS (PERCENT)

HEAT NO.	C	Mn	Si	P	S	Cr	Ni	Mo	Cu	V	N	Al	Ti	Sn	Ferrite
2041	.273	.655	.913	.010	.014	2.52	.989	.881	.128	.009	.012	.052	.011	.006	

WE CERTIFY THAT THESE RESULTS REPRESENT THE ACTUAL ATTRIBUTES OF THE MATERIAL TESTED.

ALL MATERIALS PROCURED UNDER THIS PURCHASE ORDER MEET THE REQUIREMENTS OF THE DODD-FRANK WALL STREET ACT. (CONFLICT MINERALS)

COMMENTS Chemistry determination done IAW PRL-Chemistry Rev.3

TEST PERFORMED BY CHARLES A. GOSS, LAB. MANAGER DATE 2/17/2021

Form#112 Rev.1

The recording of false, fictitious or fraudulent statements or entries on this document may be punishable as a felony under Federal Statute.

Appendix J: Hipping Process- Certification, Parameters, and Data

Pressure Technology, Inc.
7996 Auburn Road
Concord, OH 44077
440-352-0760

HIP Certification

This is to certify that PTI HIP Run Number 821054-1 was performed according to the following run parmeters.

Hold Temperature:	**1121°C (+/-14°C)**
Hold Pressure:	**15000psi (+/-500psi)**
Hold Length:	**4hours (+15mins/-120mins)**
In accordance with	**Har 02 Rev. 0** **specs per email, Dr Paul Lynch**

PTI does not clean parts Pre or Post HIP.
No getter material used.
Pressure Technology is subcontracted for HIP process only and no additional testing is performed after HIP.

Customer: **Penn State Behrend**
Purchase Order Number: **CREDIT CARD**
Date of Run: **2/23/2021**
Part Number: **Hammer 1121C**
Heat #/Serial #: **1 lot of 6 hammers and misc test pcs**
Job Number:
Quantity: **1 pieces**

Certified by:
BLD 2-24-21
Pressure Technology, Inc.

Form # 8.5-1.12.1F Rev.4.

ARGON GAS ANALYSIS CERTIFICATION

Process Gas

PTI Run Number : 821054-1

Dew Point: -73 Deg. C

Data Acquired By: TS

on:2/23/2021 12:01:58

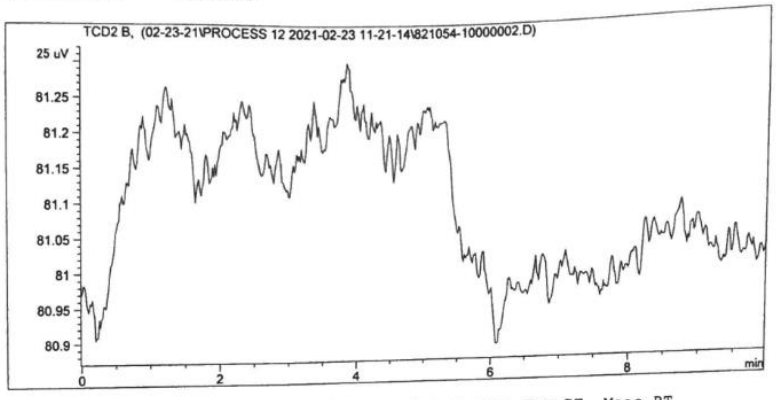

Peak Signal	#	Compound Name	Amount ppm	Exp.RT	Meas.RT
TCD2 B,	1	H2	0.000	2.771	0.000
TCD1 A,	2	H2	0.000	2.844	0.000
TCD2 B,	3	O2	0.000	3.909	0.000
TCD1 A,	4	O2	0.000	4.060	0.000
TCD2 B,	5	N2	0.000	4.828	0.000
TCD1 A,	6	N2	0.000	5.130	0.000
TCD2 B,	7	CH4	0.000	6.653	0.000
TCD1 A,	8	CH4	0.000	7.099	0.000
TCD2 B,	9	CO	0.000	7.602	0.000
TCD1 A,	10	CO	0.000	8.376	0.000
		Totals:	0.000		

Certified Gas Mixture: 160-401801605-1(ALM037469)

Certified UHP Test Gas Lot No70541035737(T241722)

The above analysis has been performed utilizing the current gas chromatography methods. PTI's received liquid Argon is certified to a minium purity of 99.997% traceable to NIST.
Pressure Technology certifies the above gas analysis meets or exceeds all customer specifications and purity standards.

Authorized by: BLO 2-24-21

8.5-1.11.2 F Rev.6

PRESSURE TECHNOLOGY of OHIO, INC. Run Data

Run Number: 821054-1 **Run Date: 2/23/21**

Time	Pressure psi	TC#1 °C	TC#2 °C	TC#3 °C	TC#4 °C	TC#7 °C	TC#8 °C	TC#9 °C	TC#10 °C	TC#11 °C
16:21:43	**15,161**	**1116**	**1117**	**1118**	**1115**	**1129**	**1107**	**1119**	**1120**	**1119**
16:36:43	15,160	1116	1118	1117	1116	1129	1112	1119	1121	1119
16:51:43	15,147	1116	1119	1118	1117	1129	1115	1120	1121	1119
17:06:43	15,135	1118	1118	1118	1116	1130	1117	1120	1121	1119
17:21:43	15,115	1115	1118	1117	1115	1129	1118	1120	1121	1119
17:36:43	15,105	1116	1118	1119	1116	1130	1119	1120	1121	1120
17:51:43	15,085	1115	1118	1118	1116	1130	1119	1120	1121	1120
18:06:43	15,066	1116	1117	1117	1116	1130	1120	1120	1121	1120
18:21:43	15,054	1115	1118	1119	1116	1130	1120	1120	1121	1120
18:36:43	15,036	1116	1118	1118	1116	1130	1120	1120	1121	1120
18:51:43	15,020	1116	1118	1117	1116	1130	1120	1120	1121	1120
19:06:43	15,005	1116	1118	1118	1115	1129	1120	1120	1121	1120
19:21:43	14,985	1116	1118	1118	1116	1129	1120	1120	1121	1120
19:36:43	14,969	1116	1118	1118	1116	1130	1120	1120	1121	1120
19:51:43	14,947	1117	1118	1117	1116	1130	1120	1120	1121	1120
20:06:43	14,928	1116	1118	1118	1115	1130	1120	1121	1121	1120
20:21:43	14,907	1117	1118	1118	1116	1130	1120	1121	1121	1120
20:22:13	**14,907**	**1116**	**1118**	**1119**	**1116**	**1130**	**1120**	**1121**	**1121**	**1120**

Temperature Set Point: **1121°C**
Temperature Specification: **1107°C - 1135°C**
Pressure Specification **15,000 ± 500 psi**
Hold Start: **16:21:43**
Hold End: **20:22:13**
Approved By: BW 2-24-21

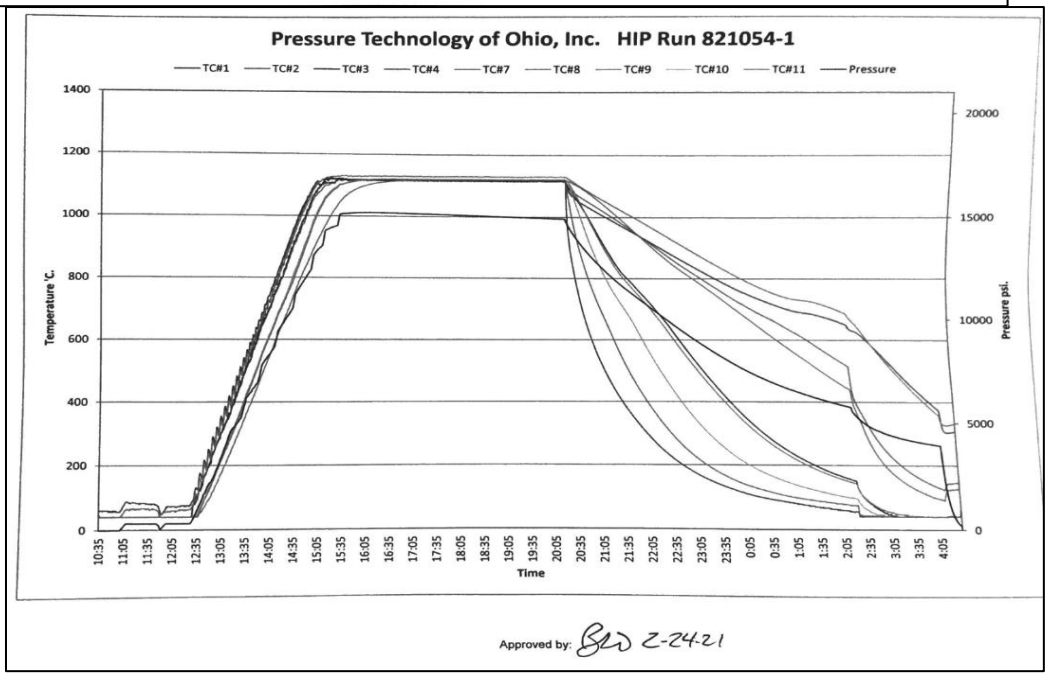

Approved by: BW 2-24-21

Appendix K: Sheet Metal of Outer Shell- Properties and Data

NLMK PENNSYLVANIA
Member of NLMK Group

METALLURGICAL TESTING LABORATORY
15 ROEMER BLVD.
FARRELL, PA 16121
CONTACT: DALE SIDDONS
TELEPHONE: (724) 983-6464 X1298
FAX: (724) 982-4423

CERTIFIED TEST REPORT

Customer:	WILCO (DBA)	ORDER #	393769-01	CUST. PO#	12482-1
Address:	3502 W. HARRY	SIZE	.050 X 36.000		
	WICHITA, KS 67213	WT SHIPPED	35350		
		HEAT #	NLPS5951		
Phone:	316-943-9379	GRADE	4130AQ		
Fax:	316-943-9664				
Representative:	Dean Schroer				

Heat Analysis # NLPS5951

ASTM TEST METHOD: E415 ☐ or E1019 ☐ (C & S only when checked) (Results are in weight %)

C	Mn	P	S	Al	Si	Cu	Ni	Cr	Mo
.29	.45	.008	.004	.03	.17	.148	.078	.83	.156
Sn	Ca	B	Nb	Co	V	Zr	Ce	N	Ti

NOTE: MELT AND MFG IN THE USA

- The material supplied is mercury and weld free
- Frequency/severity rating = passed based on Frequency/severity per spec AMS 2301K (F): 0 / (S): 0

By: _____ Date: 1-11-17
Metallurgical Laboratory Supervisor

NLMK PENNSYLVANIA
Member of NLMK Group

METALLURGICAL TESTING LABORATORY
15 ROEMER BLVD.
FARRELL, PA 16121
CONTACT: DALE SIDDONS
TELEPHONE: (724) 983-6464 X1298
FAX: (724) 982-4423

CERTIFIED MILL TEST REPORT

Customer:	WILCO (DBA)	ORDER #	393769-01	CUST. PO#	12482-1
Address:	3502 W. HARRY	SIZE	.050 x 36.000		
	WICHITA, KS 67213	WT. SHIPPED	35350		
		HEAT #	NLPS5951		
Phone:	316-943-9379	GRADE/TYPE	4130AQ (Spherodized Annealed) CR		
Fax:	316-943-9664	Testing Required:	AMS6350N/6351K, ASTM505/506/EN 10204 3.1		
Representative:	Dean Schroer		AMS2252D/2301K / (MILS-18729)		

As Processed Results											
ASTM TEST METHOD				E8			E18	E290	E45	E112	E1077
Coil #	Heat #	Gauge	Area	Yield PSI	Ultimate PSI	Elong 2%	Hardness HRBW	Bend Test 1/2T-HW	E-45 Rating 100X	Grain Size 100X	Decarb 100X
7951947	NLPS5951	.050	.0250	52150	74410	28	76	PASS	0	8	0

Heat Treated Results*			
ASTM TEST METHOD			E18
Coil #	Heat #	Gauge	Hardness HRC
7951947	NLPS5951	.050	34

*Denotes outsourced to independent laboratory (A2LA Accredited)

Hardness Test Per ASTM E-18	
	Average
Surface (HRA)	75
Core (HRA)	75.5

Requirement: The difference in hardness between the surface and core shall not be greater than 2.0

CONFORMANCE: The sample submitted has passed all testing requirements.

By: _____ Date: 1-11-17
Metallurgical Laboratory Supervisor

Appendix L: Microhardness Results- Averages and Standard Deviation

Table 32: Microhardness of Calibration Block (700 HV)

Test Block (700 HV)	Hardness (HV)	Diagonal X (Microns)	Diagonal Y (Microns)
1	710	36.3	36.0
2	694	36.6	36.6
3	698	36.6	36.3
4	700	36.2	36.6
5	696	36.7	36.3
Average	700	36.5	36.4
St Dev	5.6	0.19	0.22

Table 33: Microhardness of Test Sample Thor 1

Thor 1	Hardness (HV)	Hardness (HRC)	Diagonal X (Microns)	Diagonal Y (Microns)
1	522	51.4	42.1	42.2
2	540	52.1	41.5	41.4
3	528	51.6	42.1	41.7
4	529	51.7	41.8	41.8
5	548	52.4	40.9	41.4
6	521	51.3	42.2	42.2
7	528	51.6	42.1	41.7
8	532	51.8	42.0	41.5
9	525	51.5	42.2	41.8
Average	530	51.7	41.9	41.7
St Dev	8.7	0.35	0.43	0.30

Table 34: Microhardness of Test Sample Thor 2

Thor 2	Hardness (HV)	Hardness (HRC)	Diagonal X (Microns)	Diagonal Y (Microns)
1	525	51.5	41.8	42.2
2	537	52.0	41.1	42.0
3	515	50.9	42.4	42.4
4	546	52.3	41.1	41.3
5	540	52.1	41.5	41.4
6	535	51.9	41.4	41.8
7	531	51.7	41.6	42.0
8	524	51.5	42.0	42.2
9	525	51.5	42.0	42.1
Average	531	51.7	41.7	41.9
St Dev	9.6	0.44	0.44	0.37

Table 35: Microhardness of Test Sample Thor 3

Thor 3	Hardness (HV)	Hardness (HRC)	Diagonal X (Microns)	Diagonal Y (Microns)
1	448	45.7	45.5	45.5
2	459	46.6	44.9	45.0
3	528	51.6	42.2	41.6
4	522	51.4	42.2	42.1
5	540	52.1	41.5	41.4
6	521	51.3	42.4	42.0
7	525	51.5	42.1	42.0
8	542	52.2	41.5	41.3
9	525	51.5	42.1	42.0
Average	512	50.4	42.7	42.5
St Dev	34.2	2.44	1.45	1.57

Table 36: Microhardness of Test Sample Thor 4

Thor 4	Hardness (HV)	Hardness (HRC)	Diagonal X (Microns)	Diagonal Y (Microns)
1	540	52.1	41.6	41.3
2	535	51.9	41.7	41.5
3	546	52.3	41.4	41.0
4	543	52.2	41.1	41.5
5	549	52.5	41.0	41.1
6	525	51.5	42.1	42.0
7	543	52.2	41.3	41.4
8	542	52.2	41.3	41.5
9	538	52.0	41.5	41.5
Average	540	52.1	41.4	41.4
St Dev	7.0	0.28	0.33	0.29

Table 37: Microhardness of Test Sample Thor 5

Thor 5	Hardness (HV)	Hardness (HRC)	Diagonal X (Microns)	Diagonal Y (Microns)
1	540	52.1	41.3	41.6
2	531	51.7	41.6	42.0
3	546	52.3	41.1	41.3
4	511	50.5	42.7	42.6
5	529	51.7	41.7	42.0
6	535	51.9	41.6	41.6
7	545	52.3	41.3	41.3
8	535	51.9	41.5	41.7
9	529	51.7	42.1	41.6
Average	533	51.8	41.7	41.7
St Dev	10.5	0.55	0.49	0.41

Table 38: Microhardness of Test Sample Thor 6

Thor 6	Hardness (HV)	Hardness (HRC)	Diagonal X (Microns)	Diagonal Y (Microns)
1	535	51.9	41.7	41.5
2	534	51.9	41.7	41.6
3	522	51.4	42.3	42.0
4	519	51.3	42.2	42.3
5	538	52.0	41.4	41.6
6	543	52.2	41.6	41.0
7	532	51.8	41.8	41.6
8	559	52.9	40.8	40.7
9	518	51.1	42.3	42.3
Average	533	51.8	41.8	41.6
St Dev	13.0	0.53	0.48	0.54

Appendix M: SEM Imaging

M1: Result Report for Charpy 1 (C1)

EDAX TEAM

SFSA Cast in Steel 2021

Author: lab
Creation: 03/12/2021 2:21:35 PM

Sample Name: Thor 3_again

Area 5

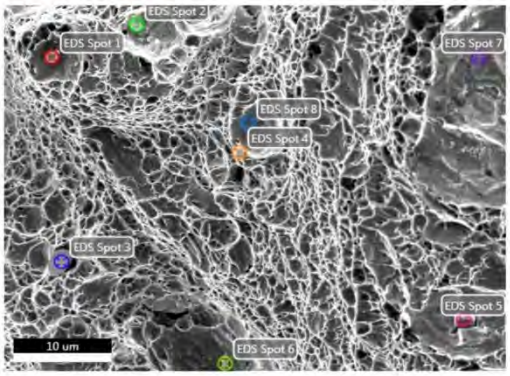

Notes:

EDS Spot 1

kV: 10	Mag: 2000	Takeoff: 34.7	Live Time(s): 25.4	Amp Time(µs): 7.68	Resolution:(eV) 124.4

EDS Spot 1

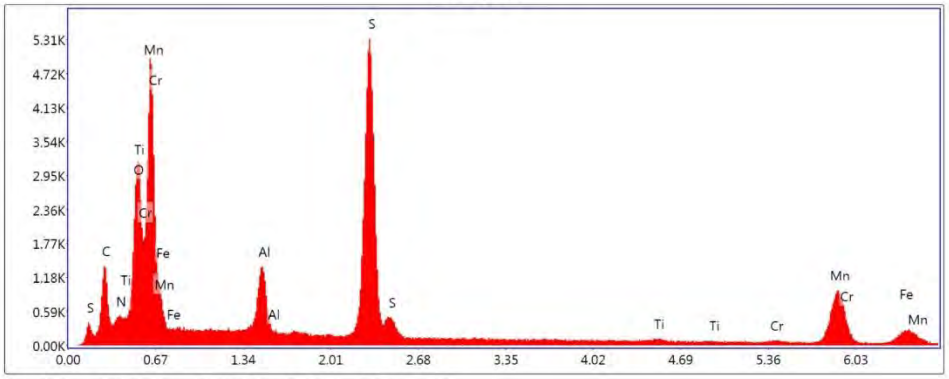

Lsec: 25.4 3.225K Cnts 0.610 keV Det: Octane Elite Super Det

eZAF Smart Quant Results

Element	Weight %	Atomic %	Net Int.	Error %	Kratio	Z	R	A	F
C K	5.75	17.61	155.31	12.38	0.0159	1.3179	0.8810	0.2092	1.0000
N K	0.00	0.00	0.04	99.99	0.0000	1.2822	0.8944	0.3328	1.0000
O K	3.45	7.94	330.28	8.54	0.0227	1.2512	0.9060	0.5257	1.0000
CrL	1.80	1.27	50.75	8.22	0.0143	0.9377	1.0296	0.8457	0.9981
FeL	3.36	2.21	75.13	10.09	0.0143	0.9338	1.0440	0.4567	0.9979
AlK	3.50	4.77	346.04	6.25	0.0290	1.0983	0.9535	0.7504	1.0068
S K	23.30	26.73	1786.26	3.63	0.2379	1.0931	0.9757	0.9240	1.0109
TiK	0.89	0.68	21.69	30.42	0.0094	0.9440	1.0071	0.9863	1.1358
MnK	57.95	38.79	465.03	6.42	0.5364	0.9044	1.0113	0.9972	1.0265

EDS Spot 2

kV: 10	Mag: 2000	Takeoff: 34.7	Live Time(s): 28.4	Amp Time(µs): 7.68	Resolution:(eV) 124.4

EDS Spot 2

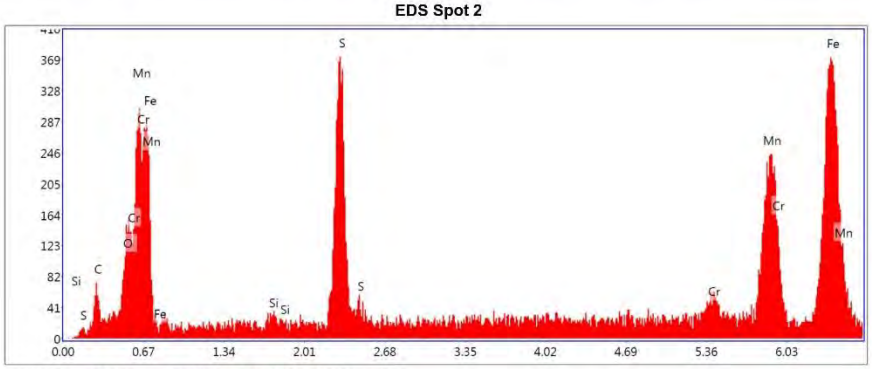

Lsec: 28.4 252 Cnts 0.610 keV Det: Octane Elite Super Det

eZAF Smart Quant Results

Element	Weight %	Atomic %	Net Int.	Error %	Kratio	Z	R	A	F
C K	0.59	2.46	3.95	36.94	0.0025	1.4032	0.8548	0.2985	1.0000
O K	0.52	1.62	10.87	19.72	0.0046	1.3331	0.8803	0.6639	1.0000
CrL	0.16	0.15	1.00	78.53	0.0017	0.9992	1.0006	1.0859	0.9981
FeL	6.83	6.14	24.23	11.48	0.0282	0.9953	1.0153	0.4158	0.9979
SiK	0.20	0.36	3.28	66.33	0.0019	1.1961	0.9386	0.7802	1.0080
S K	8.39	13.14	109.91	6.38	0.0896	1.1681	0.9544	0.9004	1.0148
MnK	83.31	76.12	117.70	7.90	0.8307	0.9754	1.0026	0.9988	1.0234

EDS Spot 3

kV: 10	Mag: 2000	Takeoff: 34.7	Live Time(s): 29.4	Amp Time(µs): 7.68	Resolution:(eV) 124.4

EDS Spot 3

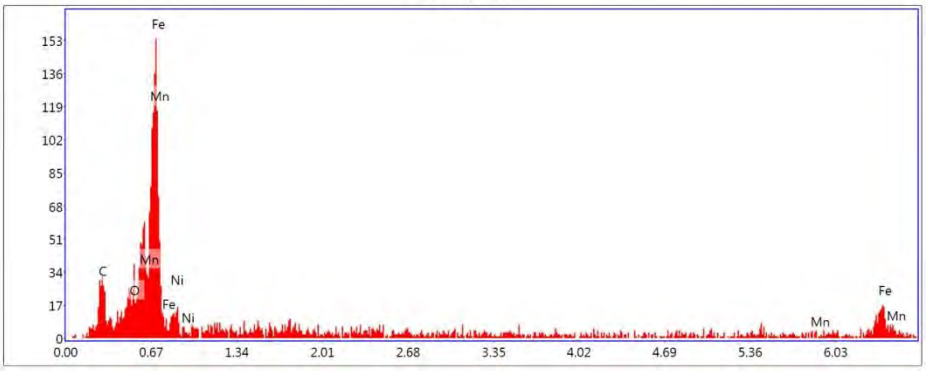

Lsec: 29.4 57 Cnts 0.610 keV Det: Octane Elite Super Det

eZAF Smart Quant Results

Element	Weight %	Atomic %	Net Int.	Error %	Kratio	Z	R	A	F
C K	10.94	32.90	3.98	23.02	0.0536	1.3236	0.8687	0.3698	1.0000
O K	6.01	13.57	5.14	19.74	0.0466	1.2573	0.8940	0.6166	1.0000
MnL	5.23	3.44	1.57	34.12	0.0445	0.9231	1.0234	0.9233	0.9981
FeL	70.62	45.67	22.01	7.25	0.5523	0.9386	1.0306	0.8350	0.9979
NiL	7.20	4.43	1.36	44.48	0.0303	0.9508	1.0444	0.4442	0.9975

EDS Spot 4

kV: 10	Mag: 2000	Takeoff: 34.7	Live Time(s): 29.1	Amp Time(µs): 7.68	Resolution:(eV) 124.4

EDS Spot 4

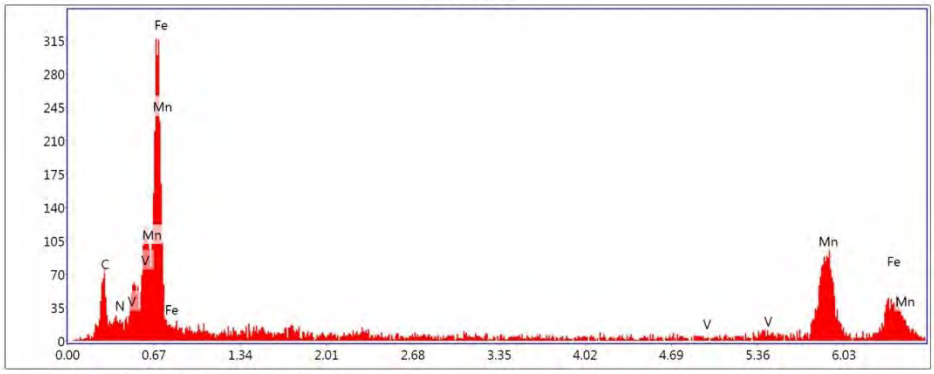

Lsec: 29.1 107 Cnts 0.610 keV Det: Octane Elite Super Det

eZAF Smart Quant Results

Element	Weight %	Atomic %	Net Int.	Error %	Kratio	Z	R	A	F
C K	2.04	8.66	7.55	20.22	0.0110	1.4147	0.8503	0.3817	1.0000
N K	0.17	0.60	0.85	84.96	0.0012	1.3770	0.8640	0.5318	1.0000
V L	3.01	3.02	4.50	22.41	0.0341	0.9921	0.9881	1.1431	0.9985
FeL	20.57	18.80	33.12	10.27	0.0900	1.0036	1.0104	0.4366	0.9979
MnK	74.21	68.92	45.55	8.59	0.7500	0.9859	1.0010	0.9986	1.0267

EDS Spot 5

kV: 10 Mag: 2000 Takeoff: 34.7 Live Time(s): 28.6 Amp Time(µs): 7.68 Resolution:(eV) 124.4

EDS Spot 5

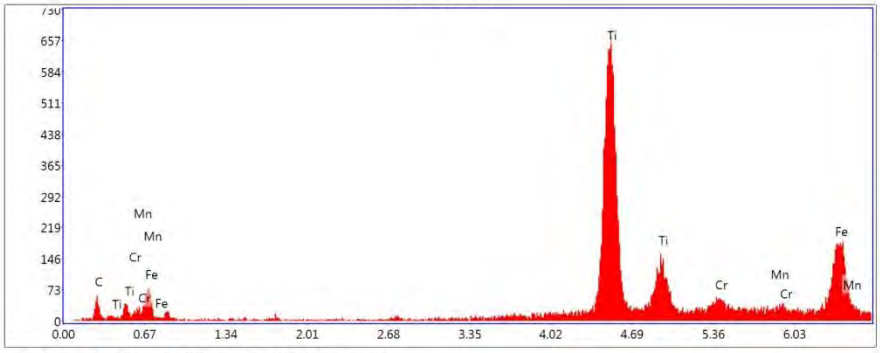

Lsec: 28.6 31 Cnts 0.610 keV Det: Octane Elite Super Det

eZAF Smart Quant Results

Element	Weight %	Atomic %	Net Int.	Error %	Kratio	Z	R	A	F
C K	0.54	2.21	7.31	16.52	0.0035	1.3999	0.8613	0.4652	1.0000
FeL	2.38	2.10	9.04	13.59	0.0081	0.9926	1.0224	0.3434	0.9979
TiK	56.23	57.92	291.28	4.64	0.5913	1.0084	0.9962	0.9975	1.0453
CrK	21.36	20.27	55.59	7.39	0.2105	0.9935	1.0030	0.9673	1.0252
MnK	19.49	17.50	34.87	8.42	0.1891	0.9693	1.0048	0.9765	1.0251

EDS Spot 6

kV: 10	Mag: 2000	Takeoff: 34.7	Live Time(s): 30	Amp Time(µs): 7.68	Resolution:(eV) 124.4

EDS Spot 6

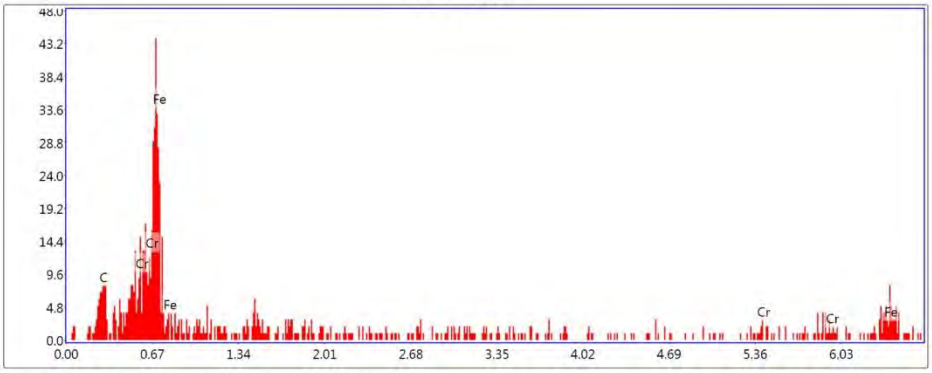

Lsec: 30.0 13 Cnts 0.610 keV Det: Octane Elite Super Det

eZAF Smart Quant Results

Element	Weight %	Atomic %	Net Int.	Error %	Kratio	Z	R	A	F
C K	11.50	37.45	1.09	43.08	0.0577	1.3454	0.8627	0.3726	1.0000
CrL	11.44	8.60	0.77	29.20	0.1115	0.9580	1.0094	1.0198	0.9981
FeL	77.06	53.95	5.83	14.10	0.5741	0.9542	1.0240	0.7823	0.9979

EDS Spot 7

kV: 10 Mag: 2000 Takeoff: 34.7 Live Time(s): 25.2 Amp Time(µs): 7.68 Resolution:(eV) 124.4

EDS Spot 7

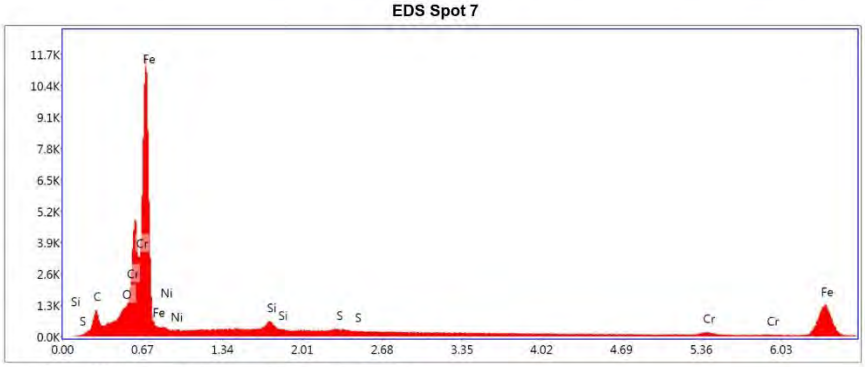

Lsec: 25.2 4.852K Cnts 0.610 keV Det: Octane Elite Super Det

eZAF Smart Quant Results

Element	Weight %	Atomic %	Net Int.	Error %	Kratio	Z	R	A	F
C K	2.68	10.79	69.64	13.62	0.0119	1.3815	0.8507	0.3214	1.0000
O K	0.90	2.74	67.83	14.02	0.0078	1.3126	0.8764	0.6566	1.0000
FeL	84.28	73.03	2201.24	3.69	0.7002	0.9801	1.0108	0.8494	0.9979
NiL	1.40	1.16	19.69	27.52	0.0056	0.9930	1.0248	0.4007	0.9975
SiK	2.16	3.72	121.22	10.31	0.0193	1.1783	0.9351	0.7551	1.0037
S K	1.02	1.55	47.04	21.26	0.0105	1.1510	0.9510	0.8809	1.0083
CrK	7.55	7.03	59.22	15.08	0.0797	0.9861	0.9985	0.9973	1.0733

EDS Spot 8

kV: 10	Mag: 2000	Takeoff: 34.7	Live Time(s): 28.3	Amp Time(µs): 7.68	Resolution:(eV) 124.4

EDS Spot 8

Lsec: 28.3 23 Cnts 0.610 keV Det: Octane Elite Super Det

eZAF Smart Quant Results

Element	Weight %	Atomic %	Net Int.	Error %	Kratio	Z	R	A	F
C K	4.25	16.35	1.86	31.49	0.0228	1.3799	0.8565	0.3882	1.0000
O K	0.60	1.74	0.67	87.01	0.0055	1.3110	0.8820	0.6961	1.0000
FeL	41.75	34.51	7.99	14.82	0.1823	0.9788	1.0171	0.4472	0.9979
CrK	53.40	47.40	5.59	13.25	0.5391	0.9824	1.0010	0.9993	1.0285

M2: Images for Charpy 2 (C2)

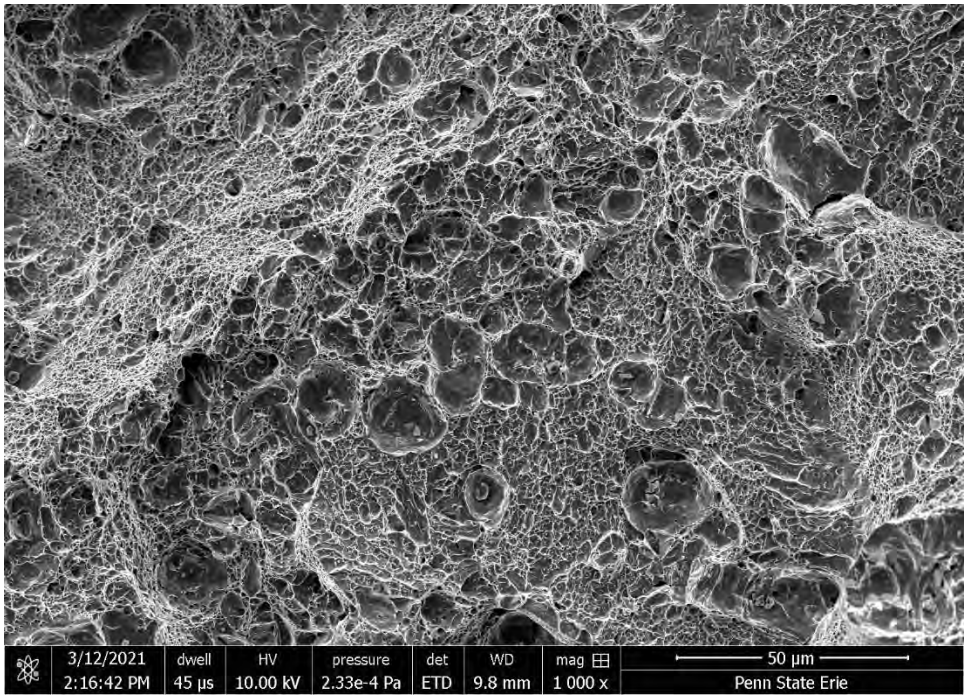

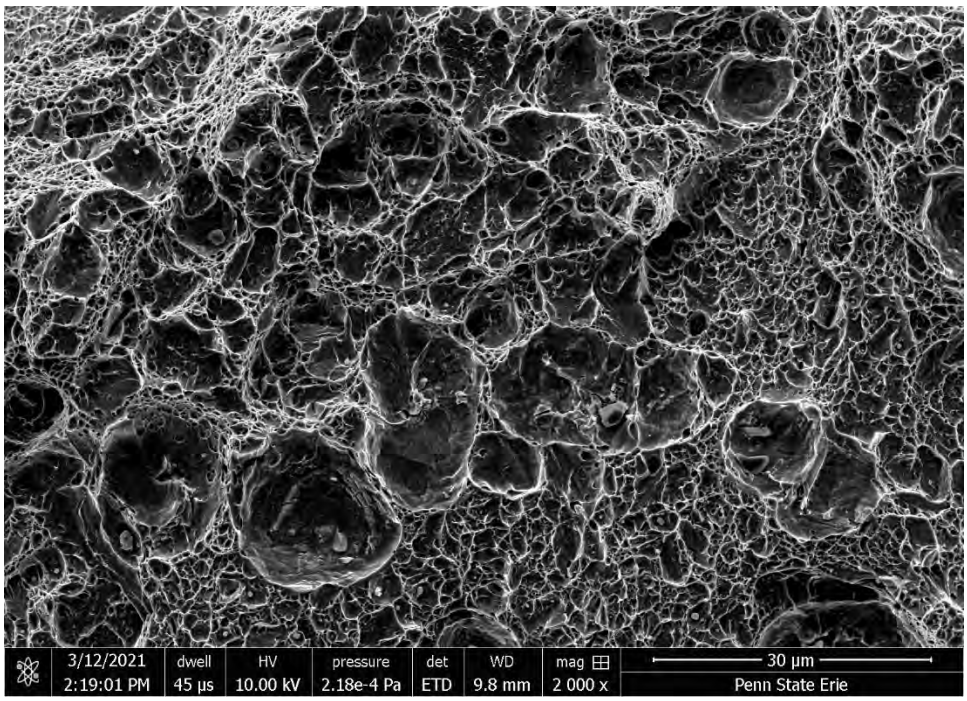

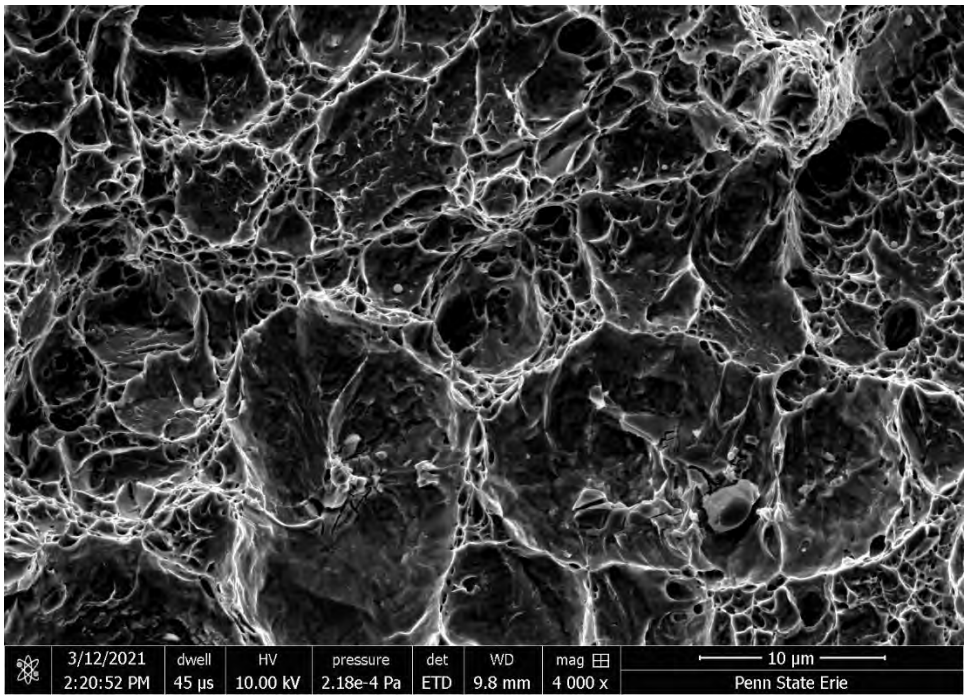
3/12/2021
2:20:52 PM
dwell
45 µs
HV
10.00 kV
pressure
2.18e-4 Pa
det
ETD
WD
9.8 mm
mag
4 000 x
10 µm
Penn State Erie

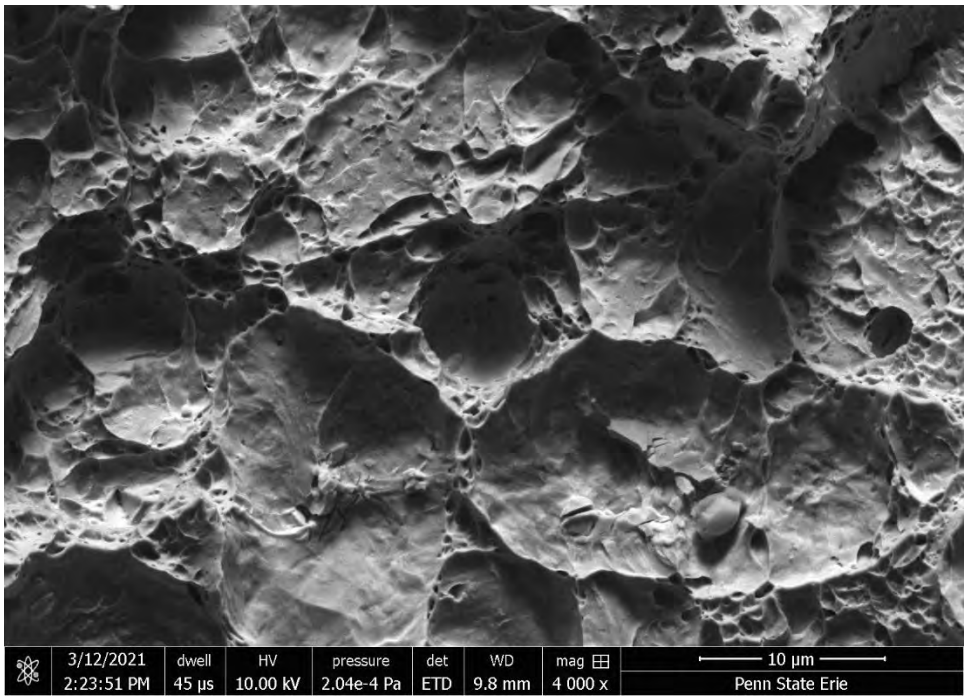
3/12/2021
2:23:51 PM
dwell
45 µs
HV
10.00 kV
pressure
2.04e-4 Pa
det
ETD
WD
9.8 mm
mag
4 000 x
10 µm
Penn State Erie

M3: Result Report for Charpy 2 (C2)

SFSA Cast in Steel 2021

Author: lab
Creation: 03/12/2021 2:40:57 PM

Sample Name: Thor 3_again

Area 6

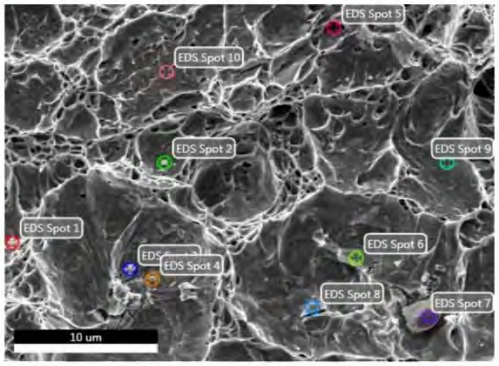

Notes:

EDS Spot 1

kV: 10	Mag: 3000	Takeoff: 34.8	Live Time(s): 24.8	Amp Time(µs): 7.68	Resolution (eV) 124.4

EDS Spot 1

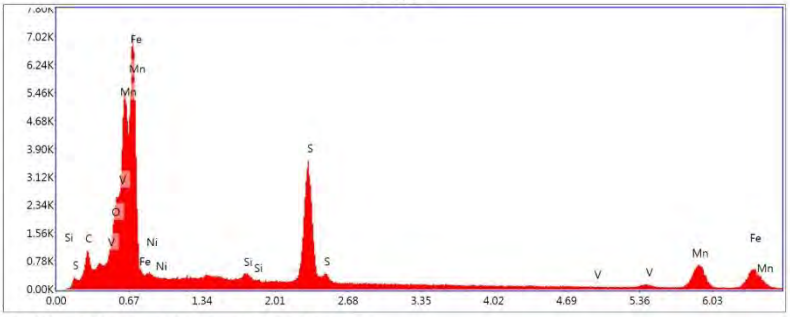

Lsec: 24.8 4.793K Cnts 0.610 keV Det: Octane Elite Super Det

eZAF Smart Quant Results

Element	Weight %	Atomic %	Net Int.	Error %	Kratio	Z	R	A	F
C K	2.04	7.64	62.57	14.64	0.0067	1.3644	0.8619	0.2415	1.0000
O K	1.64	4.62	173.40	10.26	0.0126	1.2961	0.8874	0.5899	1.0000
FeL	35.52	28.59	945.36	6.84	0.1895	0.9676	1.0231	0.5524	0.9979
NiL	1.01	0.77	25.76	25.58	0.0046	0.9802	1.0370	0.4661	0.9975
SiK	0.43	0.69	39.89	14.76	0.0040	1.1623	0.9449	0.7907	1.0079
S K	15.61	21.88	1153.72	3.98	0.1621	1.1348	0.9603	0.9058	1.0100
V K	0.33	0.29	5.91	20.23	0.0037	0.9571	1.0004	0.9919	1.1740
MnK	43.41	35.51	348.53	6.94	0.4241	0.9452	1.0050	0.9975	1.0362

EDS Spot 2

kV: 10 Mag: 3000 Takeoff: 34.8 Live Time(s): 24.8 Amp Time(µs): 7.68 Resolution:(eV) 124.4

EDS Spot 2

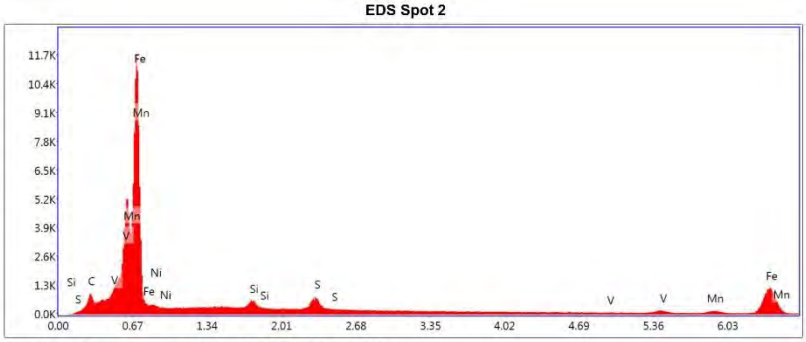

Lsec: 24.8 5.219K Cnts 0.610 keV Det: Octane Elite Super Det

eZAF Smart Quant Results

Element	Weight %	Atomic %	Net Int.	Error %	Kratio	Z	R	A	F
C K	1.38	5.82	32.79	22.43	0.0056	1.3888	0.8492	0.2925	1.0000
FeL	78.99	71.60	2020.54	3.92	0.6442	0.9854	1.0091	0.8293	0.9979
NiL	1.89	1.63	27.07	24.64	0.0077	0.9983	1.0230	0.4079	0.9975
SiK	1.88	3.38	105.90	10.94	0.0169	1.1847	0.9336	0.7570	1.0043
S K	4.38	6.92	201.92	8.44	0.0451	1.1572	0.9497	0.8826	1.0081
V K	0.94	0.94	10.05	18.45	0.0101	0.9791	0.9939	0.9934	1.0964
MnK	10.54	9.71	56.82	18.97	0.1100	0.9686	1.0006	0.9981	1.0794

EDS Spot 3

kV: 10 Mag: 3000 Takeoff: 34.8 Live Time(s): 24.3 Amp Time(µs): 7.68 Resolution:(eV) 124.4

EDS Spot 3

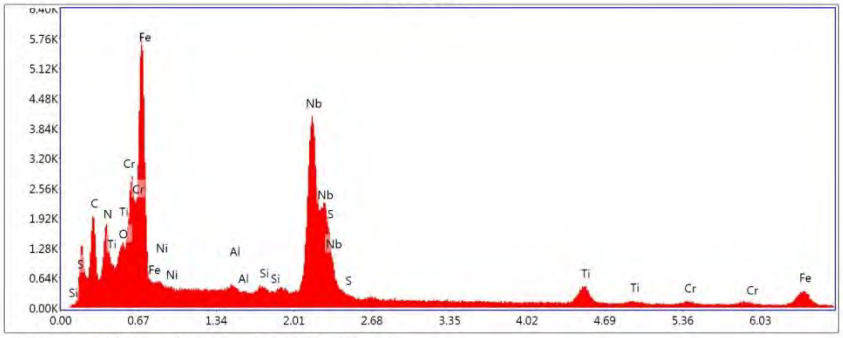

Lsec: 24.3 2.696K Cnts 0.610 keV Det: Octane Elite Super Det

eZAF Smart Quant Results

Element	Weight %	Atomic %	Net Int.	Error %	Kratio	Z	R	A	F
C K	8.92	28.43	273.79	11.10	0.0290	1.3620	0.8498	0.2386	1.0000
N K	5.24	14.30	167.07	12.58	0.0173	1.3260	0.8634	0.2490	1.0000
O K	2.49	5.97	139.75	12.93	0.0100	1.2945	0.8754	0.3090	1.0000
FeL	33.82	23.17	1011.63	6.27	0.1997	0.9667	1.0097	0.6122	0.9979
NiL	1.30	0.85	40.23	18.48	0.0071	0.9796	1.0237	0.5574	0.9975
AlK	0.46	0.65	45.32	17.31	0.0040	1.1397	0.9256	0.7501	1.0068
SiK	0.48	0.65	47.16	15.63	0.0047	1.1632	0.9342	0.8301	1.0113
NbL	33.69	13.88	1362.70	3.49	0.2863	0.8525	1.0934	0.9869	1.0101
S K	3.48	4.16	264.20	6.86	0.0366	1.1366	0.9502	0.9184	1.0053
TiK	7.83	6.26	172.90	8.24	0.0776	0.9881	0.9895	0.9722	1.0313
CrK	2.29	1.68	27.41	17.74	0.0229	0.9753	0.9980	0.9824	1.0472

EDS Spot 4

kV: 10 Mag: 3000 Takeoff: 34.8 Live Time(s): 24.8 Amp Time(µs): 7.68 Resolution:(eV) 124.4

EDS Spot 4

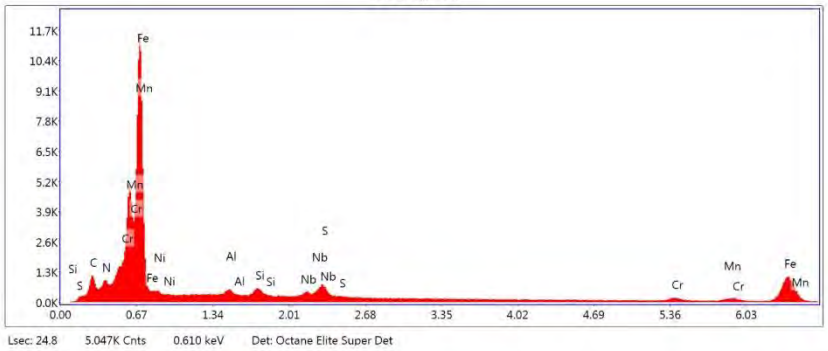

Lsec: 24.8 5.047K Cnts 0.610 keV Det: Octane Elite Super Det

eZAF Smart Quant Results

Element	Weight %	Atomic %	Net Int.	Error %	Kratio	Z	R	A	F
C K	2.59	10.20	75.78	13.64	0.0108	1.3790	0.8521	0.3013	1.0000
N K	1.50	5.06	63.71	14.03	0.0089	1.3423	0.8658	0.4394	1.0000
FeL	71.65	60.58	2003.27	4.66	0.5311	0.9783	1.0124	0.7592	0.9979
NiL	2.05	1.65	36.23	22.13	0.0085	0.9912	1.0263	0.4216	0.9975
AlK	0.91	1.59	59.64	14.23	0.0070	1.1526	0.9277	0.6655	1.0031
SiK	1.42	2.39	96.67	11.57	0.0128	1.1761	0.9363	0.7626	1.0046
NbL	2.20	1.12	64.02	14.13	0.0181	0.8616	1.0957	0.9401	1.0157
S K	3.13	4.61	172.76	8.89	0.0321	1.1488	0.9522	0.8863	1.0082
CrK	6.17	5.60	57.78	17.28	0.0649	0.9838	0.9991	0.9964	1.0742
MnK	8.38	7.21	53.51	18.62	0.0861	0.9605	1.0016	0.9980	1.0717

EDS Spot 5

kV: 10 Mag: 3000 Takeoff: 34.8 Live Time(s): 28 Amp Time(µs): 7.68 Resolution:(eV) 124.4

EDS Spot 5

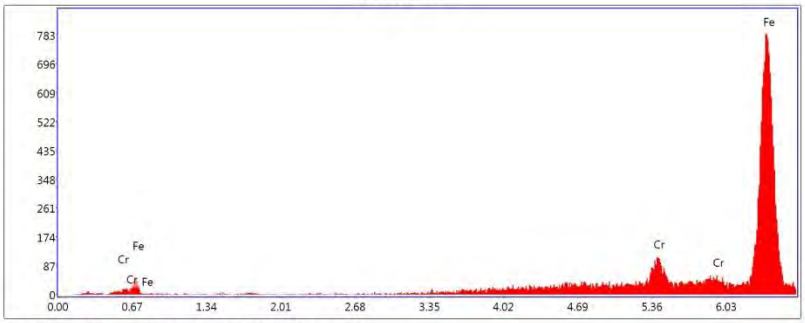

eZAF Smart Quant Results

Element	Weight %	Atomic %	Net Int.	Error %	Kratio	Z	R	A	F
FeL	4.96	4.64	5.87	16.31	0.0149	0.9963	1.0139	0.3024	0.9979
CrK	95.04	95.36	89.89	5.94	0.9682	1.0005	0.9997	0.9999	1.0184

EDS Spot 6

kV: 10 Mag: 3000 Takeoff: 34.8 Live Time(s): 23.5 Amp Time(µs): 7.68 Resolution:(eV) 124.4

EDS Spot 6

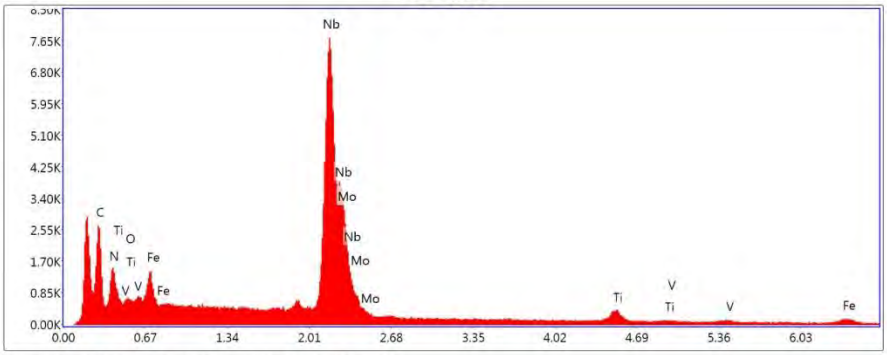

Lsec: 23.5 781 Cnts 0.610 keV Det: Octane Elite Super Det

eZAF Smart Quant Results

Element	Weight %	Atomic %	Net Int.	Error %	Kratio	Z	R	A	F
C K	15.13	46.63	433.10	11.16	0.0431	1.3886	0.8319	0.2049	1.0000
N K	5.18	13.70	121.25	15.23	0.0118	1.3521	0.8456	0.1679	1.0000
O K	2.10	4.87	93.45	14.54	0.0063	1.3204	0.8577	0.2254	1.0000
FeL	6.26	4.15	176.05	8.11	0.0326	0.9864	0.9897	0.5297	0.9979
NbL	59.77	23.82	2709.35	3.06	0.5342	0.8719	1.0756	1.0154	1.0095
MoL	5.39	2.08	221.87	8.58	0.0457	0.8612	1.0794	0.9744	1.0107
TiK	5.66	4.37	133.32	9.67	0.0561	1.0152	0.9787	0.9544	1.0244
V K	0.52	0.38	8.82	37.62	0.0051	0.9901	0.9847	0.9667	1.0324

EDS Spot 7

kV: 10	Mag: 3000	Takeoff: 34.8	Live Time(s): 24.6	Amp Time(µs): 7.68	Resolution:(eV) 124.4

EDS Spot 7

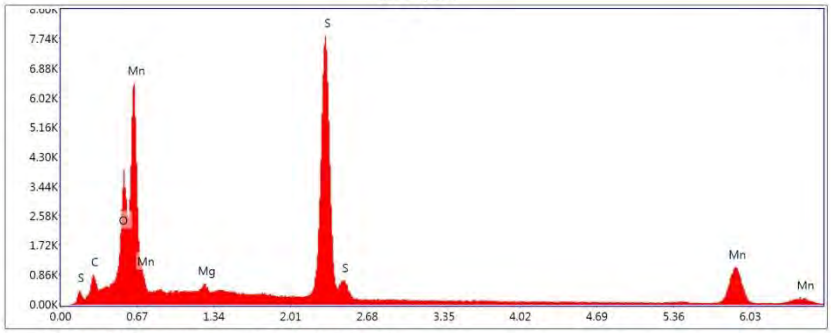

Lsec: 24.6 4.058K Cnts 0.610 keV Det: Octane Elite Super Det

eZAF Smart Quant Results

Element	Weight %	Atomic %	Net Int.	Error %	Kratio	Z	R	A	F
C K	1.86	6.24	47.86	18.36	0.0044	1.3306	0.8765	0.1778	1.0000
O K	2.31	5.82	244.81	10.11	0.0152	1.2634	0.9017	0.5196	1.0000
MgK	1.04	1.72	111.56	9.66	0.0077	1.1543	0.9411	0.6418	1.0045
S K	31.95	40.15	2759.62	3.41	0.3316	1.1041	0.9722	0.9303	1.0103
MnK	62.84	46.08	563.83	6.18	0.5868	0.9146	1.0099	0.9961	1.0250

EDS Spot 8

kV: 10	Mag: 3000	Takeoff: 34.8	Live Time(s): 23.5	Amp Time(µs): 7.68	Resolution:(eV) 124.4

EDS Spot 8

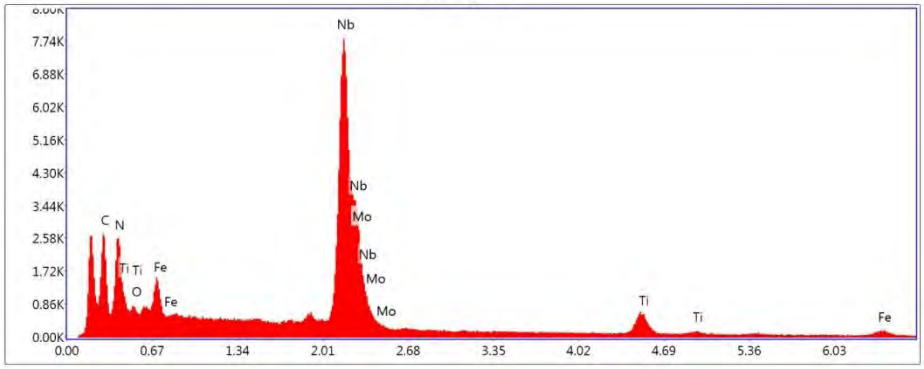

Lsec: 23.5 778 Cnts 0.610 keV Det: Octane Elite Super Det

eZAF Smart Quant Results

Element	Weight %	Atomic %	Net Int.	Error %	Kratio	Z	R	A	F
C K	12.92	36.97	440.12	10.96	0.0391	1.3616	0.8440	0.2223	1.0000
N K	10.42	25.57	301.55	12.07	0.0262	1.3258	0.8577	0.1894	1.0000
O K	2.20	4.72	105.17	14.28	0.0063	1.2946	0.8697	0.2214	1.0000
FeL	6.46	3.97	196.83	8.14	0.0326	0.9669	1.0033	0.5231	0.9979
NbL	55.25	20.44	2748.30	3.03	0.4844	0.8537	1.0877	1.0173	1.0095
MoL	2.28	0.82	103.41	12.72	0.0190	0.8431	1.0914	0.9797	1.0111
TiK	10.47	7.52	271.42	6.52	0.1022	0.9915	0.9861	0.9607	1.0238

EDS Spot 9

kV: 10 Mag: 3000 Takeoff: 34.8 Live Time(s): 25.7 Amp Time(µs): 7.68 Resolution:(eV) 124.4

EDS Spot 9

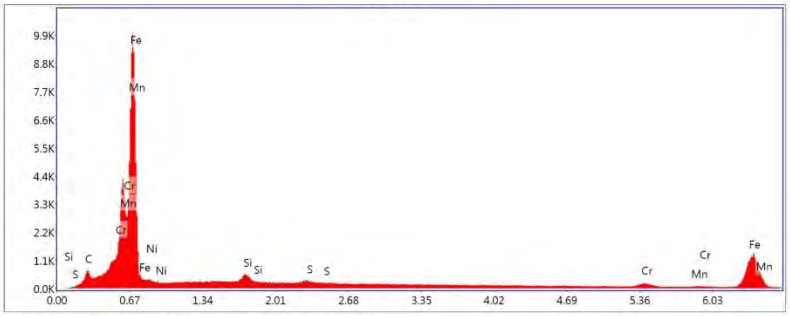

Lsec: 25.7 4.299K Cnts 0.610 keV Det: Octane Elite Super Det

eZAF Smart Quant Results

Element	Weight %	Atomic %	Net Int.	Error %	Kratio	Z	R	A	F
C K	0.79	3.43	18.35	31.03	0.0035	1.3977	0.8464	0.3203	1.0000
MnL	5.31	5.08	116.30	5.11	0.0468	0.9753	0.9988	0.9055	0.9981
FeL	80.21	75.47	1737.68	4.46	0.6202	0.9917	1.0060	0.7812	0.9979
NiL	1.45	1.30	18.15	27.06	0.0058	1.0048	1.0200	0.3971	0.9975
SiK	1.98	3.71	99.92	12.30	0.0178	1.1926	0.9312	0.7519	1.0038
S K	1.01	1.66	41.84	23.25	0.0105	1.1650	0.9474	0.8793	1.0085
CrK	9.25	9.34	65.15	15.01	0.0986	0.9994	0.9966	0.9971	1.0698

EDS Spot 10

kV: 10 Mag: 3000 Takeoff: 34.8 Live Time(s): 25.3 Amp Time(μs): 7.68 Resolution:(eV) 124.4

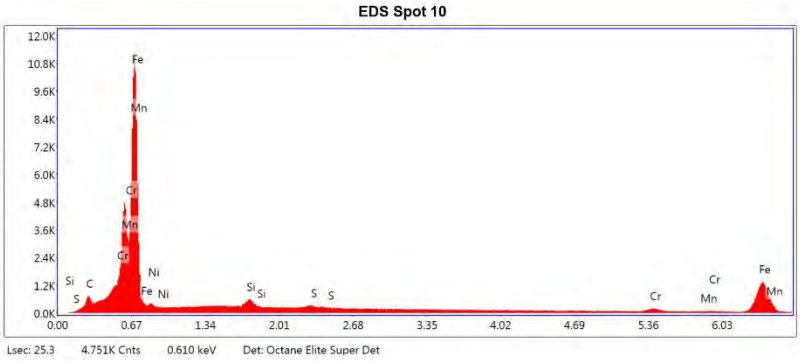

eZAF Smart Quant Results

Element	Weight %	Atomic %	Net Int.	Error %	Kratio	Z	R	A	F
C K	0.27	1.23	7.03	72.04	0.0012	1.4020	0.8450	0.3216	1.0000
MnL	5.52	5.40	134.90	4.76	0.0500	0.9783	0.9972	0.9263	0.9981
FeL	82.23	79.15	1975.04	4.33	0.6483	0.9948	1.0044	0.7942	0.9979
NiL	1.25	1.15	16.96	28.99	0.0050	1.0080	1.0184	0.3926	0.9975
SiK	1.63	3.11	89.05	11.01	0.0146	1.1964	0.9299	0.7493	1.0037
S K	0.87	1.45	38.99	23.87	0.0090	1.1688	0.9461	0.8786	1.0084
CrK	8.23	8.51	63.42	16.02	0.0882	1.0031	0.9959	0.9970	1.0724

References:

[1]. B. L. Bramfitt and S. J. Lawrence. “Metallography and Microstructures of Carbon and Low-Alloy Steels.” *ASM Handbook, Volume 9: Metallography and Microstructures*, edited by G. F. Vander Voort, ASM International, 2004, pp. 608-626. DOI: 10.31399/asm.hb.v09.a0003763.

[2]. G. F. Vander Voort. “Appendix A: Etchants for Revealing Macrostructure.” *Metallography Principles and Practice*, ASM International, 1984, pp. 509-532. DOI: 10.1361/mpap1999p509.